2014

Studies on rationally designed, allosteric, coagulation inhibitors

Rio Boothello
Virginia Commonwealth University

STUDIES ON RATIONALLY DESIGNED, ALLOSTERIC, COAGULATION INHIBITORS

A Dissertation submitted in partial fulfillment of the requirements for the degree of PhD in Pharmaceutical Sciences at Virginia Commonwealth University.

by

RIO BOOTHELLO
BPharm., University of Mumbai, India, 2009

Director: DR. UMESH R. DESAI
PROFESSOR, DEPARTMENT OF MEDICINAL CHEMISTRY

Virginia Commonwealth University
Richmond, Virginia
April 2014

Acknowledgement

My utmost thanks goes to my advisor Dr. Umesh R. Desai for always being there throughout my graduate studies. His persistent mentorship, motivation and support have made this journey a highly enriching experience. I would also like to thank my committee members Drs. Yan Zhang, Shijun Zhang, H. Tonie Wright and Carlos R. Escalante for helping me gain a better understanding in the art of grant writing through my independent proposal and reading, guiding and encouraging me throughout my graduation work. Special thanks to Drs. Tonie Wright and Faik Musayev who have been really instrumental in intriguing my interest in X-ray Crystallography and helping me develop my skills in this field.

The Dr. Desai laboratory has been an important aspect in nurturing, conserving stimulating and inspiring my love for science. This has all been possible due to the excellent work environment, which amalgamated hard work, creativity and fun to help me grow as a researcher. My heartfelt thanks goes to Drs Rajesh Karuturi and Rami Al-Horani, their experience has been really useful in trouble shooting numerous problems related to chemical synthesis and other areas of work and life. I would also like to thank Drs. Nehru Viji Sankaranarayanan and Aurijit Sarkar for their excellent assistance in all the computational modeling studies. I would like to thank all current and previous graduate students who have helped me through my graduate work particularly Akul

Mehta, Shrenik Mehta and Alhumaidi Alabbas.

My genuine love goes out to all my friends they have been tremendous in their support and patience. This includes friends in the department particularly Atul Jain, Hardik Parikh and Farhana Sakloth who have always been there to pick me up. Friends out of the department especially, Shilpa Singh for being awesome, Sweety Mehta for being like an elder sister, Soumya Warrier for being 'Soumya', Tanvi Deshpande, Priyanka Sheth, Divya Lulla, Batul Electricwalla, Khusboo Sharma, Anisha Patel, Aravind Reddy, Pratik Patel, Shankar Saran and all other friends for their constant support.

Words cannot describe the love and appreciation that goes out to my wonderful parents and sister. They have been a pillar of strength throughout my graduation and in life. Thank you for always being there for me. You have been the best family anyone could ever have.

Table of Contents

Page

List of Tables

Page

List of Figures

Page

Abbreviations

HFIP	1,1,1,3,3,3-Hexafluoro -2- propanol
TNS	2-(*p*-toluidino)naphthalene-6-sulfonic acid
2-OST	2-O sulfotransferases
3-OST	3-O sulfotransferase
APTT	Activated partial thromboplastin time
APC	Activated protein C
ASD	Allosteric databases
AUC	Analytical ultracentrifugation
AT	Antithrombin
C5E	C5 epimerase
CVLS	Combinatorial virtual library screening
CuAAC	Copper-catalyzed azide-alkyne cycloaddition
DS	Dermatan sulfate
DCM	Dichloromethane
DIPEA	Diisopropylethylamine
DMA	Dimethyl acetamide
DMF	Dimethyl formamide
EDTA	Ethylenediaminetetraacetic acid
EHBS	Extended heparin binding site
FV/FVa	Factor FV/Va
FIX/FIXa	Factor IX/IXa
FVII/FVIIa	Factor VII/VIIa
FVIII/FVIIIa	Factor VIII/VIIIa
FX/FXa	Factor X/Xa
FXI/FXIa	Factor XI/XIa
FXII/FXIIa	Factor XII/XIIa
FXII/FXIIa	Factor XII/XIIa
GA	Genetic algorithm
GlcN*p*	Glucosamine
GlcA*p*	Glucuronic acid
GP1bα	Glycoprotein 1b α-polypeptide
GAG	Glycosaminoglycan
GBP	Glycosaminoglycan binding proteins
hA	Helix A
hD	Helix D

HBP	Heparin binding proteins
HBS	Heparin binding sites
HCII	Heparin co-factor II
HIT	Heparin iduced thrombocytopenia
DEFGH	Heparin pentasaccharide
H5	Heparin pentasaccharide
H/HS	Heparin/heparan sulfate
HX	Hexasaccharides
HMWK	High molecular weight kininogen
hP	Hydrophobic domain
IdoA*p*	Iduronic acid
LC	Liquid chromatography
LMWH	Low molecular weight heparin
MS	Mass spectrometry
MWC	Monod, Wyman and Changeux model
NDST	N-deacetylase/N-sulfotransferase
NMR	Nuclear magnetic resonance
OTA	Octylamine
PT	Partial thromboplastin time
PSA	Polar surface area
PAR 1	Protease activated receptor 1
PDB	Protein data bank
QAOs	Quinazolin-4-(3H) ones
RCL	Reactive center loop
RPIP	Reverse phase ion-pairing
SIR	Selected ion recording
Serpin	Serine protease inhibitors
SAMs	Sulfated allosteric modulators
SPL	Sybyl programming language
TQD	Tandem quadrupole
TLC	Thin layer chromatography
TH	Thrombin
TF	Tissue factor
TFPI	Tissue factor pathway inhibitor
TrBA	Tributylamine
TEA	Triethylamine
UPLC	Ultraperformance liquid chromatography
UFH	Unfractionated heparin
UA*p*	Uronic acid

Abstract

STUDIES ON RATIONALLY DESIGNED, ALLOSTERIC, COAGULATION INHIBITORS

By Rio S. Boothello, BPharm.

A Dissertation submitted in partial fulfillment of the requirements for the degree of PhD in Pharmaceutical Sciences at Virginia Commonwealth University.

Virginia Commonwealth University, 2014

Major Director: Dr. Umesh R. Desai
Professor, Department of Medicinal Chemistry

Heparin is a natural allosteric modulator, with numerous structural and conformational variations leading to many reports of bleeding complications and variations in anticoagulant effects. A flurry of research has been directed towards understanding this puzzle. This work entails the utilization of three unique strategies to further our understanding of this complex issue.

Traditional synthetic, biosynthetic and biophysical approaches have failed to conquer the GAG-protein complexity. Computational analysis however could serve as a powerful approach to decipher this dilemma. A dual filter algorithm was incorporated to identify unique hexasaccharide sequences for HCII and AT. Our experimental studies exhibit a good correlation with our computational findings in addition, to the discovery of

the first reported heparin based hexasaccharide sequence (**HX1**) as a potent activator of HCII and AT.

In contrast to the enormity of GAG sequences, there appears to be a pattern where rare sequences have been identified to modulate characteristic functions in proteins. Our search led us to a biosynthetically rare GAG residue 2-*O*-sulfated glucuronic acid (GlcA*p*2S). Our computational studies indicated elements of selective recognition with coagulation enzymes propelling us towards synthesizing a polymer, **HS_{2S2S}** enriched in GlcA*p*2S and GlcN*p*2S saccharides. Our biological studies indicate its potential in activating AT and HCII in addition to a previously unobserved inhibition of thrombin but not FXa, which is corroborated by our computational studies. These studies therefore showcase the importance of studying rare sequences to further our understanding of differential recognition of proteins of the coagulation cascade.

An alternate anticoagulant strategy involves utilization of upstream enzymes like FXIa. Consequently, we devised a rational strategy, which targets the differential hydrophobic domain near the heparin binding sites of proteins through the design of molecules termed as sulfated allosteric modulators. Our endeavor led to the discovery of a library of quinazolin4-(3H)ones) dimers as selective inhibitors of FXIa. We recognized the linker length and geometry to be an important element affecting potency and selectivity. We therefore synthesized a library of 18 dimers using simple reaction schemes. Our inhibition studies do highlight a 9-fold improvement in potency.

CHAPTER 1: INTRODUCTION

1.1. Allosterism

Allostery implies regulation at a distance.[1] Largely associated with conformational and functional transitions in the target protein, "Allosterism" is a term coined by Monod and Jacob in a summary report "Cellular Regulatory Mechanism."[2] This phenomenon was initially formulated to explain the lac repressor binding on inducer and operator DNA sequences in addition to the effect observed on *Escherichia coli* dimeric threonine deaminase by L-isoleucine.[2,3] These eventually formed the basis of the Monod, Wyman and Changeux model (the MWC model) of 'concerted' allosteric transition.[2] In recent years, newer views of allostery have been hypothesized that are further reshaping the concept.[4] By definition, allostery is a phenomenon that arises from the coupling of an effector ligand binding at a remote ('*allos*') site ('*steros*') from the primary ligand site which induces structural and/or dynamic change resulting in regulation of binding of the primary ligand. The concept of allostery has expanded to numerous proteins that are known to utilize this feature.[4]

1.1.1. Allostery in the Regulation of Physiological Processes

Postulated as the most direct, rapid and efficient way to regulate protein functioning, allostery has come a long way from first being observed as early as 1903 in the sigmoidal binding curve of hemoglobin binding to O_2, which initially baffled many, but which remarkably led to the appearance of the concept of 'Allosterism' by Monod,

Wyman and Changeux.[2] The concept of allostery has now expanded from multimeric proteins to monomeric proteins and from native proteins to engineered proteins. The functions this concept regulates now range from control of metabolic mechanisms to signal-transduction pathways.[3] Numerous allosteric proteins function in normal physiology, but their roles in pathological states have now been uncovered. Comprehensive databases like the ASD (Allosteric database) have been assembled and these can be utilized to obtain information on allosteric proteins and modulators (Figure 1).[5,6]

1.1.2. Allosteric sites as Drug targets

The biological prevalence of allostery and its ability to have a huge influence in both normal and diseased states warrants its applicability as a therapeutic target. Its activation or inhibition of a particular protein, unlike standard active site direct inhibitors, makes it a unique tool to modulate the activity of a protein.

To summarize, allosteric effectors have the following advantages over conventional direct active site targets.

1. In highly conserved protein families, the allosteric effectors are more specific since they do not bind to the active sites, which tend to be conserved in such cases.[3]
2. They have lower chances of side effects, which could make them very useful in combinatorial strategies.[1]
3. They allow for modulation of protein activity rather than complete elimination of activity.[4]

4. They generally work when the endogenous ligand is bound and could therefore be used in cases where the cell is not functioning normally.

In contrast to these advantages, allosteric effectors could face a few hurdles

1. Unlike active site inhibitors, which interact with a known active site, allosteric sites are often unknown and the drug modulatory effects are difficult to predict.
2. Similar to active site effectors, allosteric effectors could also develop resistance issues.
3. There exists a higher divergence rate of allosteric sites in species homologs compared to that seen for active site inhibitors.[1]
4. Toxicity issues, generally due to high doses, which may arise from binding to additional proteins, or to formation of reactive metabolites.

Despite these challenges, allosteric effectors have displayed tremendous promise in overcoming the problems generally observed with known active site inhibitors and are therefore being pursued with increasing vigor.

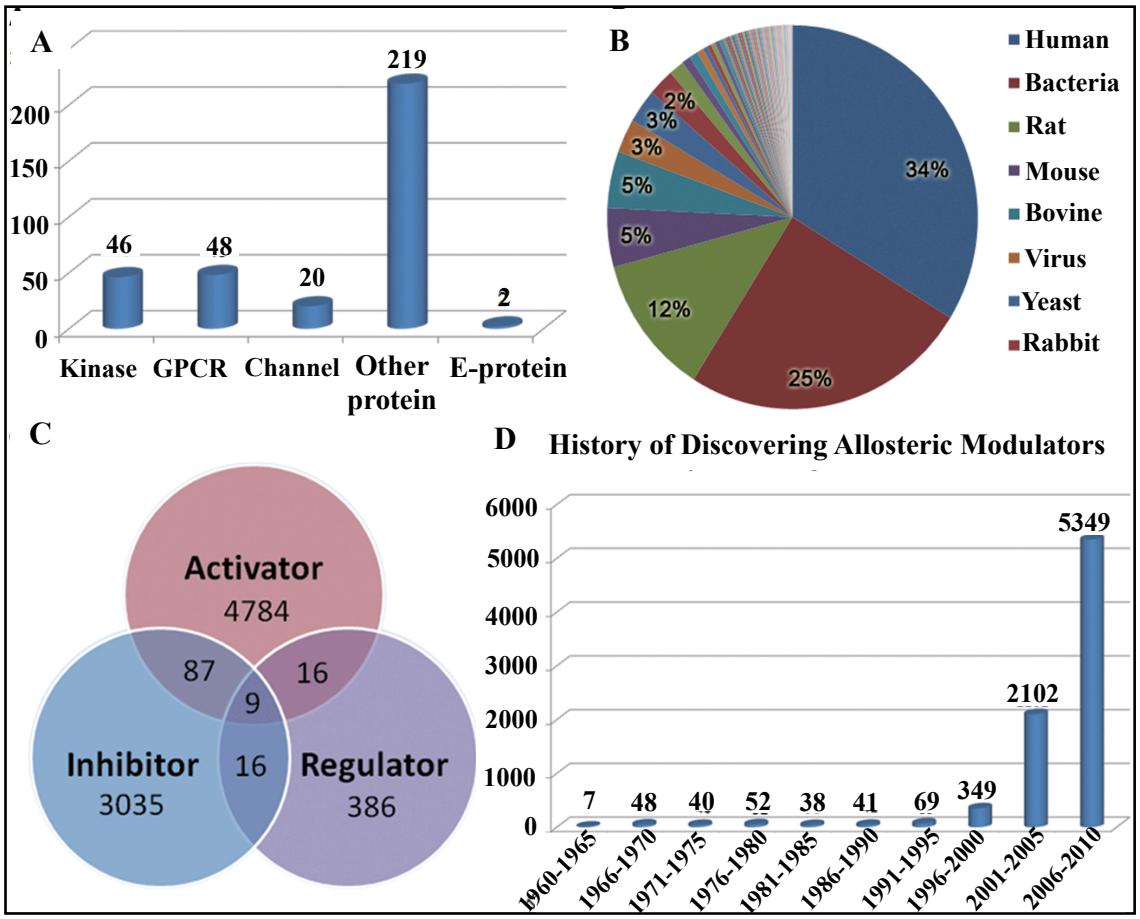

Figure 1. Statistics on the allosteric proteins and modulators from ASD. (A) Class distribution of allosteric proteins. (B) Species distribution of allosteric proteins. (C) Category distribution of allosteric modulators. (D) A history of the discovery of allosteric modulators.[6](Figure adapted from Reference 6)

1.2. Allosteric Regulation of the Coagulation enzymes

Excessive loss of blood from injury and protection against microbial infiltration are easily countered by the formation of a clot. This assures fine-tuning between blood flow and cessation, maintained by a group of highly sophisticated systems which form part of the hemostatic system. This essentially comprises the platelet dependent system, coagulation system and the fibrinolytic system, also termed primary, secondary and the tertiary hemostasis.[7] The coagulation cascade is a highly intertwined system and forms a crucial

part of this system. The concerted and finely regulated action of a constellation of proteins known as factors, the majority of which exhibit proteolytic enzymatic activity, form the cascade. This cascade principally is comprised of enzymatic conversion of zymogen to their activated form, which serves to activate a specific subsequent zymogen and further propagates the cascade.

1.2.1 The Coagulation cascade

The coagulation cascade could be fundamentally divided into the three major pathways 1.Intrinsic pathway, 2. Extrinsic pathway, and 3. The Common pathway, which are regulated by a group of physiological anticoagulant serine protease inhibitor (Serpins) (Figure 2)[8]

Intrinsic pathway

In this pathway, all clotting factors are present in the blood and are activated when blood comes in contact with activated platelets, collagen or other negatively charged surfaces as in vascular endothelium damage, lipoproteins in hyperlipidemia, or bacteria in infections. These initiate FXII attachment to the platelet membrane via the high molecular weight kininogen (HMWK), which helps anchor it to further activate to FXIIa. A small amount of FXIIa proteolytically cleaves FXI to FXIa. FXIa then converts FIX to FIXa, which forms intrinsic tenase, a trimolecular complex. Tenase then converts FX to FXa, which through the common pathway eventually culminates in the formation of thrombin and eventually clot. In a laboratory setting this pathway can be monitored using the activated partial thromboplastin time (APTT) assay.[8-10]

The Extrinsic pathway

Comparable to the intrinsic pathway, the extrinsic pathway similarly incorporates a cascade of interactions. Initiated by an injury without direct contact with nonphysiological surfaces, like endothelium damage, or by hypoxia resulting from reduced blood flow, which drives the formation of a complex between TF on cell surfaces and FVIIa located outside vascular system and hence the term extrinsic pathway. The FVIIa/TF complex, analogous in function to the tenase complex, then converts FX to its active form FXa (Figure 2). This is followed by the common pathway. In a laboratory setting this pathway is monitored using the partial thromboplastin time (PT) assay.[8,9]

The Common pathway

Apparent by its name, the common pathway is the point of convergence of the intrinsic and the extrinsic pathways. These converge with the formation of FXa, which in the presence of FV, Ca^{+2} and phospholipids converts prothrombin to its active form thrombin (TH). Thrombin primarily catalyzes the proteolysis of soluble fibrinogen to form fibrin monomers. Fibrin monomers then self polymerize to form a clot that helps cease blood flow. Thrombin is also known to activate FXIII to FXIIIa, which yields the covalent cross-linking of the fibrin polymer to form stable fibrin mesh (Figure 2). In addition, to these effects thrombin is known to catalyze its own formation from prothrombin. It can catalyze the formation of the cofactors FVa and FVIIIa effecting an efficient amplification of coagulation. Thrombin also provides positive feedback to the cascade by activating upstream proteins like factor XI, factor VIII in the intrinsic pathway, and factor

V in the common pathway. This ensures the efficient functioning of the cascade. Generally, deficiencies in any of the enzymes in the common pathway may result in major bleeding disorders.[7-10]

Natural Regulators of Coagulation.

It is necessary to have a regulatory mechanism to limit clot formation as well as to dissolve the clot when an injury has healed. This is facilitated by the presence of a variety of activators and inhibitors. The tissue factor pathway inhibitor (TFPI), the activated protein C (APC), antithrombin (AT) and heparin co-factor II (HCII) to name a few are the known anticoagulants which help restore some control over the coagulation cascade. The functions of each of these are summarized in the (Table 1). Of these, antithrombin, a **se**rine **pr**otease **in**hibitor (serpin) has garnered a lot of interest due to its accelerated inhibition of thrombin, FXa and FIXa in the presence of heparin (H).

Antithrombin activation forms the mechanism of a number of heparin-based drugs on the market. Another serpin gathering interest lately is HCII, which is known to inhibit thrombin alone and could serve as a novel target. These serpins, could be targeted to indirectly modulate the activity of the coagulation enzymes.[10]

Table 1. Natural regulators of coagulation.[10,11]

Name	Description	Function
TFPI	MW = 33,000 Da	Inhibits the TF/FVIIa complex
Activated Protein C	MW = 62,000 Da, vitamin k dependent serine protease	Cleaves FVa and FVIIa
Antithrombin	MW= 58,000, Serpin	Inhibits thrombin, FXa and FIXa
Heparin cofactor II	MW= 65,000, Serpin	Inhibits thrombin

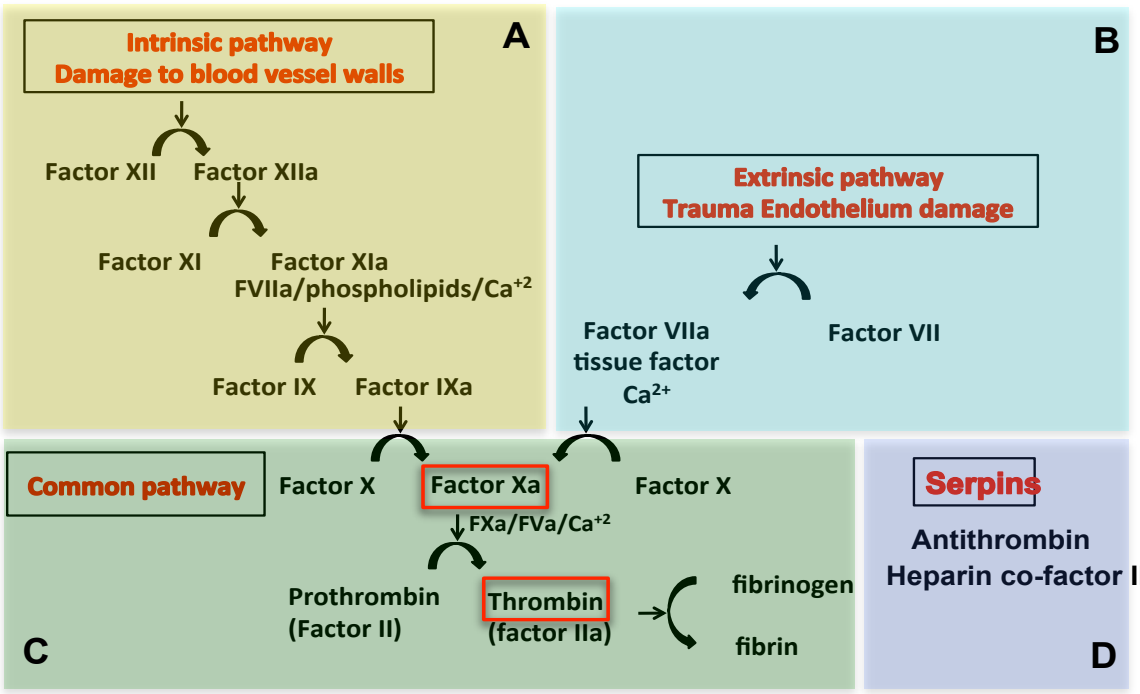

Figure 2. The coagulation system. (A) The intrinsic pathway, (B) the extrinsic pathway, (C) The common pathway (D) natural regulators of coagulation.[12]

1.2.2. Examples of Allostery in the Coagulation Cascade

The extensive interconnectivity within the coagulation system implies the presence of allostery. Allostery is indeed observed at different levels of coagulation, with many of these widely studied in terms of structure, mechanism and effects on normal functioning of these enzymes. A few examples of such systems are briefly described below to support the fact that allostery is a crucial part of the coagulation cascade and unequivocally offers new avenues in the development of drugs that could target these functions.

Thrombin

Thrombin is a serine protease of prime importance to the coagulation cascade. A part of its importance stems from its ability to interact with a multitude of substrates and cofactors to perform numerous functions in the cascade. Recent studies have indicated that the reason for this peculiar ability is the flexible structure of thrombin, which can be modulated to produce a plethora of actions.[13] Thrombin is known to possess three allosteric sites in addition to the catalytic triad containing active site as shown in (Figure 3). These serve as platforms to orchestrate the coagulation cascade.[10,13]

Exosite I – is a highly positively charged site and is responsible to be essential in the interaction with physiological substrates like PAR-1, GP1bα, and fibrinogen. This region also forms the site of interaction of known drugs like hirudin, obtained from the leech *Hirudo medicinalis*.

Exosite II – is another highly positive region decorated with numerous Arg and Lys residues. Physiologically, it is a recognition site for FV, FVIII and GP1bα.[13] This allosteric heparin-binding site has been a hotspot for drug design efforts.

Na^+ binding site – has been recognized as a vital site in regulating the activity of thrombin. Studies have indicated the importance of this site as a switch to move thrombin from the anticoagulant slow form to the procoagulant fast form. Na^+ binding ensuring its transition to the fast form.[13]

Allosteric sites have been observed in other serine proteases. A prime example includes the heparin binding exosite II, which is also seen in FXa, FIXa and FXIa thus, affording

an allosteric handle to modulate the activity of these important serine proteases through the design of newer anticoagulants.

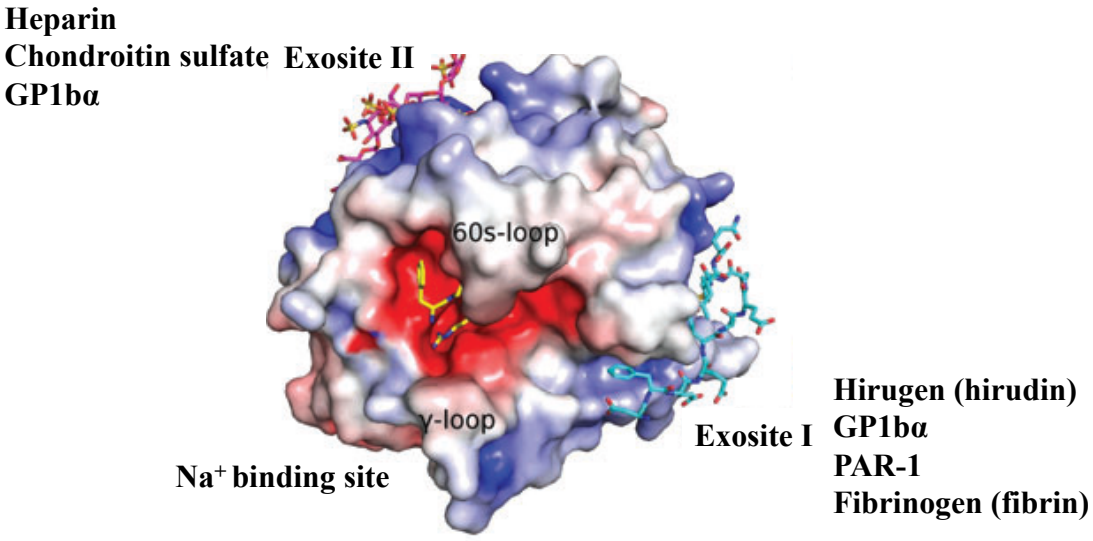

Figure 3. The allosteric sites on thrombin.[13] (Figure adapted from reference 13)

Antithrombin

Antithrombin is a serpin and a major physiological regulator of the coagulation cascade. Antithrombin in its apoform is known to be a poor inhibitor of thrombin and other enzymes. However, binding of a specific heparin pentasaccharide (H5) produces enough conformational changes to accelerate its inhibition of FXa to ~300–fold.[14] In contrast, it accelerates thrombin inhibition through a unique bridging mechanism. This involves binding of heparin at the pentasaccharide binding site of AT, while thrombin binds to non-specific residues on the other end of the heparin chain and then walks through the chain to be eventually inhibited by antithrombin, both of these mechanism are schematically represented in (Figure 4).[10,15] The allosteric nature of this interaction is known to control antithrombin inhibition of a variety of enzymes, which therefore makes

this an interesting system. Specific modulation could hold the key utilizing this as a drug target.[10,15]

Other examples of allostery in the coagulation cascade

Heparin is also known to allosterically modulate the activity of a number of enzymes in the coagulation cascade, which include enzymes like FIIa, FVIIa, FXa and FIXa. Each of these possesses a heparin binding exosite, which could be utilized in developing newer anticoagulants. Serpins like HCII are also known to accelerate allosterically towards thrombin inhibition without heparin. Studies to further understand the mechanism by which these function have been undertaken and could be utilized to further realize the potential that these possess.

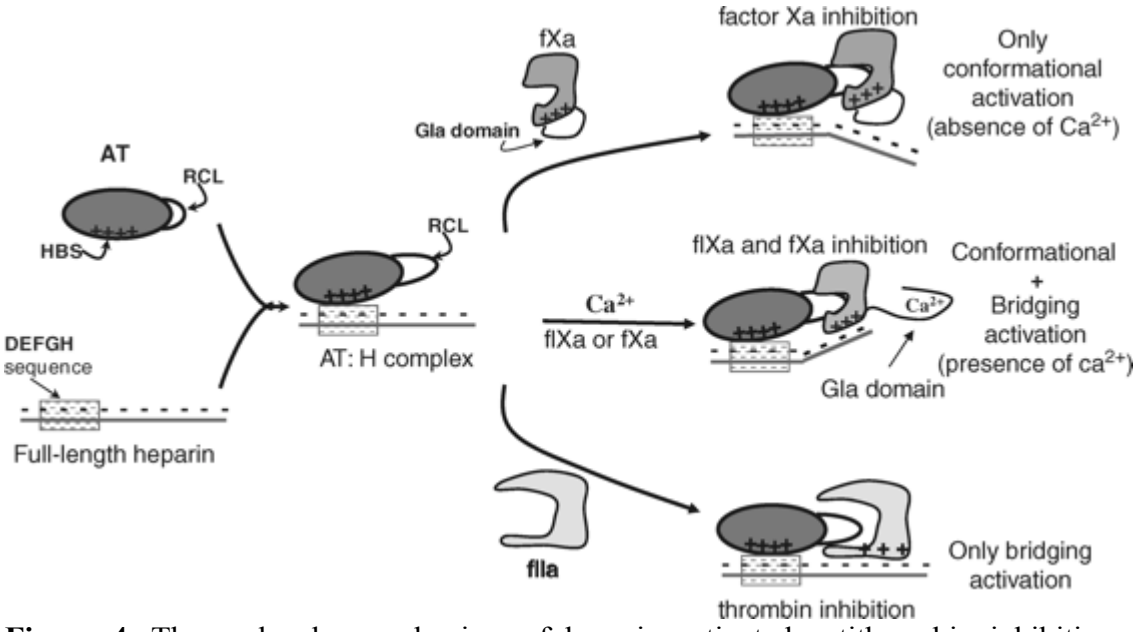

Figure 4. The molecular mechanism of heparin activated antithrombin inhibition of factor Xa, factor IXa, and thrombin. AT:H: antithrombin–heparin complex; RCL: reactive center loop; fIIa: thrombin; FXa: factor Xa; FIXa: factor IXa; Gla: Gla domain on fIXa/fXa; exosite on enzyme; HBS: heparin binding site.(Figure adapted from Reference 10)[10,15]

1.2.3. Implications for Design of Allosteric effectors

Allosteric interactions in the coagulation cascade could serve as a target for numerous anticoagulant drug design strategies. Physiologically, allosterism in the coagulation cascade is regulated by interaction between a larger protein and polymers. These therefore incorporate a higher degree of uncertainty in terms of off-target effects, heterogeneity and lack of bioavailability of these agents. Heparin is a prime example, where the heterogeneity and the lack of structural understanding of its interaction has been admirably overcome with the advent of variants of unfractionated heparin which included low molecular weight heparins (LMWH) that eventually led to the identification of heparin pentasaccharide DEFGH with a specific structure.[16] This was not only homogeneous but also selective in its interaction with AT, accelerating its FXa inhibition alone. Further studies conducted toward understanding the individual saccharide units essential for generating the acceleration indicated the presence of a trisaccharide sequence, DEF that could produce the same degree of activity, with the disaccharide EF considered to be providing stability to the active form of AT.[14,17] Similarly, a number of strategies have been utilized, which include the use of smaller oligosaccharides and synthetic small molecules, and other glycosamino glycan (GAG)-coagulation protein interactions can be similarly targeted.

Most anticoagulant drug design strategies typically aim to confer the following advantages over the physiological effectors

1. The structure of these effectors can be well characterized and be easily synthesized in larger quantities.

2. Most of the allosteric sites can modulate the interaction with more than one enzyme; hence specificity of interaction is an important feature (giving a predictable anticoagulant effect).
3. No risk of thrombocytopenia.
4. A wide therapeutic window (eliminating the need for routine coagulation monitoring)
5. Bioavailability is another important feature that these need to possess.
6. Rapid onset and offset of action and a rapid offset too, thus allowing for easier management of bleeds.
7. Presence of available antidotes could further improve the safety profile of these agents.[18,19]

1.3. Direct and Indirect allosteric effectors

Risk of bleeding is a serious drawback of current anticoagulant therapy despite the success it has enjoyed over a number of years. Observations with these agents indicate a direct correlation between the intensity of anticoagulation and the severity of risk factors. Efforts are therefore underway to discover and develop better and safer agents.[15] Targeting enzymes in the coagulation cascade could be achieved by directly inhibiting the enzyme of interest, in which case such effectors would be classified as direct inhibitors. Other effectors that interact with physiologic regulators of coagulation and accelerate inhibition of enzymes are known as indirect inhibitors.

1.3.1. Indirect allosteric inhibitors

Indirect inhibition through antithrombin activation has been a mainstay of this category. Precipitated by the advent of heparin, which was later found to activate the inhibition of a

number of enzymes in the coagulation cascade. However, antithrombin activation was considered as the primary mode of action. Several decades later heparin continues to be a major contributor in this class. Innovative design strategies and the discovery of other serpins, like heparin cofactor II, promise to be the new strategies towards developing more, safer indirect anticoagulants.

Antithrombin activators

Antithrombin: structure and kinetics of inhibition

Antithrombin, as the name suggests, is a physiological inhibitor of thrombin in addition to a variety of other coagulation enzymes like FXa and FIXa. This highlights the importance of this serpin. Physiologically, antithrombin exists as 58,200 Da plasma protein with relatively slow rates of inhibition of its target on its own.[20] However, coupled to its high plasma concentration (~2.3 μM) and its known interaction with cell-surface polysaccharide species like heparan sulfate, results in an acceleration of its activity culminating in a rapid inhibition of procoagulant proteinases.[20] Homozygous antithrombin knockout mice appears to be incompatible with life, however heterozygous mutation produces structurally defective variants.[21,22] The crystal structures of antithrombin in both the apoform and in presence of pentasaccharide have been solved, further providing insight into the function of this important enzyme.[22] A glycoprotein with 432 residues, it is known to possess four glycosylated Asn residues in its stable major α-antithrombin form. β-antithrombin, also known as the minor form, is not glycosylated at Asn135. The crystal structure indicates nine α-helices surrounding three β-sheets.[23-25] The presence of a dominant five-stranded β-sheet A approximately in the

center of the inhibitor and an exposed 15–residue sequence comprising the reactive bond Arg393-Ser394, also known as the reactive center loop (RCL), are the two distinctive features.[26-28] Another unusual feature seen only in AT and HCII is the presence of two residues, P15-P14 (Gly379-Ser380) at the N-terminal end of the reactive center loop, which are inserted as a short β-strand between strands 3 and 4 of the β-sheet A in the inhibitor (Figure 5A). [15,29] This partial insertion of the RCL plays a major role in the process of proteinase inhibition. The structure of antithrombin cleaved at the reactive bond shows the complete insertion of RCL as strand 4a in β-sheet A (Figure 5B) with the remainder of the protein remaining largely unchanged. This structural change initiates an approximately 70Å movement of the P1 residue from the top of the molecule to the bottom.[30,31] This dramatic conformational change yields an additional thermodynamic stabilization of the molecule and is considered to be a critical event in the disruption of the catalytic triad of a target proteinase, eventually resulting in its inactivation.[32-35]

This mechanism has been widely referred to as the serpin mousetrap mechanism, where the serpin (AT) acts as a bait to trap target enzymes like FXa, FIXa and thrombin (E) in an equimolar, covalent inactive complex (E*-AT*) (Figure 6). Initial interaction between the RCL and the proteinase active site forms a Michaelis complex (E:AT), which is then followed by the rapid cleavage of the P1-P1' scissile bond in the RCL to form an acylated intermediate (E*-AT*). Another competing reaction known as the substrate pathway, involves rapid cleavage of the acylated enzyme (E-AT) to give the free enzyme and substrate. This does not contribute during normal experimental conditions.[15]

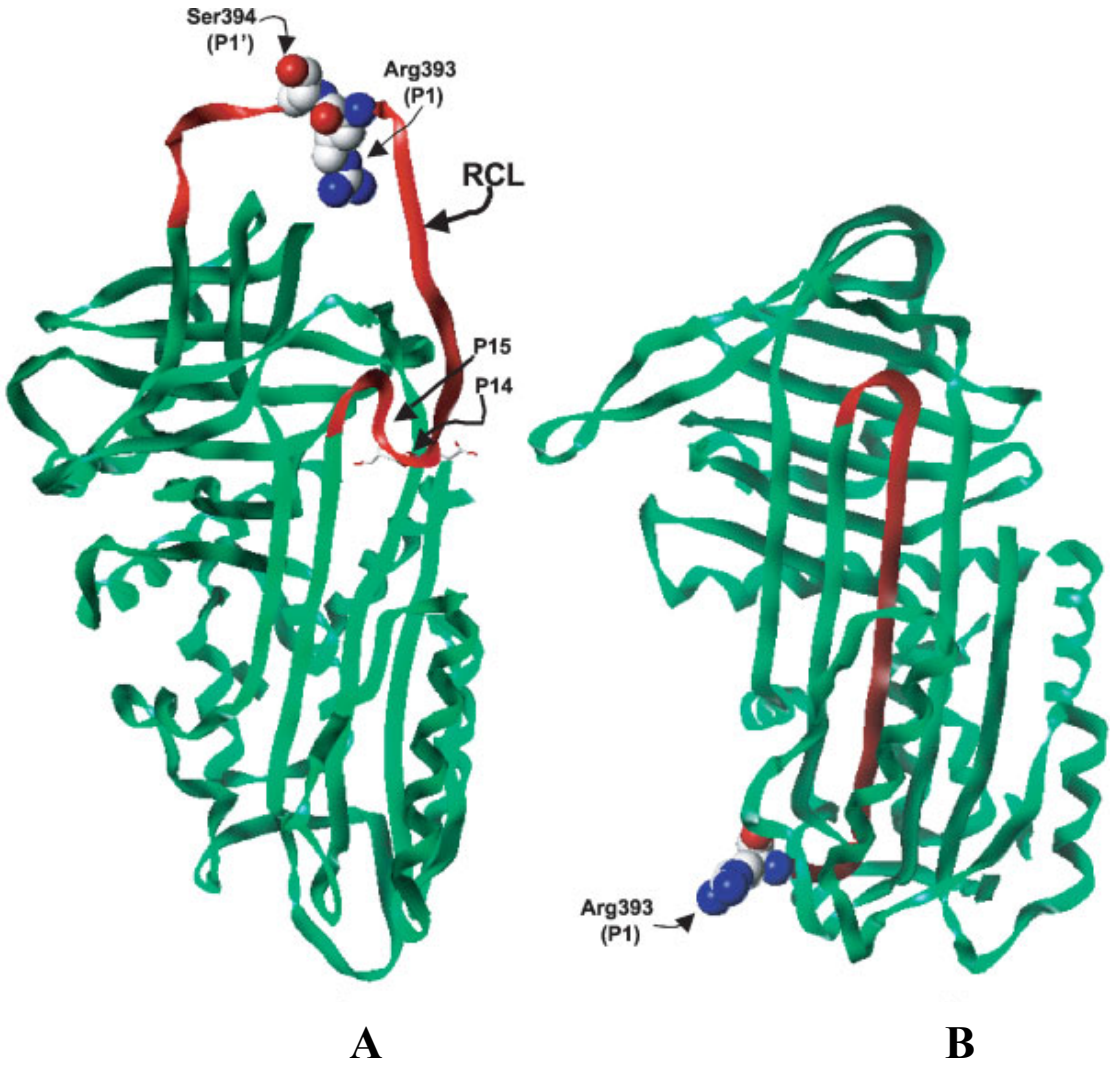

Figure 5. Ribbon diagram of native (**A**) and cleaved (**B**) plasma antithrombin. The structure of plasma antithrombin was obtained from PBD (pdb id'1ath') (Figure adapted from Reference 10)

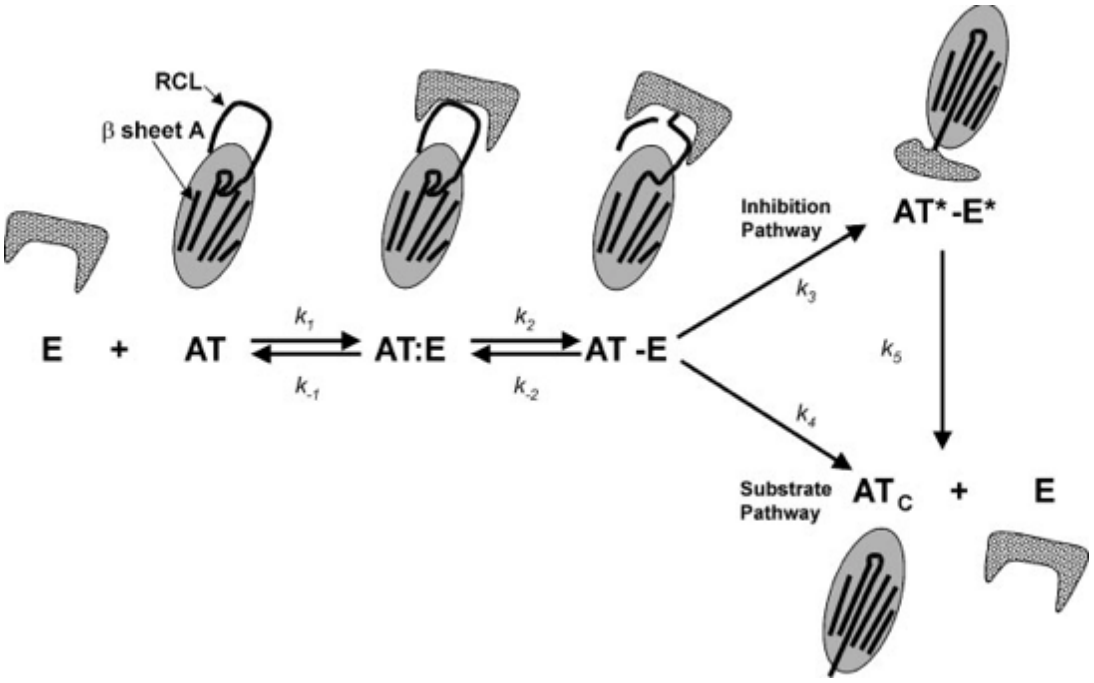

Figure 6. A model of the serpin 'mousetrap' mechanism of inhibition. (Figure adapted from Reference 10)

Heparin induced activation of antithrombin

Serpins are generally known to inhibit their target enzymes by diffusion controlled acceleration rates of ~10^6-10^7 M^{-1} sec^{-1}. Uncatalyzed rates of antithrombin inhibition, however, are drastically low with *in vitro* rates of ~7-11 x 10^3 M^{-1} sec^{-1} for thrombin and ~2–3 x 10^3 M^{-1} sec^{-1} for FXa.[36-39] The native structure of AT highlights a peculiarity in the RCL, which exhibits partial insertion forcing P1 and other important residues to adopt a conformation that hinders the interaction with enzymes like thrombin and FXa. Owing to this, the anticoagulant effect of antithrombin is suboptimal physiologically.[40] Heparin, a natural linear polysaccharide, was identified to possess anticoagulant effect in 1916.[41] It was later deciphered that this effect was seen due to its acceleration of antithrombin inhibition of a number of coagulation enzymes as shown in (Table 2).[26] Since then much

of research has been dedicated understanding the mechanism of its action and developing agents, which could mimic this interaction.

Mechanism of heparin activation

Heparin is known to accelerate antithrombin by two distinct mechanisms, namely the conformational and the bridging mechanism. The conformational change mechanism involves a major change in the structure of antithrombin on interacting with heparin, which accelerates its inhibition of FIIa and FXa. In the case of the AT-FXa system, binding of the highly specific heparin pentasaccharide H5 to heparin, at an exosite produces a conformational change in the RCL and β-sheet C. The partially inserted P1-P1' reactive center and an exosite on AT is now exposed, which is then better recognized by FXa, resulting in accelerated cleavage of the P1-P1' bond and rapid formation of covalent inhibited complex.[32,39,42,43] This phenomenon is also seen with other enzymes, but it is more important in the inhibition of FXa.

In contrast, the bridging mechanism is found to be crucial in the acceleration of thrombin inhibition. Specific binding to antithrombin of heparin H5 sequence, present in the full-length heparin is followed by thrombin binding to the same chain at non-specific sites to form ternary complex comprised of antithrombin-heparin-thrombin as shown in Figure 4. This is then followed by diffusion of thrombin along the polyanionic heparin chain, resulting in ~2000 –fold inhibition under physiological conditions.[17,44,45] A polysaccharide of ~18 residue saccharide units is required to simultaneously hold thrombin and antithrombin for accelerated inhibition. Thus, in this case the H5 sequence alone cannot potentiate inhibition. Recent evidences however suggest that such a

mechanism could be used by the AT-FXa system too, however this is seen in the presence of Ca^{2+} with full-length heparin. Similarly, UFH is also known to accelerate AT inhibition of FIXa 300-500-fold through the conformational mechanism and ~1000-fold using the bridging mechanism.[43] The mechanism of action for thrombin, FXa and FIXa is summarized in (figure 4).[10,46]

Heparin binding site

The allosteric heparin binding exosite is located around 20 Å away from the RCL in AT. This exquisitely structured site specifically recognizes the H5 sequence from a variety of structurally different heparin chains. The heparin-binding site is predominantly positively charged made up of the positively charged residues of helices A and D, and the polypeptide N-terminus. The crystal structure of antithrombin with the pentasaccharide sequence has been solved and indicates four important residues (Arg47, Lys114, Lys125, and Arg129) and the domain called the pentasaccharide binding site (PBS).[22,47-51] Full-length heparin called the extended site formed by residues Arg132, Lys133, and Arg136 at the C-terminal end of helix D and is known as the extended heparin binding site (EHBS).[47] The interaction of H5 with the PBS induces conformational change with allosteric effects. This allostery is seen on both sides the RCL end as well as the heparin binding site end. The P1-P1' bond (Arg393-Ser394) is the target for proteinase cleavage.[52,53] Antithrombin inhibits a number of coagulation enzymes and the interaction with heparin is know to accelerate it to varying degrees towards inhibition of other proteinases as seen in (Table 2). Though this provides for a major block in the coagulation activity, it could however lead to bleeding risk. Therefore, controlling the

activation towards its intensity and specificity of target enzyme can help develop safer and more useful anticoagulants.

Table 2. Acceleration rates of antithrombin towards inhibition of proteinases in the presence of heparin and the mechanistic contribution of this acceleration.[26]

Serpin	Proteinase	Bridging	Conformational	Max rate $(M^{-1} s^{-1})$
AT	Thrombin	~2400-fold	~1.7-fold	~3.7 x 10^7
AT	Factor Xa	~70-fold	~300-fold	~4.4 x 10^7
AT	Factor IXa	~600-fold	~700-fold	~2.0 x 10^7
AT	Trypsin	~2.2-fold	~3.2-fold	~1.4 x 10^6

Classes of antithrombin based anticoagulants

Heparin is the one of the most widely used anticoagulant, impelling enormous research activities towards discovering/designing newer agents, aimed at both improving on heparin as well as refining the selectivity towards targeting specific enzymes. These molecules can be classified into 1. Heparin-based activators 2. Heparin-pentasaccharide DEFGH and its variants 3. Nonsaccharide-based activators.

Heparin-based activators

Heparin is a glycosaminoglycan (GAG), which continues to be a mainstay of anticoagulant therapy for decades, however advances over the past years have yielded worthy successors to this pivotal drug. Structurally, heparin is a polysaccharide consisting of chains ranging from 5,000-40,000 in weight, with an average of ~14,000. Heparin is predominantly made up of alternating unit of glucosamine or uronic acids.

These are sulfated at varying levels, with N-sulfation and/or sulfation at 2, 3, or 6 positions. The uronic acids generally involved include the β-D-glucuronic acid or α-L-iduronic acid with varying degree of sulfation (Figure 7).[54-57] The high degree of sulfation makes heparin a highly negatively charged molecule. The heterogeneity in structure, molecular weight and polyanionic character make it a novel and equally challenging class of anticoagulant.

The diversity in heparin was moderately reduced through the use of enzymatic and chemical approaches in developing smaller heparins with an average molecular weight of ~4,000 – 6000, also known as the low molecular weight heparins (LMWH).[58,59] A variety of these have been made available commercially as seen in (Table 3). Synthetic variants using natural polysaccharide like hyaluronic acid, chitosan, dextran, galactomannan and fucan have been sulfated but, these fail to replicate the activity seen with heparin.[60-64]

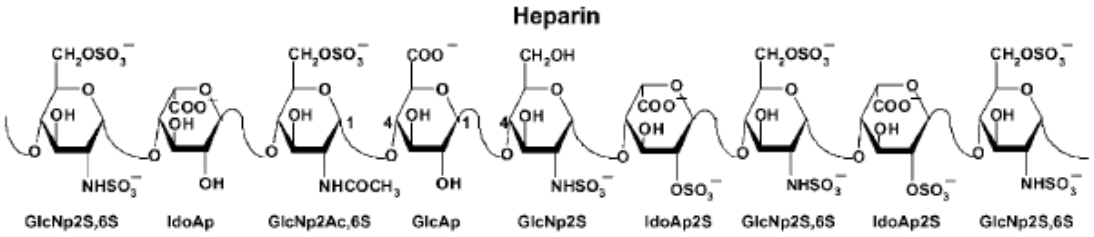

Figure 7. Structure of heparin.

Table 3. Comparative properties of low molecular weight heparin preparations.[15]

Brand name	Manufacturer	Key reagent in depolymerization	M_R	Ratio anti-fXa: anti-IIa
Ardeparin	Wyeth-Ayerst US	Peroxides	5,300	2.0
Dalteparin	Pharmacia, US	Nitrous acid	6,000	1.9 – 3.2
Enoxaparin	Aventis, US	Alkali	4,500	3.3 – 5.3
Nadroparin	Sanofi, France	Nitrous acid	4,300	2.5 – 4
Reviparin	Knoll AG, France	Nitrous acid	3,900	3.6 – 6.1
Tinzaparin	Leo Labs, Ireland	Heparinase	6,500	1.5 – 2.5

Anticoagulant heparin, however, has been associated with numerous complications. One of the major concerns is, that of heparin induced thrombocytopenia (HIT). Most of these complications have been attributed to non-specific interactions and to major structural differences. Another problem associated with the heparin is the lack of ability to inactivate clot bound thrombin, which is attributed to the thrombin binding to γ-fibrin at exosite II, thus blocking the heparin-binding site.[65-70]

Lower molecular weight heparins have a significantly lower bleeding rate but, they do not completely eliminate the bleeding risk. Different methods of preparations are known to bring about variations in their anticoagulant properties, prompting the FDA to suggest each clinical LMWH be treated as an unrelated independent drug.[71-76] Nevertheless, newer heparins continue to be developed at a frantic pace. Technological advances in

related fields have led to expectation of developing structurally and biologically superior heparins.

Heparin oligosaccharides

The heparin pentasaccharide sequence DEFGH has been identified as the specific tight binding sequence and is known to bring about a conformational modification of antithrombin, which produces acceleration in it inhibitory properties. Structurally, it is made up of two domains, the trisaccharide DEF and the disaccharide GH domain. The disaccharide sequence consisting of →4)IdoAp2S (1→4)GlcNp2S6S (1→ is known to be the most abundant disaccharide sequence in heparin, whereas the trisaccharide sequence consisting of GlcNp2S,6S(1→4) GlcAp(1→4)GlcNp2S,3S,6S is the least abundant sequence in heparin.[77,78] The most characteristic feature includes the presence of a central glucosamine residue, F, consisting of three sulfates at 2-, 3-, and 6-positions, which is rarely present outside the pentasaccharide H5 sequence. Both these domains play different roles with the trisaccharide playing an important role in inducing conformational changes while the disaccharide is involved in stabilization of this change and improving the overall affinity of H5. The crystal structure of the pentasaccharide with antithrombin has been obtained and this provides for insights of the residues involved at a molecular level as seen in (Figure 8).[15]

The pentasaccharide is known to produce acceleration of selective AT inhibition of FXa alone. This is due to the ability of the pentasaccharide to utilize the conformational mechanism of activation alone, which is a major player in the activation of AT towards

FXa inhibition. Thrombin inhibition, on the other hand, utilizes the bridging mechanism and thus is not inhibited.

The major complications in heparin generally arise from its non-specific interactions, which were primarily attributed to its complex structure. Reducing this complexity by chopping down the size of heparin to oligosaccharides like heparin pentasaccharide has helped improve this specificity. Since the discovery of the pentasaccharide numerous efforts have been made to develop even better oligosaccharide units. Some of this work explored natural variants of the pentasaccharide, (Petitou and coworker). Similarly, synthetic variants were designed to conduct a structure activity relationship study to design more potent sequences. A few of these efforts have been summarized in (Figure 9).

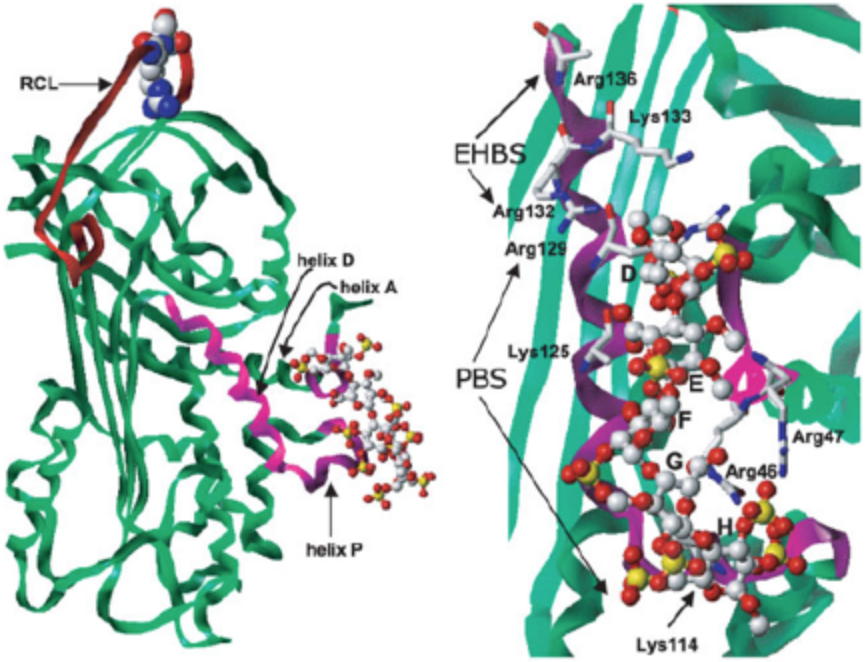

Figure 8. Crystal structure of pentasaccharide with antithrombin displaying the interaction with antithrombin. (Figure adapted from reference 10)[15,25]

Synthetic nonsaccharide based activators

The hypothesis that synthetic small molecules could mimic the activity of heparin has recently resulted in efforts aimed at the development of small molecule activators of heparin and heparin pentasaccharide. These have utilized computational tools like HINT to obtain molecules that could structurally resemble the heparin trisaccharide sequence DEF, which was the smallest oligosaccharide sequence to still possess activity. On this basis, a group of small molecules were identified, followed by a series of structural screens, from which (-)-epicatechin sulfate was found to be small molecule activator of antithrombin. Using a similar approach several other molecule where designed with a maximum of ~80–fold activity obtained. However, the detailed competitive binding and molecular binding studies indicated that these molecules bind to the extended heparin-binding site (EHBS) (Figure 7). Thus, developing agents, which could target the pentasaccharide, binding site or both the pentasaccharide and the extended heparin binding sites could result in a more active molecule.[58,59,79-82]

Heparin co-factor II activators

Heparin cofactor II (HCII) is a 65.5KDa plasma protein that belongs to the serine protease inhibitor (Serpin) family. Since its initial discovery in 1974 by Bringinshaw and Shanberge, little information has been obtained despite its high plasma concentration of 1 μM.[83,84] Initially named heparin cofactor A and other names, such as antithrombin BM, dermatan sulfate cofactor and leuserpin-2, it was eventually named heparin cofactor II by Tollefsen and Blank.[85] Its major inhibitory activity was observed against thrombin in the

presence of dermatan sulfate, which produces a 1000–fold acceleration in inhibitory activity.

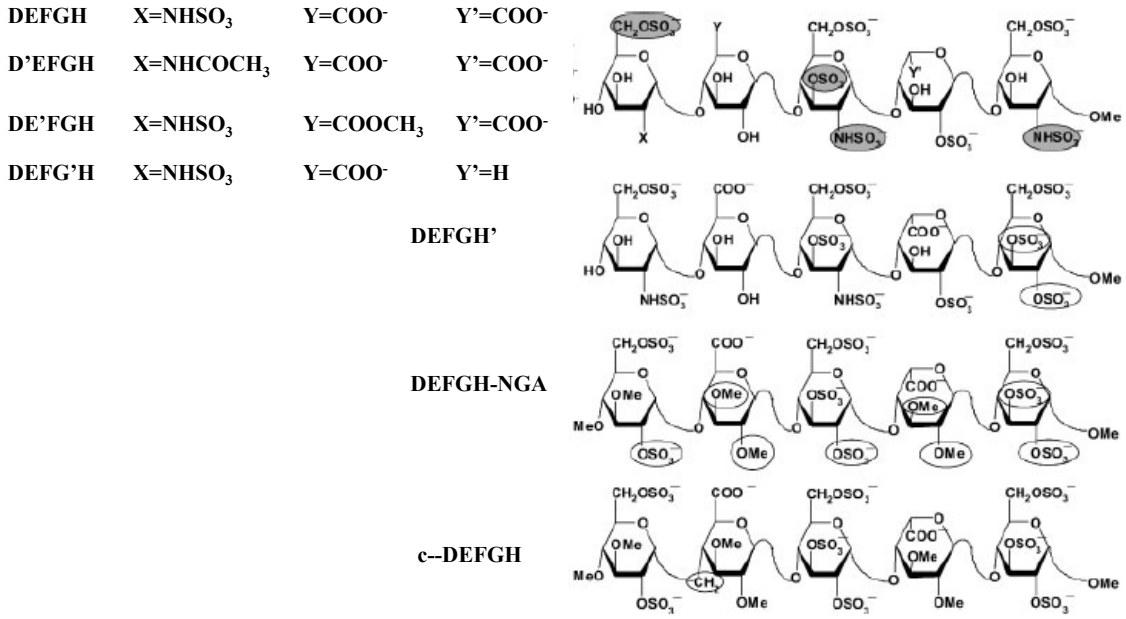

Figure 9. Structure of natural pentasaccharide DEFGH derivatives.[15]

Structure, function and the kinetics of inhibition by heparin cofactor II

The crystal structure of heparin cofactor II has been solved both in the native form and in the presence of thrombin. This reveals some structural insights into the functioning of this serpin. HCII is composed of 480 amino acid residues. On a three-dimensional level, it is structurally quite similar to AT, with a six-stranded β-sheet A due to the partial incorporation of the RCL that effectively reduces its flexibility and accessibility to proteolytic attack. Superposition of AT and HCII structure indicated a deviation in RMSD of 1.8Å, consistent with similar functions, which involves the expulsion of the RCL to further inhibit circulating serine proteases. A major difference between AT and HCII is the presence of Leu at the P1 position instead of the Arg residue normally seen in

serpins. The heparin binding sequences in HCII obtained on sequence alignment indicates the conservation of similar residues. The N-terminal acidic tail, which comprises 160 amino acids, consists of two hirudin-like domains, EDDDY*LD and EDDDYID. Both these consists of several acidic amino acids and a sulfated tyrosine, which are responsible for interaction with exosite I of thrombin.[29]

Physiologically, despite its high concentration, HCII does not seem to be vitally important, with individuals predisposed to HCII deficiency not showing an increased risk of venous thrombosis. Recent studies have postulated that HCII plays the role of an adjunct to AT in hemostasis regulation. HCII, however seems to play a major role during pregnancy with studies indicating that HCII deficiency is embryonically lethal. Increased HCII levels during pregnancy further add to this claim. HCII has also been shown to play a major role in vascular injury with high levels of HCII showing a decrease in atherosclerosis and restenosis, whereas reduced levels have been shown to produce increased cardiac events.[86-89]

Comparable to AT, HCII is quite similar in its mechanism of inhibition of serine proteases, the only difference being the presence of Leu at P1 instead of an Arg, generally seen in serpins. HCII is known to inhibit thrombin in addition to other proteins like chymotrypsin and neutrophil cathepsin G. Its rate of inhibition of thrombin is very slow (600 $M^{-1}s^{-1}$). Thrombin specificity is conferred by the presence of two hirudin-like domains in the N-terminus of HCII. Unlike AT, which is substantially activated by only heparin, HCII shows a ~1000–fold increase in activation in the presence of heparin, heparan sulfate and dermatan sulfate and several other types of polyanions such as

polysufates, polyphosphates, and polycarboxylates (Table 4). These agents function through the release of the RCL from in the partially inserted state to a fully exposed state.

Table 4. Second order rate constants of proteases inhibition by human HCII in the presence of various cofactors.[26,90]

Serpin	Target Proteases	Cofactor	Second order rate k_2 ($M^{-1}s^{-1}$)
HC-II	Thrombin	-	6×10^2
		UFH	5×10^6
		LMWH	5×10^6
		Dermatan sulfate (DS)	$\sim 5 \times 10^6$
		Hexasaccharide DS	10^7
		Chondroitin sulfate E	2×10^6
		Dextran sulfate	5×10^6
	Thrombin	Sucrose octasulfate	$\sim 10^6$
	Chymotrypsin	-	2×10^4
	Cathepsin	-	2×10^2

Heparin cofactor II-dermatan sulfate interactions

The inhibition of thrombin by HCII is accelerated nearly 1000-fold in the presence of DS. Though AT is structurally similar to HCII, with similarities in the heparin binding site, nevertheless heparin pentasaccharide DEFGH binds HCII poorly in comparison to its affinity for antithrombin.[91] Dermatan sulfate produces acceleration by a basic bridging mechanism, providing a template for HCII and thrombin to bind. Structurally, DS is a

linear polymer of D-glucuronic acid or iduronic acid alternating with *N*-acetyl–D-galactosamine residues. Like heparin, DS is heterogeneous as a result of a varying degree of O-sulfation and the two types of uronic acid residues.[92] Physiologically, dermatan sulfate is found in the vessel wall. The surface of fibroblasts and vascular smooth muscle cells generally contain dermatan sulfate proteoglycans. A subpopulation of oligosaccharides obtained by partial depolymerization of DS binds to HCII at physiological salt concentration. In a manner similar to heparin pentasaccharide H5, a distinct small fragment of dermatan sulfate binds with increased affinity to HCII. This hexasaccharide contains three L-iduronic acid (2-SO_3) *N*-acetyl D-galactosamine (4 and/or 6-SO_3) disaccharide units.[90]

Heparin cofactor II as a target

The DS-HCII system has number of important physiological roles. Unlike AT, HCII in the presence of heparin or dermatan sulfate is only activated towards thrombin inhibition. This unique specificity can be used to develop agents with reduced bleeding risks. HCII deficiency does not appear to enhance risk for thrombosis and at the same time it prevents arterial thrombosis. A major advantage of HCII activation is its ability to target clot-bound thrombin but not other coagulation proteases and its postulated that HCII contributes to ~20-30% of thrombin inhibition in coagulation, a feature not seen in AT.[90,91]

All these advantages point towards the development of HCII activators to produce an indirect pathway of coagulation regulation. Numerous attempts are now being made toward developing agents targeting HCII. Investigations include oversulfated dermatan

sulfate, chitosan polysulfate, fucoidan, clam dermatan sulfate, green algae sulfated polysaccharide and fucosylated chondroitin sulfate. Smaller oligosaccharides like sucrose octasulfate have also been recently identified as a HCII activator.[93]

1.3.2. Direct allosteric inhibitors

Direct inhibitors are generally agents, that target the catalytic triad located in the active site of serine proteases. However, with the growing knowledge and the discovery and understanding of other allosteric sites in the serine proteases, these sites are is now a subject of interest for designing agents, that could target these sites and thus inhibit the coagulation enzymes directly. The hypothesis behind this strategy is that the active sites of most serine proteases are quite similar, thus making it difficult to develop selective agents. Allosteric sites structurally however, are relatively different for these enzymes and could therefore be utilized in developing more selective agents. Additionally, controlled modulation of these enzymes through allosteric inhibition offers for lesser risks. Nevertheless a number of selective thrombin and FXa inhibitors have been discovered with few recently making it to the market.

Downstream targets

Direct thrombin and FXa inhibitors

Thrombin and FXa are the major downstream targets of various anticoagulant therapies. Structurally, these are quite similar enzymes and have a similar mechanism of action. Agents utilizing these targets are now slowly replacing unfractionated heparin (UFH) in the market.

Thrombin is a serine protease with a three dimensional structure similar to most serine proteases. Targeting thrombin directly produces a substantial degree of coagulation through additional prevention of thrombin-mediated feedback of factors FV, FVIII, FXI, and FXIII. Numerous crystal structures of both the native form and the co-crystallized form in the presence of an inhibitor have been deposited in the protein data bank (PDB). Thrombin could either be targeted at its active site or the two-polyanionic exosites and the Na^+ binding site, which serve as allosteric targets. Numerous agents have been discovered and/or designed that specifically target thrombin. Table 5 summarizes a list of these agents.

Directly inhibiting FXa is another approach, which is gaining popularity with many of these agents making it to the clinic recently. Directly targeting FXa has been hypothesized to be more effective then thrombin inhibition, due to the fact that one molecule of FXa is responsible for the generation of 1000 thrombin molecules.[94,95] Thus, regulation of thrombin production rather than inhibiting it also ensures that the natural clotting process post surgery can function more smoothly. Two new FXa inhibitors, rivaroxaban and apixaban have recently been approved for use clinically.[96-99]

Table 5. List of direct thrombin inhibitors.

Drug name	Binding site
Melagatran	Active site
Dabigatran	Active site
Hirugen	Exosite I
Bivalirudin	Exosite I

Direct agents, however, do not completely eliminate the risks observed with indirect agents. Risk of bleeding is a major complication in these agents, though the intensity is decreased to safer levels but not completely eliminated. Certain natural agents like hirudin have added problems like anaphylaxis while other agents produce liver toxicity. Thus, the current challenge to overcome in the design of these agents involves eliminating bleeding risk, liver toxicity and histamine release, while maintaining good oral bioavailability and duration of action.

Novel upstream targets

Major bleeding risks have led to the hypothesis that utilizing an upstream enzyme could produce controlled inhibition without producing the deleterious effects of other stronger downstream agents. Targeting upstream enzymes from the intrinsic pathway, particularly FXIa, has been postulated to potentially achieve a safer degree of anticoagulation.

Structure and function of FXIa

FXIa is a major player in the intrinsic pathway. It is involved in the activation of FIX to FIXa, which eventually activates FX to FXa. The crystal structure of its zymogen form, FXI, and the catalytic domain of its active form (FXIa) have been solved, thereby providing insights into the overall structure and working of this enzyme. Physiologically, it exists as a homodimer linked by a disulfide bond, with each monomer consisting of 607 amino acid residues. Its three dimensional structure is analogous to a cup and saucer arrangement with the catalytic domain surrounded by four apple domains (Figure 10). These are responsible for the recognition of FIX in the coagulation cascade in addition to

heparan sulfate, GPIb and other ligands. Like thrombin and FXa, FXIa also consists of a heparin-binding site in the A3 apple domain, and strikingly another heparin binding site in the catalytic domain.[100-102]

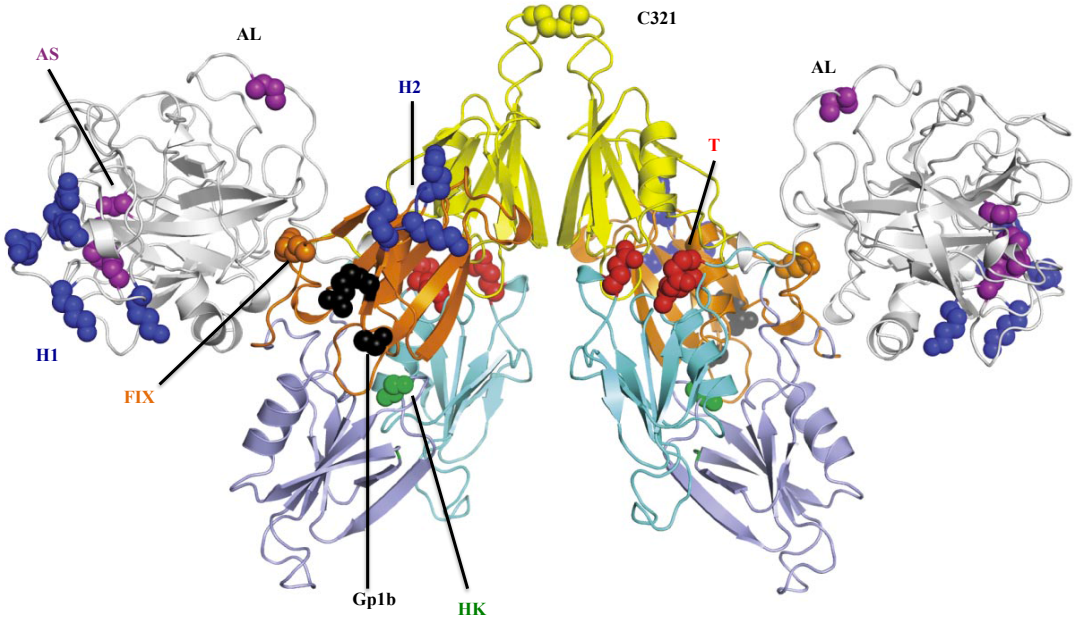

Figure 10. The structure of zymogen FXI. The catalytic domain is in white. Sites of residues implicated in ligand binding are red for thrombin (T), green for HK, black for GPIb, blue for heparin sites (H1 and H2), and orange for FIX. Positions for the activation loop (AL) cleavage site (Arg360-Ile370) residue Ile370 and active site (AS) residues Ser557, Asp462, and His413 are shown in purple. (Figure adapted from Reference 94)

Targeting FXIa

The utility of FXIa as a drug target has been revealed by a number of *in vitro* models of coagulation. Additionally, studies on its deficiency in humans and in animal models of thrombosis and hemostasis has further supported the claim that it could indeed serve as a safer target to modulate the coagulation system. In vitro studies have measured the action of FXIa on both the extrinsic and the intrinsic pathways by utilizing the PT and the APTT assays respectively. These studies displayed the importance of FXIa in the

intrinsic pathway, where FXIa inhibition affected clot formation in the APTT assay. This further supports the inference that FXIa is more essential in the amplification than in the initiation of coagulation.[103,104] FXI deficiency, which is seen in a condition called hemophilia C, generally observed in the Ashkenazi Jews, was found to show minor risk to bleeding. Bleeding in this condition was only seen on occurrence in response to surgery or trauma, however in women the deficiency did not affect pregnancy or delivery. This, indicates that FXI is more important in conditions of thrombosis and does not necessarily affect hemostasis.[105-107] The occurrence of ischemic stroke was found to be significantly reduced in FXI-deficient patients.[108] Genetic studies in mice have demonstrated that FXI-null mice do not develop clots in $FeCl_3$-induced carotid artery model, additionally showing no effect on bleeding time.[109] These observations, validate the use of FXIa inhibition as a target to develop anticoagulants.

FXIa inhibition as an anticoagulant target is a rather new premise, with a review of literature revealing of very few molecules targeting this enzyme. These are arginine-containing acyclic peptidomimetics, guanidine-containing arylboronic acid and natural products like clavatadines A and B, β-lactam derivatives, and amidine containing macrocyclic indoles.[104,110-115] All of these recognize residue in the catalytic triad of FXIa active site. However, there exist minute differences in the active sites of various serine proteases and thus the advent of allosteric site inhibitors. Two heparin binding site exist on FXIa as mentioned earlier, with the one on the catalytic domain showing a 100–fold greater affinity and an allosteric mechanism of action, whereas the one in the A3 domain is postulated to have a more template based mechanism (Figure 10).[116,117] These could be

targeted to develop allosteric inhibitors of FXIa, with the potential advantage that the heparin-binding site of all serine proteases is structurally different and thus allows for use of these differences in developing selective agents.[103]

CHAPTER 2: RATIONALE

Allostery involves conformational and functional transitions in individual protein molecules.[1] In a more classic sense, molecules, which function in this fashion are based on the principle of influencing the activity of an enzyme by binding to a site remote from the active site of the enzymes. Numerous reports of systems functioning by this route have been reported and well studied.

Glycosaminoglycans (GAGs) have been subjected to extensive studies because of their prevalence in nature. Numerous functions have been sustained by the plethora of protein-GAG interactions, which have been recognized and continue, to be, identified thereby propelling our understanding of this complex yet highly important system of interactions. A majority of this study is focused on protein interactions with heparin. The steady commercial availability of heparin and its use in fractionation and heparin-sepharose affinity chromatography make it a well-studied polymer. The presence of heparan sulfate in cells and their subsequent interactions in numerous physiologically relevant interactions has also garnered interest. The importance of heparin in the coagulation system has been a hot topic for research with the advent of heparin as one of the earliest anticoagulants and it continues to be utilized at present.

The anticoagulant effect of heparin led to widespread studies aimed at deciphering the mechanistic and structural aspects of this interaction. The antithrombin-heparin interaction can now be considered the paradigm for studying GAG-protein allosteric

interactions. Studies indicated the mechanism with which heparin interacts with AT to be a conformational/bridging based interaction. Similarly, a number of serine proteases have been reported to possess a highly positive heparin-binding site, including FXa, thrombin, FXIa and FIXa.

The complexity of heparin interactions with proteins and the resulting functions it alters can be attributed to the phenomenal structural diversity in heparin polymers and their sulfation pattern. Numerous efforts have been made to reduce this complexity through the identification of smaller more defined units. The heparin pentasaccharide has been the most notable example of a highly specific unit with well-studied interactions. However, the interactions of heparin with other serpins like HCII and serine proteases like thrombin, FXa and FXIa have not been thoroughly understood. Numerous research efforts have therefore been employed to obtain a comprehensive understanding of both the mechanistic and structural diversity of heparin.

The rationale of the current work is based on improving our understanding of this incidence. The studies address two questions:

1. **Can computational strategies be devised to exploit the structural diversity of heparin sulfate in activating serpins.**
2. **Can allosteric sulfated quinazolin-4(3H)-ones be developed as more potent inhibitors of FXIa?**

These questions have been approached through two projects addressing question 1 and one project addressing question 2.

a. Novel hexasaccharide based activators of heparin cofactor II and antithrombin (Discussed in chapter 3)
b. Differential recognition of coagulation proteins by a heparan sulfate containing 2-*O*-sulfated glucuronic acid (Discussed in chapter 4)

The goal of both these projects was to develop computational strategies that could utilize the structural information for the proteins efficiently to recognize sequences with high affinity and specificity. This was followed by an experimental validation. Project 1a, involves the computational design of heparin-based hexasaccharide sequences followed by the selection of high affinity and specificity structures through the dual-element algorithm developed in our laboratory. The algorithm helped recognized two specific sequences, which could be utilized as novel dual activators of HCII and AT.

Project 1b takes into account the structural enormity of the heparan sulfate disaccharide library and utilizes very rare sequences indicated to be of high interests through our computational studies and further reported occurrences and mechanistic evaluations. This is followed by the enzymatic synthesis of a polymer rich in the rare disaccharide sequence and its mechanistic evaluation. The questions answered through the evaluation could help unearth newer interaction in addition to understanding the structure prevalence in nature.

Question 2 utilizes a completely different approach at selectively targeting the heparin-binding site in FXIa. FXIa, which belongs to the intrinsic coagulation pathway, has been increasingly recognized as a safe alternative to other downstream targets. The active site of serine proteases is conserved and is comprised of a catalytic triad making it

difficult to design selective agents by targeting specific differences in the active site. The heparin binding sites of such proteins are decorated with positively charged arginine/lysine residues, however the hydrophobic domain bordering these have been hypothesized to be different. We therefore utilized the dual element strategy, using a molecular design containing an electrostatic element and a hydrophobic moiety. The electrostatic moiety should recognize the heparin-binding site, the hydrophobic moiety could be used to identify complementary binding sites, that selectively target a specific protein. Our approach has been deemed successful through the synthesis and identification of sulfated quinazolinone dimers. We further this approach through the identification of more potent and selective agents, while utilizing these advances to gain a mechanistic understanding of these molecules.

CHAPTER 3: NOVEL HEXASACCHARIDE BASED ACTIVATORS OF HEPARIN COFACTOR II AND ANTITHROMBIN.

3.1. INTRODUCTION

GAGs have been ubiquitously found in nature.[118,119] Structurally, these are polymers of alternating glycosamine and uronic acid residues, which are irregularly decorated along the chain with either sulfates or acetate moieties. Heparan sulfate, chondroitin sulfate, dermatan sulfate and hyaluronan comprise the most prevalent GAGs found in nature in addition to numerous other GAGs localized in various tissues. These are increasingly being recognized to play critical roles in many biological processes, including hemostasis, growth and differentiation, immune responses and pathogen invasion.[120-123] A phenomenonal structural diversity exists among the GAGs and these are introduced in a spatiotemporal fashion by utilizing a template-free arsenal of 16 enzyme isoforms.[122]

Heparan sulfate and heparin, which reportedly are the most extensively studied, are primarily composed of alternating 1→4 linked uronic acid and glucosamine residues that are decorated with sulfate and *N*-acetyl groups. Theoretically, 96 different disaccharide sequences are possible for H/HS arising from uronic acid (UA*p*) residues that can bear either an –OH or a $–OSO_3^-$ group at their 2- and 3-positions and glucosamine (GlcN*p*) residues that may contain either an –OH or $-OSO_3^-$ group at their 3- and 6-positions, as well as either an $–NH_3^+$, $–NHSO_3^-$ or –NHAc group at its 2-position. However, only 23 sequences have been identified in nature.[124] The structural

complexity is demonstrated by a simple calculation where 0.8 billion distinct sequences are possible for a HS oligomer containing six repeating disaccharide units. For a hexapeptide this number is 64 million, while a hexanucleotide could be one of the 4096 sequences.[125] Further complications arise from the conformational variability of the iduronic acid (IdoA*p*) residues, which exist in multiple forms of which $^{1}C_{4}$ and $^{2}S_{0}$ are usually preferred.[126] These combinations of structural and conformational possibilities make GAGs a very difficult prospect to study.

Computational analysis might serve as a powerful approach to the complex protein-GAG interactions. However, this is not a straightforward approach with the polyanionic nature and the poor surface complementarity posing major obstacles.[127] However, our recent efforts have yielded a combinatorial virtual library screening (CVLS) approach, which utilizes the genetic algorithm-based automated docking program GOLD.[91,128] The technique was efficiently utilized in recognizing the binding mode of heparin pentasaccharide, which is consistent with that seen in the crystal structure.[129] The success of this approach for this pair suggests its utility in similar systems.

Out of contrast to the vast heparin structural diversity, the heparin pentasaccharide sequence is the only one that targets AT with a higher specificity. This sequence has been extensively studied and numerous structural activity relationships have been performed to recognize the features essential for its specificity to AT and the resultant activation. Similarly, heparin cofactor II has been studied widely, due to its structural and functional similarity to AT and the possible advantages it offers in terms of its safety and selectivity profile.[86,88,92] An alternative oligosaccharide sequence can similarly be devised for this

serpin too. With this in view, studies conducted reported a hexasaccharide sequence as the minimal moiety required to interact with HCII.[92,130] Further, studies however fail to register the same level activation for this system.[130] The concept however has attracted a flurry of research aimed towards identifying such a sequence. The CVLS approach could serve as good starting point to identify such sequences for the HCII-dermatan sulfate system in a manner akin to the AT-heparin pentasaccharide system. However, the syntheses of simple oligosaccharides have been found to be a painstaking process, which incorporates numerous steps.[16,131-133] Consequently, in this work we have utilized our computational approach and successfully identified sequences with the potential to be utilized as an anticoagulant functioning through the unique HCII-thrombin system in addition to the AT-FXa system.

3.2. RESULTS

3.2.1. Computational studies (Work performed by Drs. Raghuraman, Mosier and Sankaranarayanan)

Structure of the Activated Form of Heparin Cofactor II

Two experimentally determined structures of heparin cofactor II are available, native and S195A thrombin-complexed.[29] The overall structure of native HCII is similar to that of native antithrombin. Superposition of the structure of native HCII on that of native antithrombin (PDB file: 2ant)[25] gives a RMSD of 1.8 Å for 352 equivalent C^{α} atoms (not shown). Likewise, superposition of C^{α} atoms of the residues that define the heparin-binding site in antithrombin, i.e., Arg46, Arg47, Lys114, Lys125, Arg129, Arg132 and

Lys133, with corresponding residues in heparin cofactor II results in a RMSD of 1.5 Å indicating a high degree of similarity between the two native serpins.

The structure of GAG-activated heparin cofactor II is not available as yet. However, the structure of the serpin in complex with S195A thrombin displays extensive similarities with that of the heparin pentasaccharide-activated antithrombin (Figure 11). The S195A thrombin-complexed HCII shows an expelled reactive center loop (RCL), as found in pentasaccharide-activated antithrombin.[22,134] The reason for the expulsion of the RCL appears to be the extensive exosite interactions that the RCL makes with S195A thrombin. Likewise, exosite interactions also stabilize the heparin-induced, conformationally activated antithrombin, as borne out in experiments with factor Xa and factor IXa, its conformational activation targets.[42,135] Thus, the overall structure of HCII in the S195A thrombin-complexed state is similar to that of the pentasaccharide-activated antithrombin.

Further evidence that these forms are nearly identical comes from the superposition of the corresponding C^{α} atoms. Figure 11 shows the superimposed activated forms of the two serpins. The RMSD in C^{α} atoms of the core amino acid residues was found to be 2.4 Å suggesting significant similarity in the orientation of most structural domains including β-sheets and helices. More importantly, the RMSD for corresponding basic residues in helices A and D was found to be 1.5 Å indicating a high degree of similarity between the two activated forms in this region. These structural similarities indicate that the S195A thrombin-complexed HCII is likely to be the H/HS-activated form of the serpin.

However, differences exist between the two activated serpins in the relative orientation of helices A and D, and in the extension of RCL. Whereas A helices (hA) superpose nearly completely, the D helices (hD) display a significant ~30° angle between the two serpins (Figure 11). Likewise, the RCL in the activated forms show a significantly greater extension of the loop in the S195A thrombin-complexed HCII than in the pentasaccharide-activated AT (Figure 11). In addition, helix D of heparin cofactor II contains an additional electropositive residue, Arg184, which has no counterpart in antithrombin. Thus, although the two serpins in their native and activated forms are nearly equivalent, subtle differences are evident. Despite these differences, the S195A thrombin complexed HCII structure is very similar to the pentasaccharide-activated AT structure and is a good model for investigation of H/HS interactions, especially considering that the structure of GAG-activated HCII is unknown.

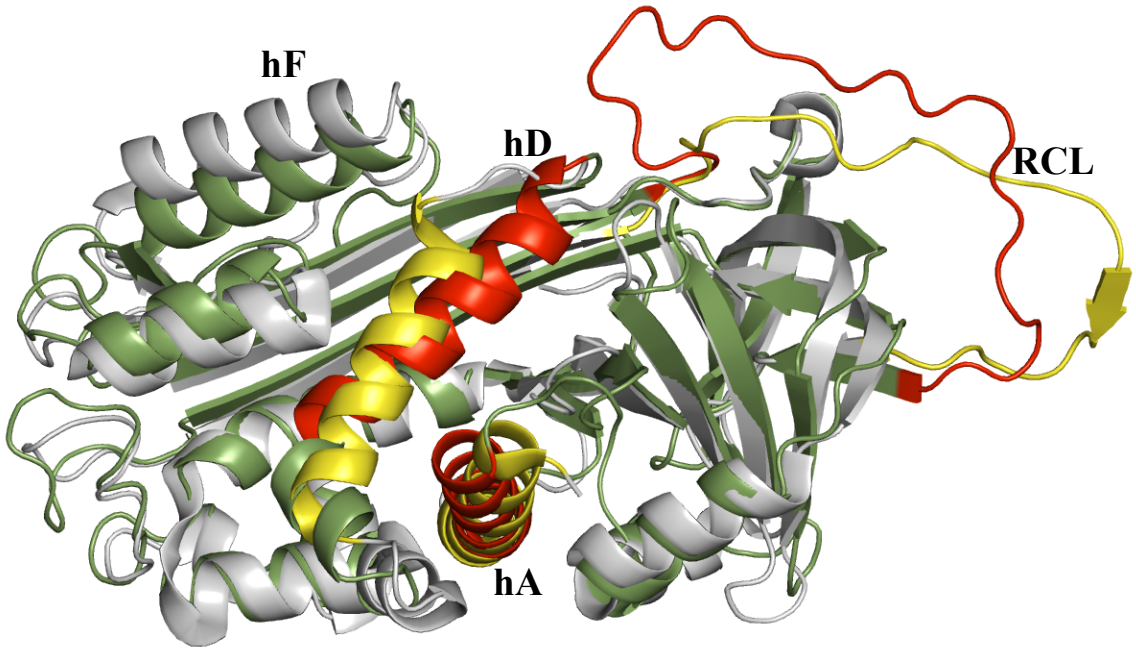

Figure 11. Comparison of the structure of S195A thrombin-complexed heparin cofactor II with heparin pentasaccharide activated antithrombin. Core polypeptide sequences, devoid of residues of the *N*-terminus and the RCL, were to give an overall RMSD of 2.4 Å. Note the small rotational difference in helix D axis and at the *N*-terminal end of helix A between the two proteins, while the expulsion of RCL in heparin cofactor II is much greater than that in antithrombin. Antithrombin ribbon is shown in green and red (hD, hA and RCL), while HCII is shown in gray and yellow (hD, hA and RCL).

Filtering of sub-optimal HS sequences from a library of 46,656 sequences

Computational docking approaches represent a powerful means of assessing binding affinity, specificity and binding geometry. Yet, modeling GAGs is challenging because the high negative charge density tends to induce false positive recognition. In addition, most GAG-binding sites on proteins are surface–exposed and shallow, which encourage poor complementarity.[136-142] Our previous CVLS protocol was applied to a small library of H/HS sequences (~7,000 sequences) and screened a limited domain of 3D space to assess 'specificity' of binding.[128] However, the repertoire of nature's sequences is huge,

of which the majority are never studied rigorously. Recently, we have designed a robust genetic algorithm-based combinatorial virtual library screening approach that utilizes a dual-filter process to identify hexasaccharide sequences in heparin that recognize antithrombin with high specificity. This sequential dual-filter algorithm utilizes GOLD score, a measure of 'affinity', as the first filter, followed by convergence of binding geometries, a measure of 'specificity', as the second (Figure 12).

In the present study with heparin cofactor II, we used a comprehensive library of HS hexasaccharide sequences built from all of the 23 disaccharide building blocks reported to date (Figure 13B). To address the conformational variability possible in IdoA*p* residues, two major ground state conformers $^{1}C_{4}$ and $^{2}S_{O}$, were explicitly modeled, increasing the number of building blocks to 36 to give a library of 36^{3} = 46,656 hexasaccharide sequences. The H/HS binding site in activated heparin cofactor II was defined to include the domain formed by helices A and D and the polypeptide *N*-terminus.[29]

GOLD-based docking, with 10,000 iterations and 10 GA evaluations, of the 46,656 hexasaccharides was carried out to identify sequences with good HCII recognition. Figure 14 displays the histogram of GOLD scores. The profile is Gaussian, showing that a majority of HS sequences (83.5%) bind heparin cofactor II with average GOLD score (30–80 units). Nearly 15.7 % of sequences bind poorly (GOLD score below 30 units), while 0.8 % hexasaccharides recognize the serpin with high GOLD scores between 80 to 106 units. This included 2 sequences with GOLD score higher than 100 and 45 sequences with score between 90 and 100 units. In comparison to the heparin–

antithrombin system[128], these overall GOLD scores are approximately 20 to 30 units lower suggesting that the affinity of HS hexasaccharides for heparin cofactor II may be lower than that for pentasaccharide binding to antithrombin. We chose 47 sequences (the top 0.1%) as candidates for the convergence ('specificity') test (not shown).

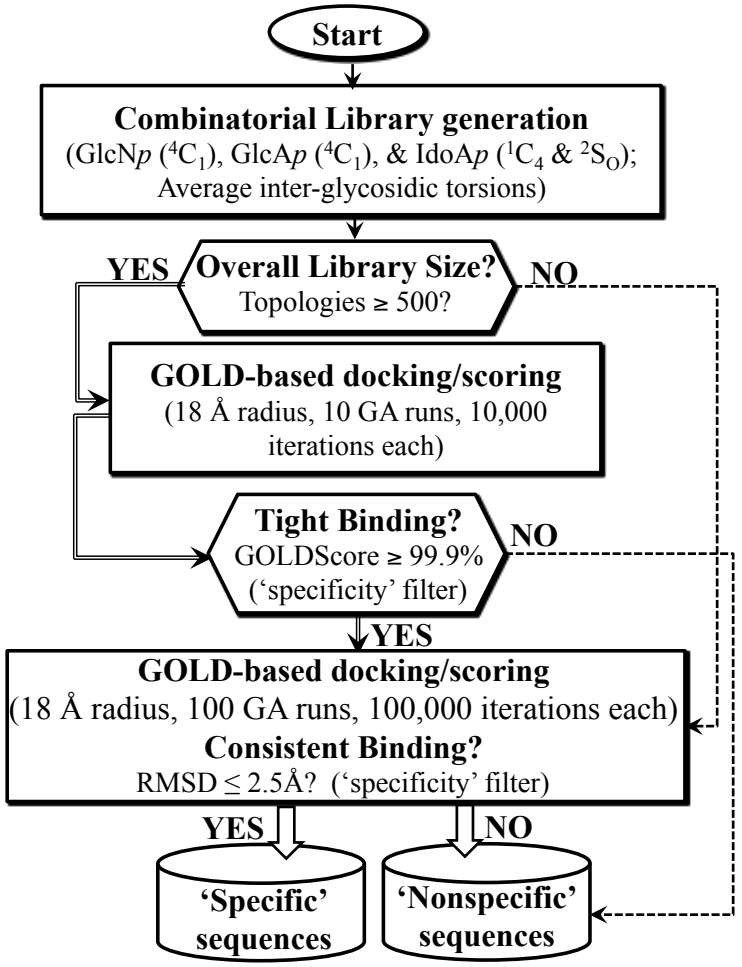

Figure 12. Dual-filter algorithm used to screen a combinatorial library of 46,656 H/HS hexasaccharide sequences. The hexasaccharide library was built from 36 naturally occurring disaccharide building blocks using the average backbone model and screened using two filters, an 'affinity' filter and a 'specificity' filter. The affinity filter corresponded to a GOLD score in the top 0.1% or less hexasaccharide sequences, while the specificity filter corresponded to reproducibility of binding geometries in successive experiments to within RMSD of less than 2.5 Å. See Experimental Section for details.

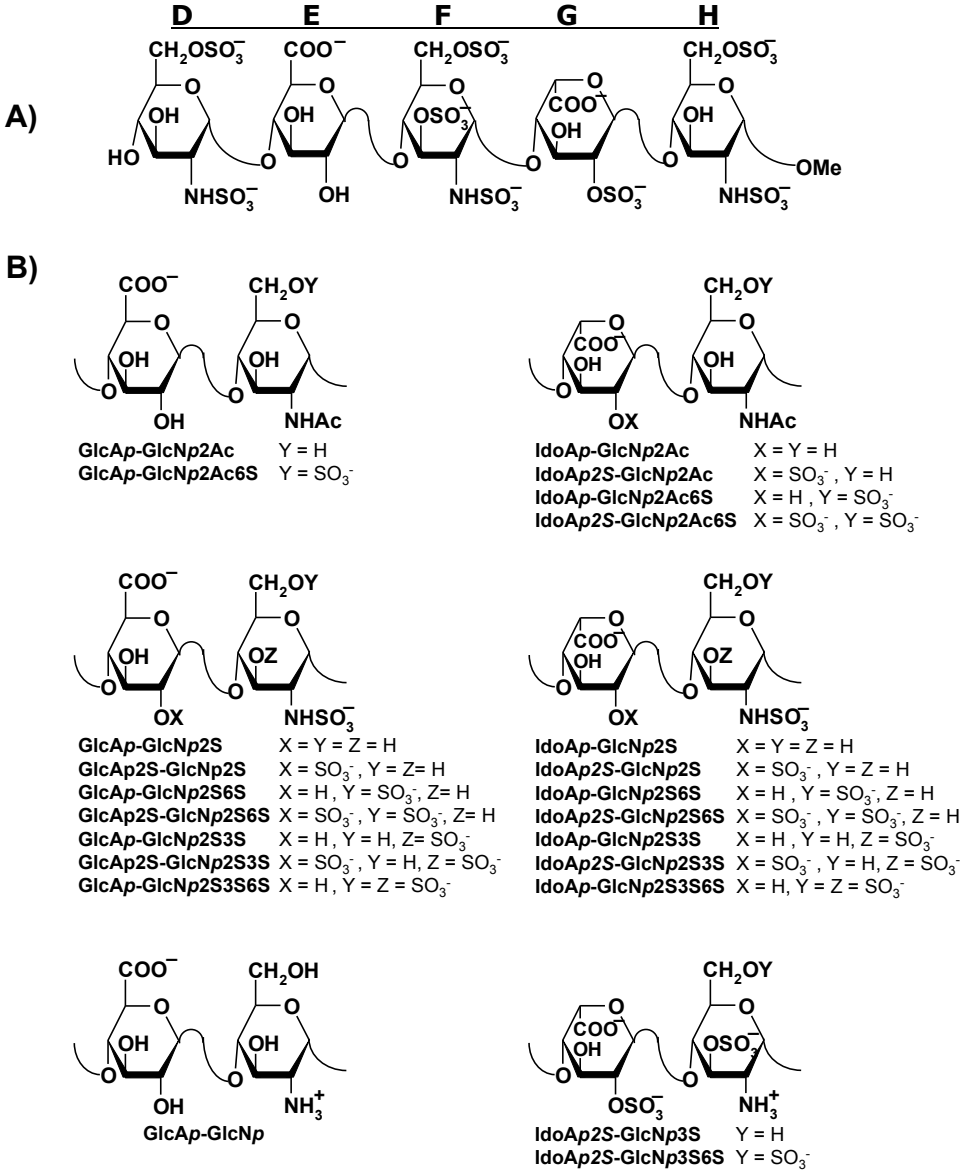

Figure 13. Structure of high-affinity heparin pentasaccharide (A) and naturally occurring disaccharide building blocks used in the construction of combinatorial virtual library (B). Heparin pentasaccharide DEFGH (A) binds antithrombin with high-affinity and high specificity, yet does not recognize heparin cofactor II. Disaccharide building blocks used in the combinatorial library construction (B) include GlcA*p* disaccharides on the left and IdoA*p* disaccharides on the right. X represents substitution possible on the 2-position of uronic acid residue, while Y and Z represent that on the 3- and 6-positions of the glucosamine residue, respectively. Ten GlcA*p*- and 13 IdoA*p*-containing disaccharides are found in nature, respectively, of which the IdoA*p* residue can either be $^{1}C_{4}$ or the $^{2}S_{O}$ form, thus giving a total of 36 disaccharide building blocks.

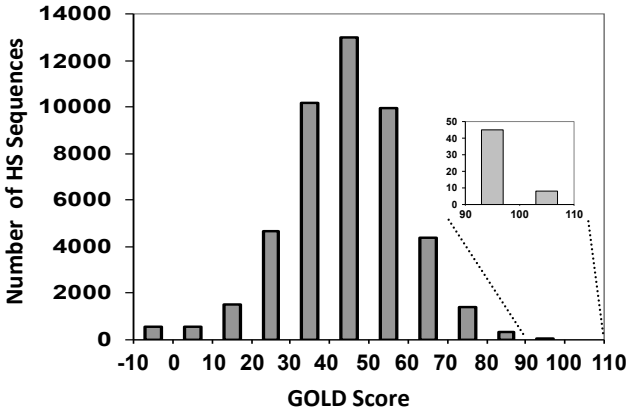

Figure 14. Histogram of number of HS hexasaccharide sequences for every 10 unit change in GOLD score. Modified GOLD score was calculated for all 46,656 hexasaccharides docked onto heparin cofactor II following the first phase of combinatorial library screening. Inset shows an expanded portion of the histogram in the range 90–110 GOLD score units.

Structural Features of the 'High-Affinity' HS Hexasaccharides

Structural analysis of the sequences identified through the 'affinity' filter reveals interesting insight into recognition of heparin cofactor II. Of the 47 hexasaccharides, only 4 carry the maximal possible sulfation load of 9 groups, while the library contains a total of 1728 sequences with the maximum load. This suggests that the majority of the high-affinity sequences are not highly sulfated. It also suggests that the GOLD fitness function does not arbitrarily select for higher sulfation level, although the binding site in heparin cofactor II is highly electropositive. The GOLD fitness function is driven by hydrogen bond and van der Waals' potential functions only, and not by Coulombic interactions, making it particularly suited for weeding out GAG structures with low complementarity. The 8 topologies corresponding to the common heparin hexasaccharide sequence, [IdoA*p*2S-GlcN*p*2S6S]$_3$, which also carry 9 sulfate groups, have GOLD scores in the

range of –2.7 to 66.4 units, suggesting that these sequences recognize heparin cofactor II with poor affinity. These results are consistent with solution experiments with heterogeneous, polydisperse heparin sample that show poor heparin cofactor II affinity in the range of 45–140 mM.[143-145]

The ratio of IdoA*p* and GlcA*p* containing disaccharides in our combinatorial library was 2.6:1, while it was found to be 1.2:1 in the 47 hexasaccharides. This implies a significant enrichment of GlcA*p*-residues. Additionally, the 47 identified hits do not contain the hexasaccharide sequences related to the high-affinity pentasaccharide (IdoA*p*2S [$^{2}S_{O}/^{1}C_{4}$]-GlcN*p*2S6S-GlcA*p*-GlcN*p*2S3S6S-IdoA*p*2S [$^{2}S_{O}/^{1}C_{4}$]-GlcN*p*2S6S), which were found to have GOLD scores in the range of 50–54. This result is also consistent with Maimone and Tollefsen, who have shown that heparin molecules with or without the high-affinity antithrombin-binding pentasaccharide sequence equally activate HCII.[130]

Finding Needle(s) in the Haystack: Only two HS hexasaccharides are predicted to recognize heparin cofactor II with high-specificity.

The convergence ('specificity') filter used in our dual-filter algorithm is a robust strategy to identify sequences that possess exceptional complementarity to the receptor. This filter utilizes 3 experiments of 100 GA runs each, in which each GA run is allowed to evolve over 100,000 iterations, resulting in 6 final binding geometries. Binding is deemed to be specific if the RMSD among these geometries is ≤ 2.5 Å. Of the 47 sequences that were subjected to this stringent criterion, only 2 sequences (**HX1** and **HX2**) were found to recognize activated heparin cofactor II with high specificity (Figure 15A).

Several points about the structure of these two hexasaccharide sequences are striking. None of the GlcN*p* residues have an acetyl group at the 2-position. This is striking because natural heparan sulfate consists of nearly 50–60 % GlcN*p*2Ac residues.[146,147] The total number of sulfate groups in these sequences are 8 (**HX1**) and 7 (**HX2**). This averages to about 2 to 3 sulfate groups per disaccharide sequence. In contrast, the degree of sulfation of human liver HS was found to be 1.2, while that of porcine liver HS and porcine intestinal heparin was found to be 1.0 and 2.6, respectively.[146,148] Thus, these sequences are significantly more sulfated than natural HS, but either equal to or slightly less sulfated in comparison to natural heparin. Yet, these sequences are not heparin-like because the IdoA*p* composition is 0.0% whereas for heparin, it is > 80%.[122,149]

Significance of Our Two Step Approach of Identifying Potential HCII-Binding HS Sequences

The identification of the 2 "high-specificity" HS hexasaccharides is based upon the geometry convergence of 47 top-scoring sequences that comprised 0.1 % of all hexasaccharides in the virtual HS library. Yet, it is possible that some of the filtered sequences from the first affinity screen may have been false negatives due to pre-termination of the genetic algorithm or insufficient number of iterations (see 'Experimental Section'). In other words, putting these filtered sequences through the more robust, but time-consuming geometric convergence test may reveal additional "high-affinity" sequences.

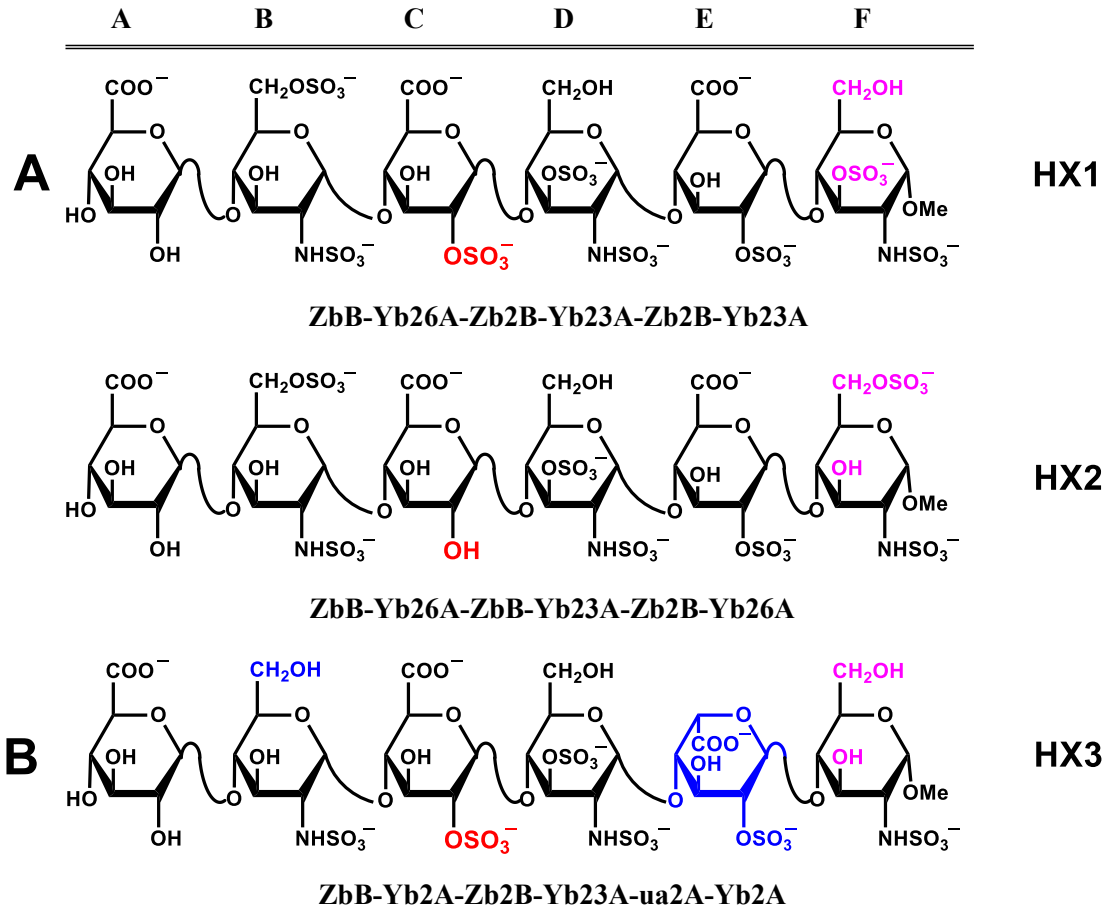

Figure 15. Structures of HS hexasaccharide sequences A) HX1 and HX2, which are predicted to recognize heparin cofactor II with 'high affinity-high specificity' and B) HX3 'high affinity' sequence. A) Sequences HX1 and HX2 are predicted to bind HCII with *'high affinity-high specificity'* from the combinatorial virtual library screening. These sequences have almost 85% of similar residues. The major difference in the sequence is with the position of sulfation at residue C (red) and F (magenta). Each sequence contains more than one residue that is rarely found in naturally occurring heparan sulfate, including GlcA*p*2S and GlcN*p*2S3S. See text for details. B) Sequence HX3 which was predicted to bind HCII with 'high affinity' from the critical analysis of CVLS. But this sequence failed at the second filter ('specificity'). This sequence had IdoA*p* containing disaccharide (blue). See text for details. For naming conventions of hexasaccharides see Appendix A.

To test if potential high-affinity HS sequences may be present in the set of HS sequences that did not pass the affinity test, we randomly choose 47 of these sequences, 5 from each of the 10 histograms bins in Figure 14, and subject them to the geometry

convergence test. Our results revealed that only one (**HX3**) of the 50 sequences passed the test. This sequence had an IdoA*p* containing disaccharide (Figure 15B). Additionally, the binding mode of this sequence is approximately 15-20° away from the 'high specificity' sequences. The calculation of RMSD for this sequence (**HX3**) (for triplicate runs) was >2.5Å (Figure 16A). This result suggests that our two-step docking approach is well suited to eliminate false positives; it is unlikely that false negative solutions have been overlooked.

Docking of 'high specificity' and 'high affinity' sequences with other serpins and Coagulation enzymes

The 2 "high-specificity" HS hexasaccharide sequence from our dual filter algorithm and one 'high affinity' sequence obtained from critical analysis of the first filter were used for further docking with other serpins and coagulation enzymes. Since the binding site of both HCII and AT results in a RMSD of 1.5 Å indicating a high degree of similarity between the two native serpins, all three sequences were docked in triplicate to the crystal structure of AT (PDB ID: 1TB6)[134] which resulted in 6 solutions for each of the sequence. The application of 'specificity' filter to these solutions yields an RMSD >2.5Å for all 3 sequences (**HX1to HX3**) (Figure 16A). Further in order to check whether these sequences were similar in binding to other serpins and coagulation enzymes, the same triplicate docking was done for these 3 sequences. The molecular docking was carried out for serpins like alpha-1-antitrypsin (α1-PI) (PDB ID: 1EZX),[34] plasminogen activator inhibitor-1(PAI1) (PDB ID: 1B3K),[150] protein C inhibitor (PCI) (3DY0)[151] and Protease Nexin-1(PN1) (PDB ID: 4DY0)[152] and the coagulation enzymes like thrombin (TH)

(PDB ID: 1XMN),[137] factor IXa (FIXa) (PDB ID: 3KCG),[153] factor Xa(FXa) (PDB ID: 2GD4)[154] and factor XIa(FXIa) (PDB ID: 2F83).[102] The RMSD analysis of these docked sequences showed that the 'highly specific' sequences (**HX1 and HX2**) of HCII were completely non-specific in recognition to both serpins and coagulation enzymes (Figure 16). Similarly the high affinity sequence (**HX3**) was also found to be non-specific in recognition. This result suggests that the sequences **HX1** and **HX2** are 'highly specific' in HCII recognition.

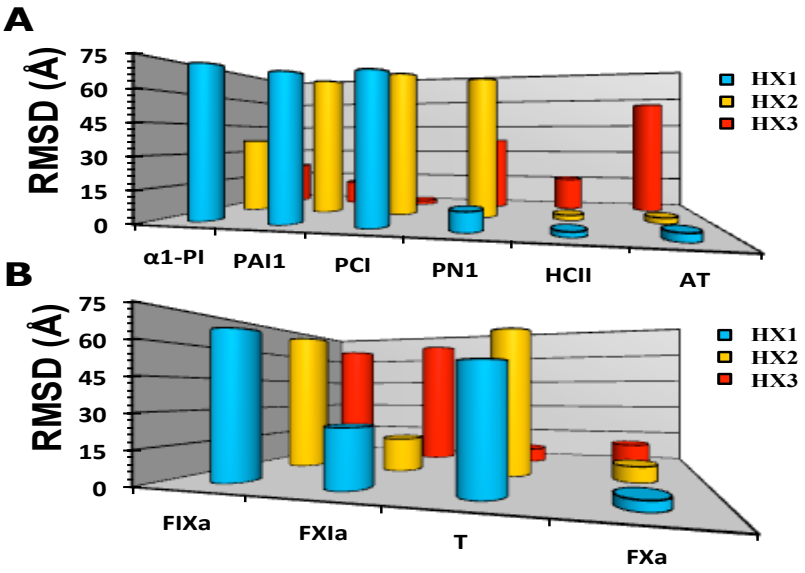

Figure 16. RMSD plot for the 3 specific sequences A) with serpins and B) with Coagulation enzymes.

Molecular Interaction Profile of the two Predicted 'High-Affinity, High-Specificity' Sequences

Both the sequences bind activated HCII in an essentially identical orientation with the non-reducing end recognizing helix A, while the reducing end is oriented toward the *C*-terminus of helix D (Figure 17A and Figure 18A). This suggests good specificity in the recognition of activated HCII. In fact, a RMSD of 0.9 Å is found for backbone atoms of

the central tetrasaccharide BCDE among the highest scoring docked solutions for each sequence, which increases to 2.5 Å, if one considers the backbone atoms of all six residues. Both **HX1** and **HX2** sequences strongly hydrogen bond to activated HCII. The HS hexasaccharides orient at a ~60° angle relative to the axis of helix D. This alignment is significantly different from heparin pentasaccharide binding to antithrombin, which orients almost parallel to the axis of helix D.[22,134] When both **HX1** and **HX2** were docked to antithrombin they bind ~10° relative to heparin pentasaccharide sequence (Figure 17B and Figure 18B). The hexasaccharide sequences **HX1** and **HX2** forms a strong hydrogen bond with residues, Arg103, Arg184, Lys185, His188, Arg192 and Arg464 (Figure 19). Closer inspection of interaction at the atomic level reveals that the high scoring residues – Arg464, Arg184 and Arg192 – form multi-valent hydrogen bonds. Specifically, Arg464 forms 3 strong hydrogen bonds, two with the B_{2S} group and one with the C_{2S} group, Arg184 forms 2 hydrogen bonds with the D_{2S} and E_{2S} groups, while Arg192 forms 1 – 2 hydrogen bonds with F_{3S} group. Together these four sulfate groups on the GAG are responsible for over 85% of the calculated hydrogen bonds. This analysis suggests that a core, conserved tetrasaccharide BCDE with the minimal sequence GlcN*p*2S—GlcA*p*2S—GlcN*p*2S—GlcA*p*2S appears to be critical for high-affinity, high-specificity binding to activated heparin cofactor II. Additionally, sulfation at 3 positions in residue D, introduces additional interactions with Lys185, respectively.

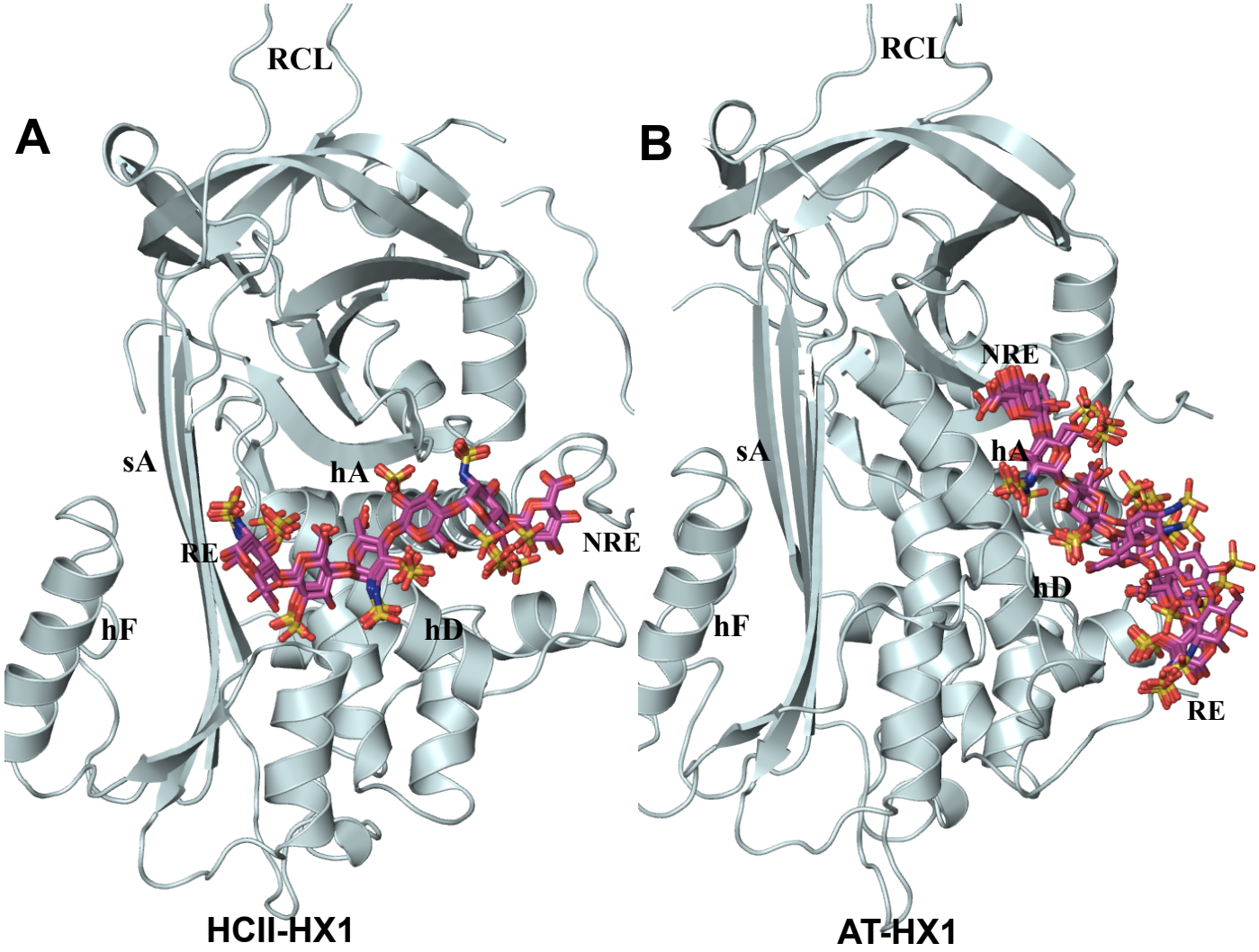

Figure 17. Overlay of **HX1** on HCII and AT.

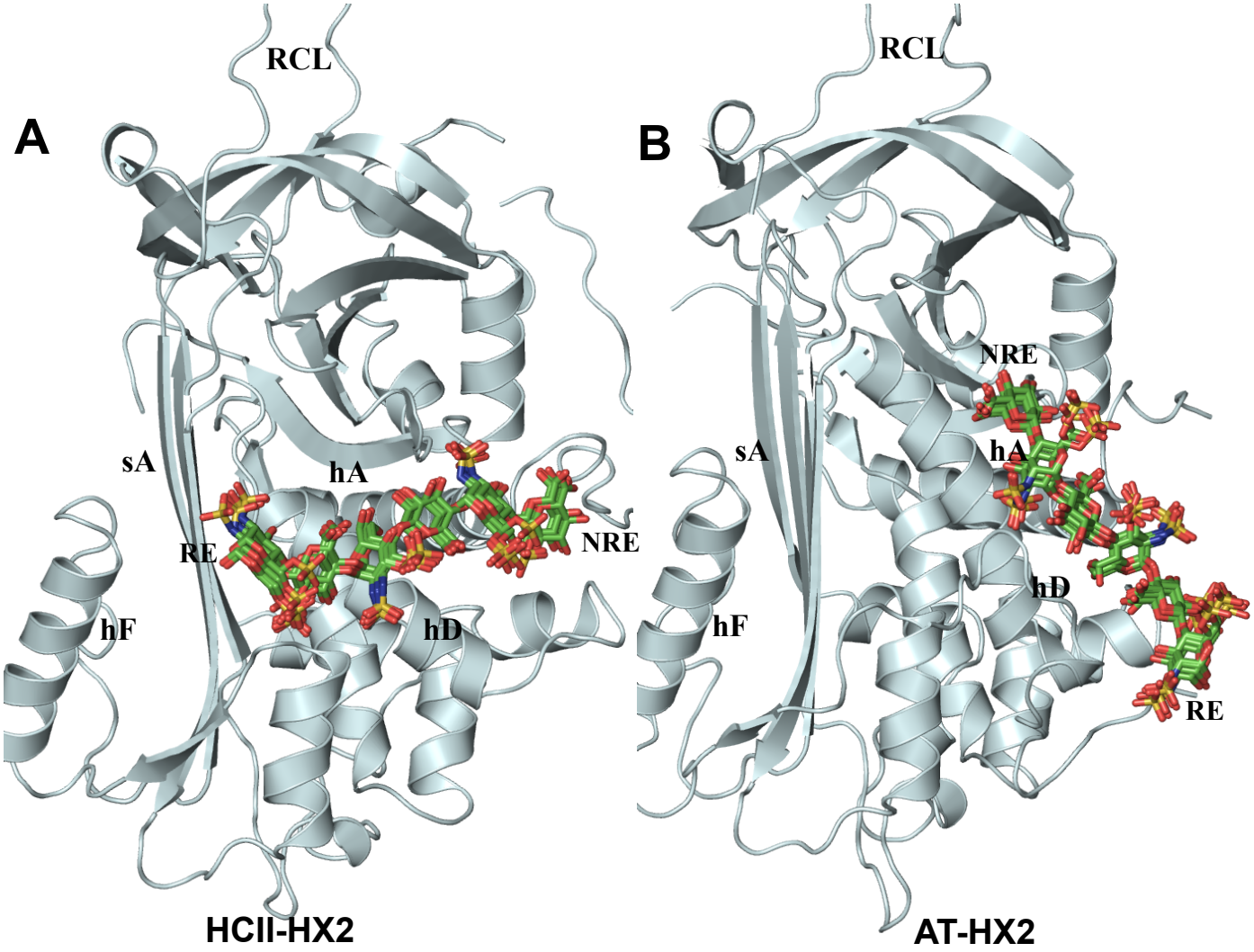

Figure 18. Overlay of **HX2** on HCII and AT.

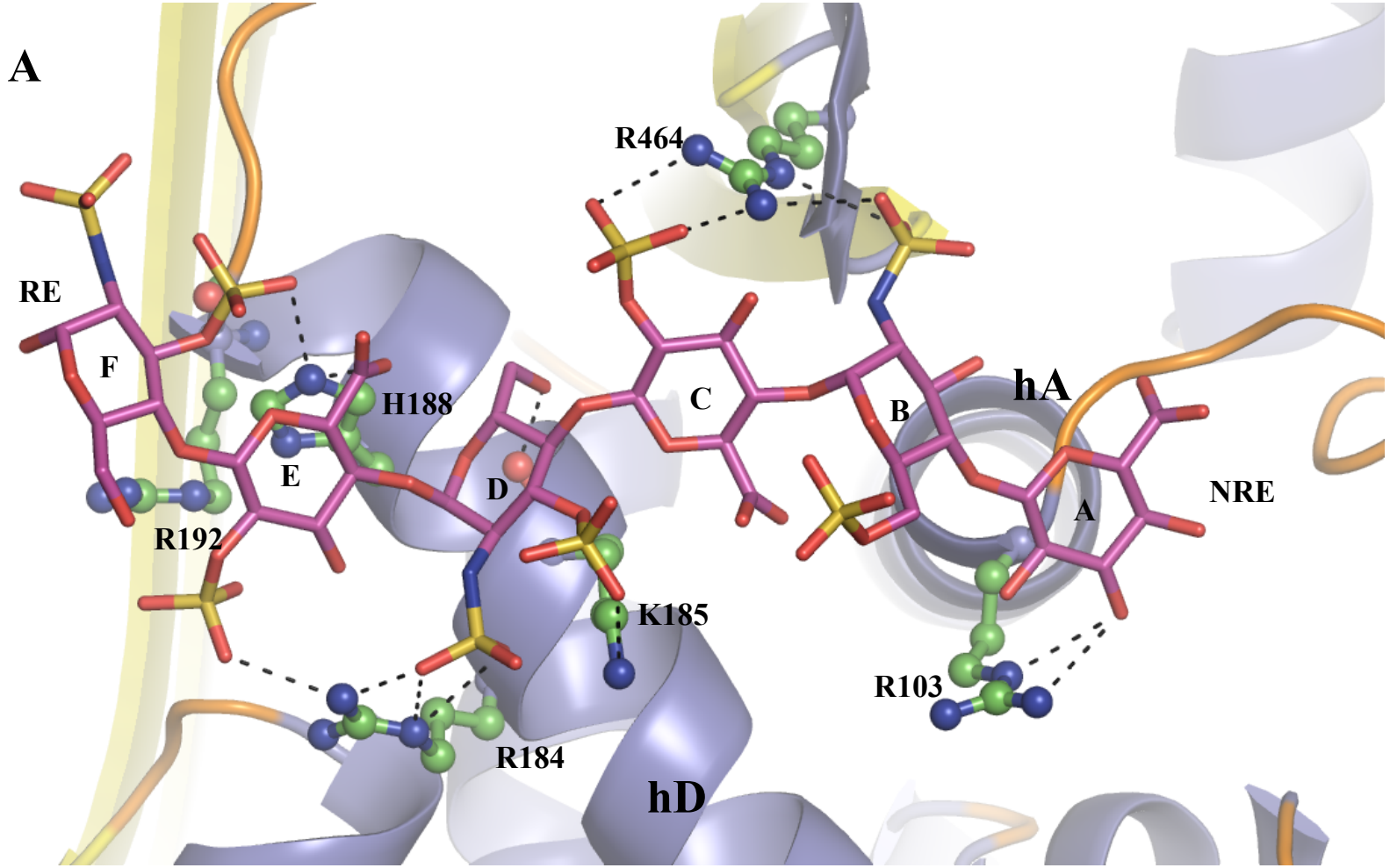

Figure 19. Interaction of HX1 with HCII

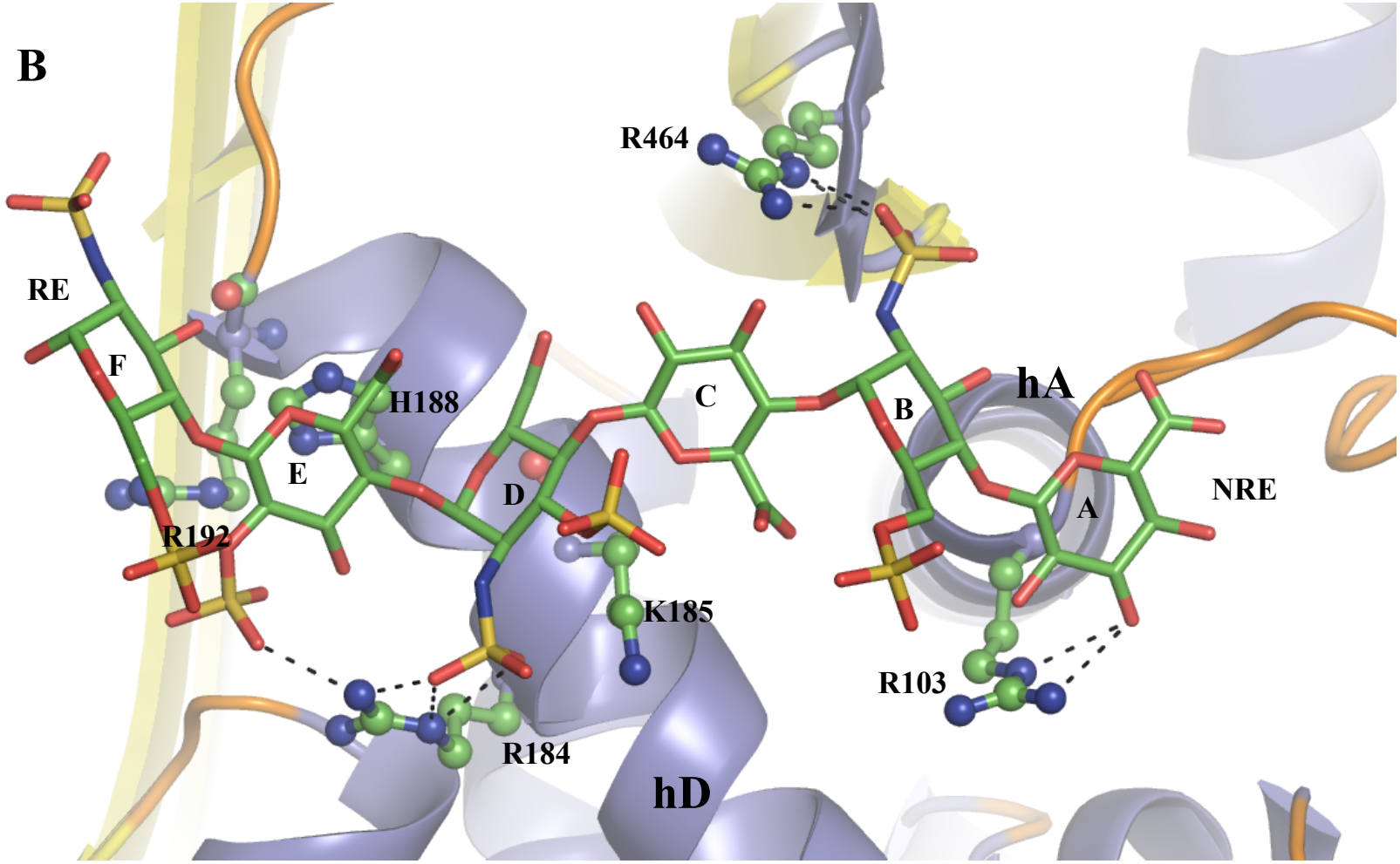

Figure 20. Interaction of HX2 with HCII

3.2.2. Synthesis of the Hexasaccharides

The hexasaccharides (**HX1-HX3**) were synthesized by the Oscarson lab at UCD School of Chemistry and Chemical Biology, University College of Dublin, Ireland.

3.2.3. Hexasaccharides Bind to HCII and AT With Good Affinity

To put the computational predictions to test, we studied the interaction of the designed hexasaccharides with HCII and AT utilizing intrinsic tryptophan fluorescence spectroscopy, as reported in literature.[155,156] All three hexasaccharides demonstrated a characteristic saturable change in fluorescence emission at 340 nm (λ_{EX} = 280 nm) under pH 7.4, *I* 0.06, 25 ºC conditions indicative of good interaction (Figure 21). Whereas a decrease in fluorescence was observed for each hexasaccharide binding to HCII (-26 to -33%), an increase was noted for AT (32 to 46%). Although the changes for the two related serpins are dramatically distinct, these are in line with those reported in the literature for other oligosaccharides.[14] Also, heparin pentasaccharide H5 also shows equivalent order of changes (-24% and 32%, respectively, Table 6). The affinities for HCII derived from the fluorescence profiles were calculated to be in the range of 29 to 45 μM for the three HXs. These compare favorably to the HCII affinities reported for high affinity hexasaccharide sequences extracted from UFH and DS (20-40 μM).[92,130] Interestingly, H5 was found to bind with an affinity of 9.2 μM, which was better than the HXs. In comparison to HCII, the HXs bound antithrombin with much more varied affinities. **HX1** and **HX2**, the two primary hexasaccharide sequences targeted by computational design, displayed affinities of 7.9 and 49 μM, while **HX3** interacted with a K_D of 75.3 μM (Figure 20, Table 6). These affinities are much weaker than the low nM

affinity noted for H5 in the literature.[14,57]

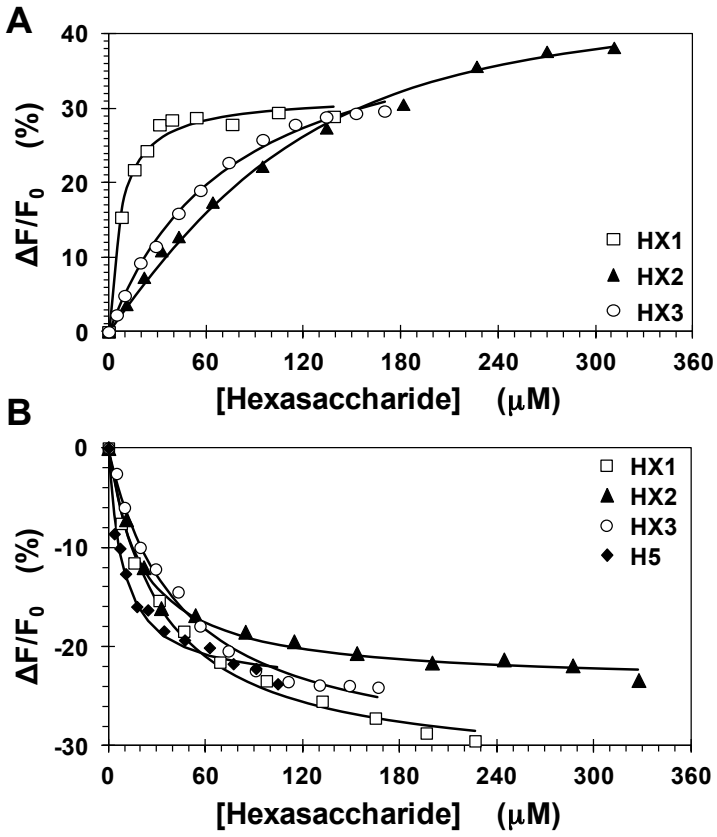

Figure 21. Affinity of hexasaccharides **HX1**–**HX3** for antithrombin (A) and heparin cofactor II (B) in 20 mM sodium phosphate buffer, pH 7.4, containing 25 mM NaCl at 25 °C. The affinity was measured from the proportional change in fluorescence emission ($\Delta F/F_0$) at 340 nm (λ_{EX} = 280 nm) as a function of the concentration of the HX, which was fitted using quadratic eq 1 (solid line) to derive the maximal fluorescence change (DF_{MAX}) and equilibrium dissociation constant (K_D). See 'Experimental Section' for additional details.

Table 6: Equilibrium dissociation constant (K_D) and maximal fluorescence change (DF_{MAX}) for hexasaccharide–serpin complexes.[a]

	AT		HCII	
	K_D	ΔF_{MAX}	K_D	ΔF_{MAX}
	(mM)	*(%)*	*(mM)*	*(%)*
HX1	7.9±0.5[b]	32±4	29.4±6.9	-33±5
HX2	48.7±8.7	46±4	17.6±4.0	-26±3
HX3	75.3±5.9[c]	45±4	44.5±3.8	-32±2
H5	0.05±0.006[c]	32±3	9.2±1.2	-24±1

[a]Measured using intrinsic (Trp) fluorescence in 20 mM sodium phosphate buffer, pH 7.4, containing 25 mM NaCl, at 25 °C. See Materials and Methods for additional details. [b]Error represents ±1 S.E. [c]Taken from Desai *et al.*[5]

3.2.4. Hexasaccharides Activate Serpin Inhibition of Target Protease

To assess the influence of HXs on the ability of serpins to inhibit their target protease, we studied the kinetics of HCII inhibition of TH and AT inhibition of FXa in a discontinuous assay at pH 7.4, *I* 0.06, 25 ºC, as described earlier.[93] The exponential decrease in residual protease activity as a function of time was used to derive the observed pseudo-first order rate constant (k_{OBS}) (Figure 22). The k_{OBS} of inhibition was found to increase linearly with the concentration of HX–serpin complex, which was used to obtain the second-order rate constant for the uncatalyzed inhibition (k_{UNCAT}) from the intercept and HX-catalyzed inhibition from the slope (k_{HX}) (Table 7).

The k_{UNCAT} for HCII–TH system and AT–fXa system was found to be 1.1–1.3

$\times 10^3$ $M^{-1}s^{-1}$ and $2.2–2.4\times 10^3$ $M^{-1}s^{-1}$, respectively (Table 7). These values compare favorably with basal rates reported in the literature.[14,93] The k_{HX} for HCII–TH reaction in the presence of **HX1** was measured to be 2.4×10^5 $M^{-1}s^{-1}$, which implies an acceleration of ~208-fold. **HX2** and **HX3** displayed an acceleration of ~43- and 71-fold, respectively. Likewise, heparin pentasaccharide H5 was found to induce a 49-fold acceleration in HCII–TH reaction. With regard to AT inhibition of FXa, **HX1** and **HX2** revealed accelerations of ~346- and ~380-fold, respectively, while **HX3** displayed a weaker acceleration of ~63-fold (Table 7, Figure 22). In comparison, H5, a clinically used anticoagulant targeting the AT – fXa system, displays accelerations in the range of 275 – 300-fold.[14]

To assess whether the observed accelerations arise from direct interaction of the proteases by HXs, we performed inhibition studies in the absence of the respective serpins. Using chromogenic substrate hydrolysis assay, the residual protease activities were monitored at HX concentrations as high as 500 μM against both TH and FXa. No inhibition of either enzyme was noted in these studies (not shown) suggesting that the HXs function only through an indirect mechanism of action. Overall, HXs were found to significantly affect serpin inhibition of target proteases. **HX1** was found to simultaneously induce robust acceleration of both AT and HCII against their preferred targets, as predicted on the basis of computational design.

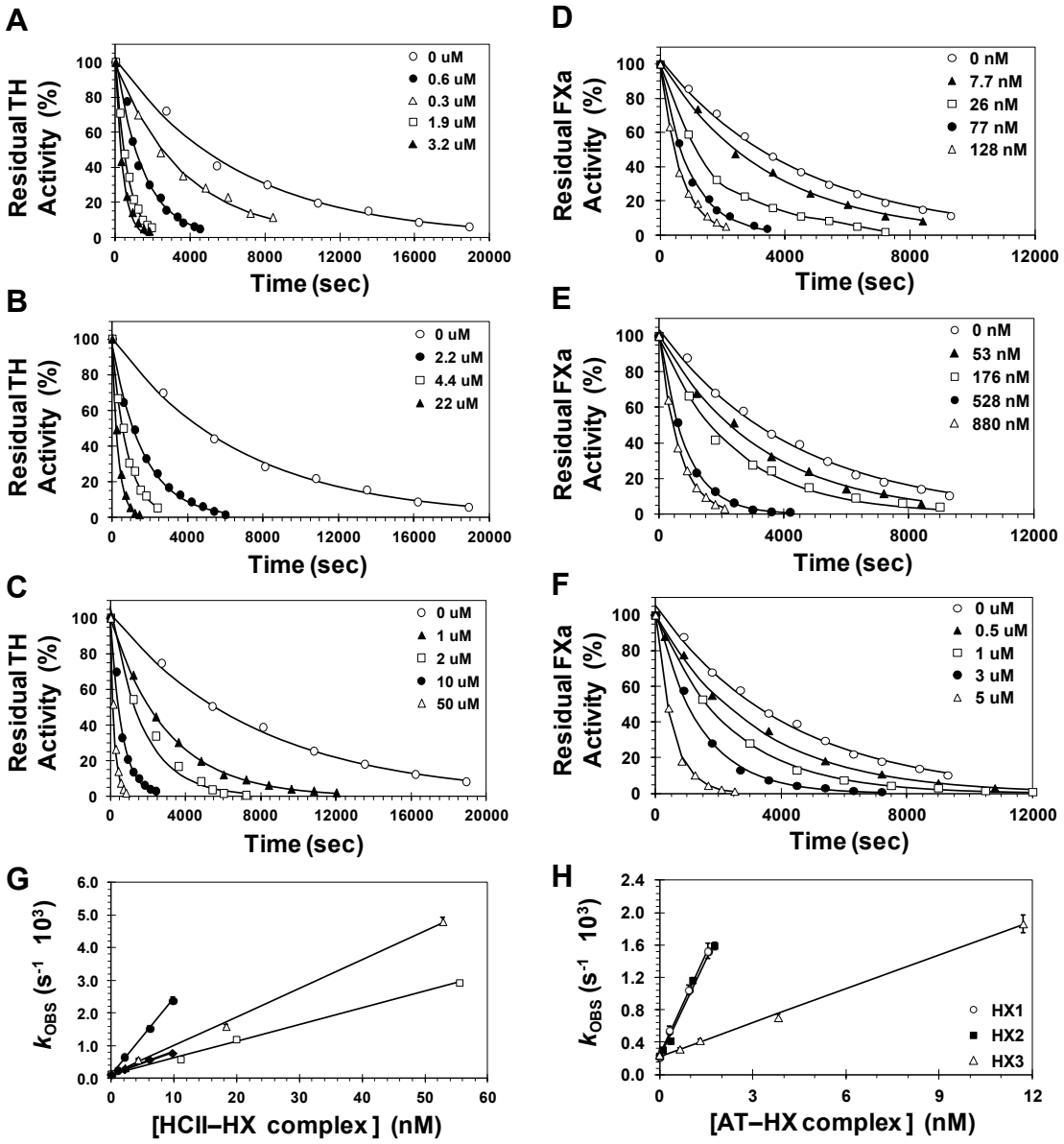

Figure 22. Kinetics of serpin inhibition of target protease in the presence of hexasaccharides **HX1–HX3** in 20 mM sodium phosphate buffer, pH 7.4, containing 25 mM NaCl at 25 °C. The residual TH activity (A, B and C) or FXa activity (D, E and F) was measured from the initial rate of substrate hydrolysis under pseudo-first-order conditions as a function of time in the presence of **HX1** (A and D), **HX2** (B and E) and **HX3** (C and F) and fixed concentrations of HCII (A, B and C) or AT (D, E and F). Panel G and H shows the profile of the observed pseudo-first order rate constant of HCII (G) or AT (H) inhibition (k_{OBS}) at different HX concentrations and its analysis using linear equation 2 (solid lines) to obtain the uncatalyzed (k_{UNCAT}) and catalyzed (k_{HX}) rate constants. See 'Experimental Section' for additional details.

Table 7: Acceleration in serpin inhibition of coagulation enzymes brought about by HX.[a]

	AT-FXa			HCII-TH		
	k_{UNCAT}	k_{HX}	Activation[b]	k_{UNCAT}	k_{HX}	Activation[b]
	$(M^{-1}s^{-1})$	$(M^{-1}s^{-1})$		$(M^{-1}s^{-1})$	$(M^{-1}s^{-1})$	
HX1	$2.4\pm0.2\times10^{3}$[c]	$8.3\pm0.3\times10^{5}$	346±41	$1.1\pm0.2\times10^{3}$	$2.4\pm0.1\times10^{5}$	208±48
HX2	$2.1\pm0.5\times10^{3}$	$8.0\pm0.5\times10^{5}$	381±114	$1.2\pm0.3\times10^{3}$	$5.1\pm0.2\times10^{4}$	42.7±12.4
HX3	$2.2\pm0.3\times10^{3}$	$1.4\pm0.1\times10^{5}$	62.4±7.0	$1.3\pm0.3\times10^{3}$	$8.8\pm0.2\times10^{4}$	70.5±16.7
H5[d]	$2.3\pm0.1\times10^{3}$	$6.1\pm0.3\times10^{5}$	275±25	$1.4\pm0.2\times10^{3}$	$6.8\pm0.4\times10^{4}$	49.0±17

[a]Measured using discontinuous enzyme inhibition assay in 20 mM sodium phosphate buffer, pH 7.4, containing 25 mM NaCl, at 25 °C. See Experimental Methods for additional details. [b]Refers to the ratio of catalyzed and uncatalyzed rate constants. [c]Error represents ±1 S.E. [c]Taken from Lindahl *et al.*[6]

3.2.5. Hexasaccharides are Potent Anticoagulants in Human Plasma

To assess if the promising activation of HCII and AT against TH and fXa, respectively, translates into promising anticoagulation potential in human plasma, we utilized the activated thromboplastin time (APTT). The ability of the HXs to prolong clotting was quantified in the form of the concentration required to double the clotting time (Figure 23). A **HX1** concentration of 85 μM doubled APTT, while 323 and 824 μM levels were needed for **HX2** and **HX3** (Figure 23). In comparison, 34 μM **H5** was minimally needed for 2×APTT. This implies that **HX1** and **H5** are approximately equipotent in this human plasma anticoagulation test, while other two HXs are much less potent. A plausible explanation for this difference is the higher affinity of **H5** and **HX1** for the two serpins in comparison to the other HXs. Interestingly, the observed 85 μM 2×APTT for **HX1** is

only about 10 and 3-fold lower than its affinity for AT and HCII, respectively. In contrast, H5 demonstrates a loss of ~6800 and 3.7-fold, respectively.

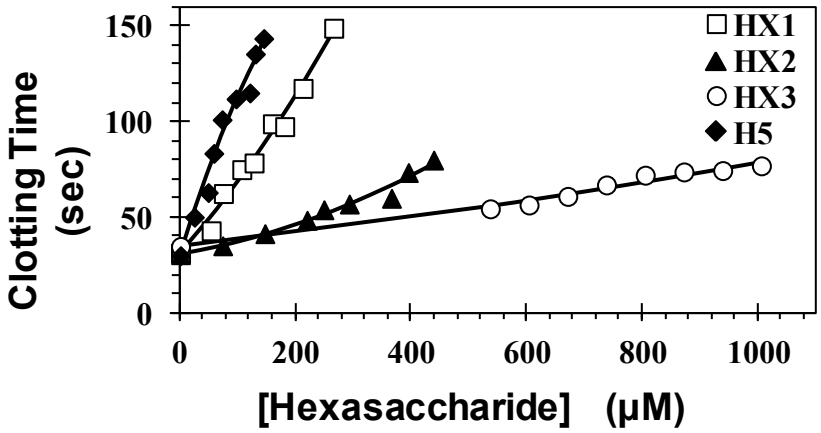

Figure 23. Pooled human plasma clotting time at varying levels of hexasaccharides **HX1–HX3** and heparin pentasaccharide H5 measured using the APTT assay. Solid lines are trend lines, which were used to calculate the concentration required to double the clotting time.

3.3. DISCUSSION

3.3.1. Designing Hexasaccharides Targeting HCII.

The heterogeneity and the non-specific heparin-based interaction were thwarted by the advent of a more specific pentasaccharide sequence identified for AT. The first total synthesis of the pentasaccharide in low yields laid the foundation to achieve a degree of understanding to this otherwise unknown interaction.[131] We have utilized a computational based approach to identify a similar specificity for the closely related serpin HCII. Three hexasaccharides were synthesized to test our hypothesis, which included **HX1** and **HX2** as molecules specific for HCII and, **HX3** predicted to be non-specific. Structurally, each of these possesses an alternating uronic acid and glucosamine units, sulfated strategically to unearth specific interactions with HCII identified computationally (Figure 19 and 20).

HX1 and **HX2** are identical with minor changes at the B residue 2-position sulfate and the F residue 3-position sulfate (Figure 24). Comparatively, H5 possess an iduronic acid at the G residue, replaced by a glucuronic acid for **HX1** and **HX2** (residue E). However, **HX3** does retain the iduronic acid at the same residue but lacks the important 6-OSO_3^- groups at the D residue (Figure 24) These hexasaccharides do possess an extra glucuronic acid residue in comparison to H5. The basis of these structural modifications are derived through our computational strategy and its translation into actual measured activity (Table 7) does indicate the robustness of our strategy.

3.3.2. Reported Structural Studies for the AT-FXa system

AT is a major regulator in maintaining normal hemostasis. It achieves this by targeting major coagulation proteases like FXa, thrombin and FIXa.[15] Heparin was the first known activator of AT but, is highly non-specific due to its large anionic and heterogenous character. Reducing its overall size and anionic character produced a striking improvement in specificity showcased by the small and specific heparin pentasaccharide (**DEFGH**, Figure 24).[132,157,158] Additionally, the improved specificity reduces the possibilities of non-specific interactions with other proteins.[159] The natural pentasaccharide was further studied through the synthesis of a plethora of synthetic variants.[16,17,132,133] Each of these extensive libraries has helped advance more potent and stable variants (Table 8). Important structural data established from these studies indicate that the 6-position of residue D, 3- and 2-position of residue F, and 2-position of residue H, are crucial for binding to antithrombin (Figure 24). Further synthetic derivatives revealed the replacement of the $NHSO_3^-$ group in all three glucosamine residues with

OSO_3^- and the addition of alkyl ethers at the free hydroxyl groups produce an enhancement of activity[132] (**DEFGH-NGA**, Table 8). Additionally, altering the backbone O-glycosidic bond with a C-glycosidic bond did not affect the activity (**C-DEFGH**, Table 8).[45] Similarly, the addition of a hydrophobic unit (**95**, Table 8) did not alter activity.[133] The AT-H5 system is a well-studied system and extending this to the HCII-TH system has been widely pursued.

Table 8: List of natural pentasaccharide and its derivatives.[a]

DEFGH derivatives				
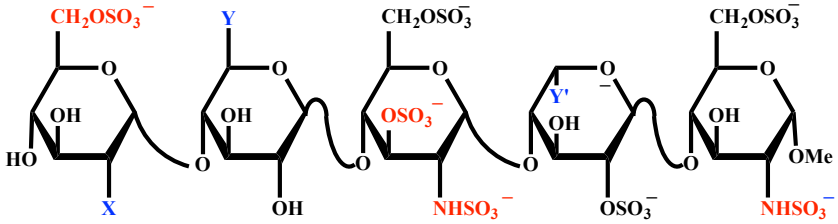				
Pentasaccharide[b]	**X**	**Y**	**Y'**	**Anti-FXa activity** *U/mg*
DEFGH	$NHSO_3^-$	COO^-	COO^-	700
D'EFGH	$NHCOCH_3$	COO^-	COO^-	350
DE'FGH	$NHSO_3^-$	$COOCH_3$	COO^-	35
DEFG'H	$NHSO_3^-$	COO^-	H	~0
Pentasaccharide	**Structure**			**Anti-FXa activity**
DEFGH''	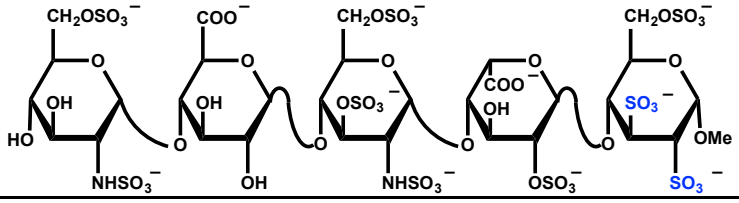			1250

DEFGH-NGA	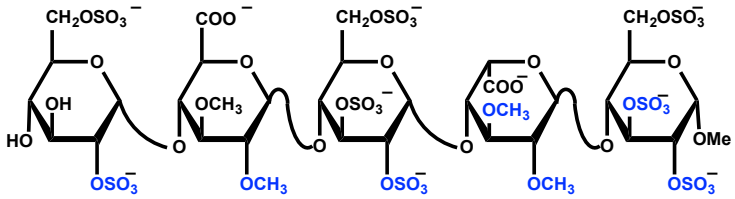	1323
C-DEFGH	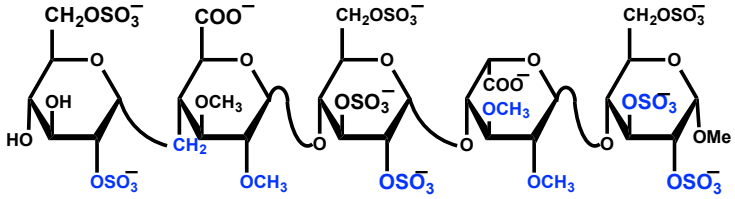	880
Idraparinux	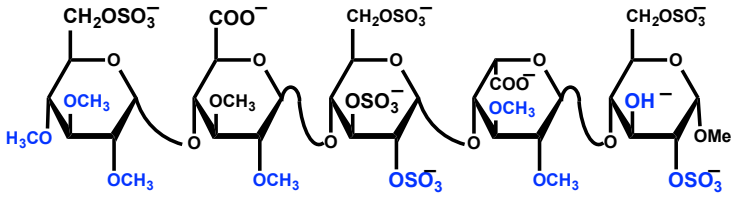	~700
95	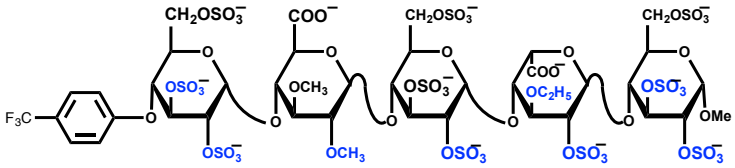	943

[a]Pentasaccharide derivatives as antithrombin based anticoagulant. Red refers to the residues known to be important in the pentasaccharide sequence and blue refers to the changes incorporated in comparison to the original DEFGH pentasaccharide sequence found in heparin.[b]Compiled from van Boeckel and Petitou[160] and Petitou *et al.*[45]

3.3.3. Reported Structural Studies for the HCII-TH system

HCII has evolved to be an adjunct to AT in regulating the circulatory levels of thrombin. Unlike AT, HCII only targets thrombin, affecting both the clot bond and the free form of thrombin.[145] Its adjunct role postulated to be more essential in pathophysiological responses, has resulted in a flurry of research aimed at developing agents targeting this system. Literature reports include the polymeric saccharide based effectors like dermatan sulfate, heparin and heparan sulfate,[161] chitosan polysulfate,[162] fucoidan,[163] fucosylated

chondroitin sulfate[164] shown to produce a drastic acceleration of HCII for thrombin inhibition. The polymeric structure of these however, incorporates numerous complexities in terms of their structure and purity, making it almost impossible to reproducibly use these in a clinical setting. Thus the impetus to identify smaller, well characterized effectors.

In an attempt to replicate the high affinity heparin pentasaccharide in the HCII system, the polymeric mix of dermatan sulfate and heparin were successfully reduced in two different studies to a hexasaccharide as a minimal effective unit for HCII.[92,130] These were elucidated as shown in Figure 25 indicating the structure of the heparin-based hexasaccharide and the dermatan sulphate-based hexasaccharide. Reports suggest the hexasaccharide comprises ~5% of disaccharides present in dermatan sulfate. This has been reportedly synthesized.[165] Similarly, studies with the heparin-based hexasaccharide indicates a dual interaction and acceleration of HCII in addition to potentiation of AT mediated inhibition of FXa, a feature indicated in the HXs studied here. Numerous reports incorporating depolymerization strategies have identified hexasaccharides based effectors,[22,166,167] however the maximum activity afforded by these has been ~100-fold, moderate in comparison to the ~2000-fold observed for heparin and dermatan sulfate.[92] Non-saccharide based sucrose octasulfate specifically activates HCII with a 2000-fold activation, however its affinity for HCII is poor at 1.45±0.30 mM. Conversely, contrasting reports indicate it to be a direct potent inhibitor of thrombin with an IC_{50} of 4.5±1.1 μM, albeit with an efficacy of less than 10%.[168]

3.3.4. Hexasaccharides Predictably Interact with AT

The hexasaccharide sequences studied herein, produced a potent activation of AT comparable to DEFGH especially **HX1** and **HX2**, with **HX3** inducing a poor 63-fold activation. Structurally, **HX1** and **HX2** are similar to the pentasaccharide sequence DEFGH, the major difference being the replacement of the iduronic acid at residue G with a gluocuronic acid (residue E) (Figure 14). The structural change does not affect the acceleration however, could conversely affect the affinity denoted by the moderate affinity observed in comparison to H5 (Table 6). Minor structural changes include the addition of sulfates at the 2-position of C residue and the 4-position of the F residue (Figure 24), both of which are not studied to be vital for activity. Predictably, **HX3** which lacks the essential sulfate group at the 6-position (Figure 24) of the B (D in pentasaccharide) residue produces a loss in acceleration and affinity, despite of this derivative possessing an iduronic acid at the E residue.

3.3.5. Identification of Hexasaccharide based Potent Activator of HCII

The computationally designed hexasaccharides we studied, possess a moderate affinity for HCII, however comparable to that reported for similar hexasaccharides.[92,167] The activation profile for these indicated a high 208-fold acceleration induced by **HX1**, albeit without any direct inhibition of thrombin. In comparison, to the well-studied AT-H5 system, little is known about the features required to induce specificity towards HCII. However, a comparison to the reported heparin hexasaccharides (Figure 25) does indicate a structural dependence to the improvement in acceleration. The reported sequence ABCDEF (Figure 25) is essentially similar to the HXs studied, with minor changes

including the replacement of the iduronic acid at residues A and C by a glucuronic acid in HXs, additionally the glucuronic acid in residue E has been replaced by a iduronic acid in **HX3**. The effects of these changes does indicate the importance of the sulfate at the 2-position on each residue, especially the residue C with the addition of a sulfate group increasing acceleration quantified by lack of a sulfate in **HX2**, producing a decrease in acceleration. Whereas, modification in the saccharide backbone does not affect the acceleration with both glucuronic or iduronic acid tolerated (Figure 15). Consequently, the identification of **HX1** could serve as the initial step towards developing more potent and selective agents to target HCII more specifically.

3.3.6. Utilization in Arterial/venous Thrombosis Models

AT conventionally targets venous thrombosis through the activation of thrombin and FXa. However, HCII possess a peculiar characteristic of specifically targeting clot bound thrombin and could therefore be utilized in an arterial thrombosis model. **HX1** possess an activation potential for both AT and HCII and could therefore be utilized as a newer agent in the unexplored field of dual agents, targeting both venous and arterial thrombosis. Similarly, the affinity these possess for AT is considerably lower than that reported for the heparin pentasaccharide (50 nM). The same affinity, which induces specificity, is responsible for the bleeding complications reported with the use of the heparin pentasaccharide. However, the HXs have a reportedly lower affinity for AT and could therefore induce a measured anticoagulant effect thereby reducing the risks of bleeding complications.

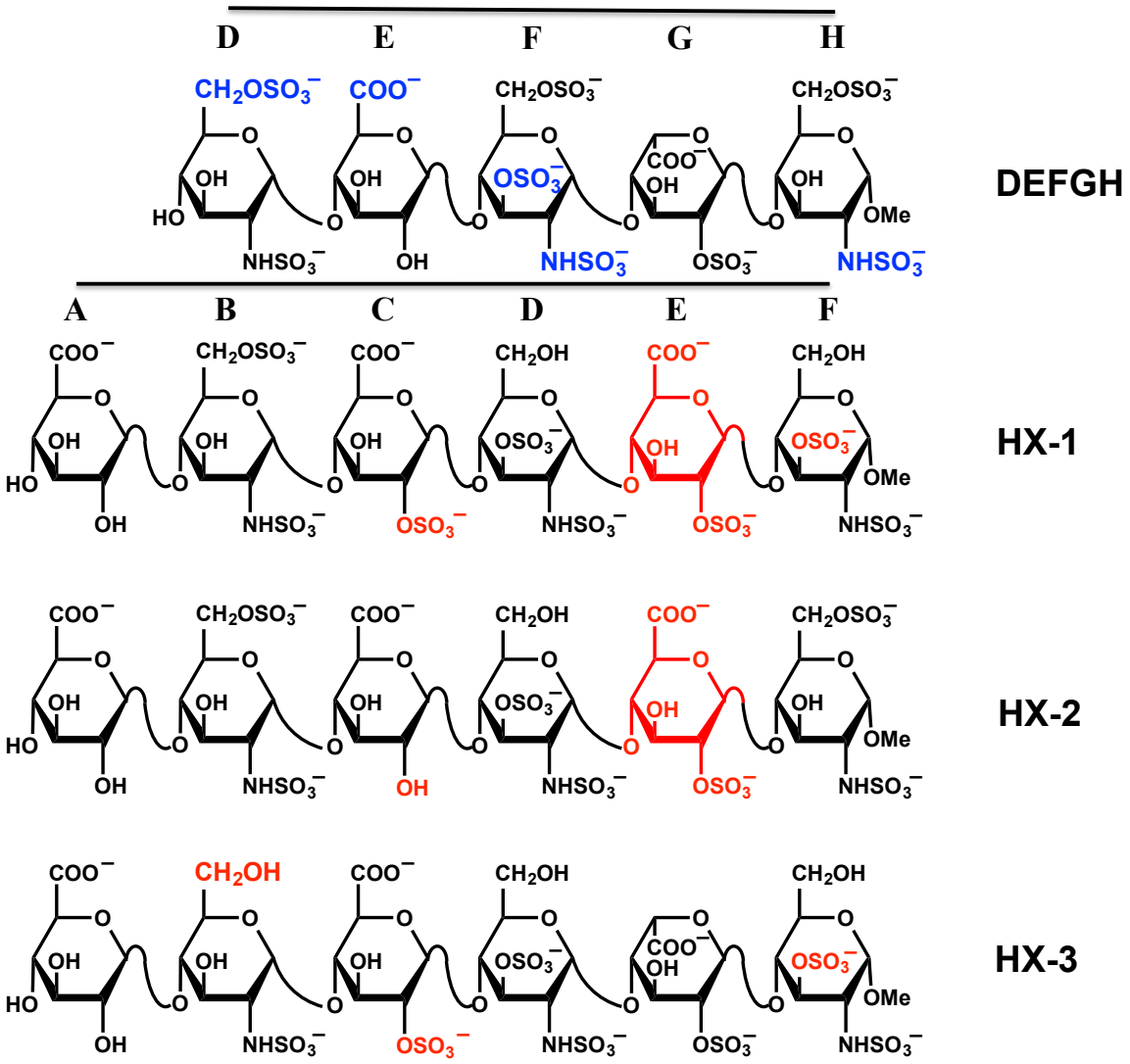

Figure 24. Structural comparison of the DEFGH sequence and the HXs synthesized. Blue refers to the residues deemed important as per reported studies. Red refers to the residues altered in the HXs in comparison to DEFGH.

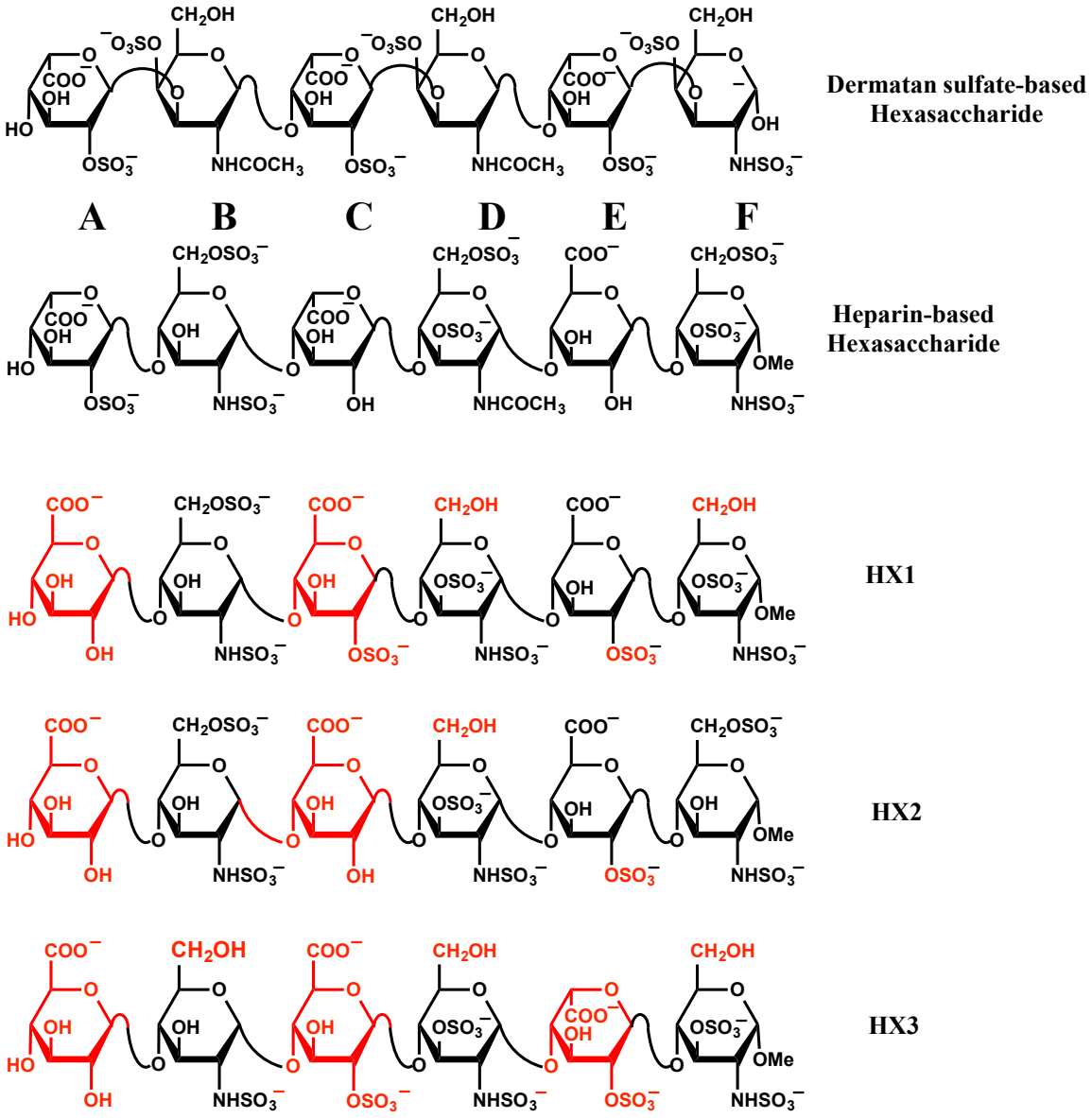

Figure 25. The structure of the reported dermatan sulfate and heparin-based hexasaccharide sequences and the comparison of the HXs and the heparin based hexasaccharide sequence. Red refers to the backbone saccharide units altered in comparison to the heparin-based hexasaccharide ABCDEF.

The interaction of heparin/heparan sulfate (H/HS) with heparin cofactor II was commonly assumed to be non-specific,[130,144,161] primarily because the GAG chains could not be separated into individual high and low affinity fractions. This also poses major

difficulties in structure elucidation since crystallization of a complex using the highly heterogeneous, polydisperse GAG is nearly impossible. Our work suggests that there exist at least two hexasaccharide sequences that are predicted to recognize activated heparin cofactor II with high-affinity and high specificity. Both sequences contain at least two GAG monosaccharides of the GlcN*p*2S3S or GlcA*p*2S type that are rare in natural preparations of H/HS.

The fact that each sequence has at least two such rare monosaccharides suggest a rapidly diminishing probability of finding these structures naturally. Yet, the hexasaccharides are expected to be accessible through chemical synthesis,[169] which may catalyze interest in clarifying the mechanism of H/HS activation of heparin cofactor II as well as advance the concept of designing potent heparin cofactor II agonists as specific inhibitors of thrombin. Considering that the structure of H/HS–HCII complex is not available, our combinatorial virtual library screening results have far reaching implications.

Our dual-filter algorithm appears to be a powerful tool for deciphering specificity of binding. For GAG-protein pairs that are difficult to study through NMR spectroscopy and X-ray crystallography, our virtual approach provides an avenue for gaining initial insight into ligand – protein interactions.

3.4. Experimental Methods

3.4.1. Computational Methods

Software. SYBYLX v2.0 (Tripos Associates, St. Louis, MO) was used for molecular visualization, minimization and for preparation of protein structures from the

Protein Data Bank (www.rcsb.org/pdb). GOLD, v5.1[170] was used for molecular docking experiments. GAG sequences were built combinatorially in an automated manner using in-house SPL (SYBYL Programming Language) scripts.

Protein preparation. The coordinates for the activated form of heparin cofactor II were extracted from the crystal structure of the S195A thrombin-HCII Michaelis complex (PDB entry 1JMO).[29] For comparative purposes, the co-ordinates of heparin pentasaccharide – antithrombin co-complex were extracted from protein databank file 1TB6.[134] Protein preparation was performed using the "prepare protein" module in SYBYLX, v2.0 and included removal of water molecules, adjustment of the protonation states of amino acid residues to physiological conditions, addition of hydrogen atoms and the structure was minimized with fixed heavy-atom co-ordinates using the Tripos Force Field for 1,000 iterations subject to a termination gradient of 0.05 kcal/(mol-Å).

Co-ordinates for HS Virtual Library. The co-ordinates for HS hexasaccharide sequences present in the combinatorial virtual library were generated using a series of SPL scripts and HS disaccharide building blocks. Although the total number of possible disaccharides (UA*p*(1→4)GlcN*p*) is 48, only 23 have been experimentally observed (Figure 13B).[124] Of these 23, 13 disaccharides contain IdoA*p*, while 10 contain GlcA*p* residue. Because IdoA*p* residue in HS can exist either in the $^{2}S_{O}$ or $^{1}C_{4}$ conformations,[126,171] each IdoA*p*-containing disaccharide was modeled explicitly in these two different states. Thus, our virtual library consisted of 26 IdoA*p* and 10 GlcAp disaccharide building blocks generating a total of 46,656 (36 x 36 x 36) hexasaccharide sequences.

Each H/HS sequence within these libraries were denoted using the GLYCAM force field[172] symbols or letters for base monosaccharides (GlcN*p*, IdoA*p* and GlcA*p*) and further modified by the substituents (–H, $–SO_3^-$, or $–COCH_3$, see Appendix A). Appropriate side-chain modifications were made to generate the 36 building blocks. Each disaccharide was minimized using glycosidic bond torsion constraints (restraining force constant = 0.01 $kcal \cdot mol^{-1} \cdot deg^{-2}$). Analysis of the available crystal structures showed that the inter-glycosidic torsions ϕ_H (O5-C1-O1-C4') and ψ_H (C1-O1-C4'-C5') fall within a relatively narrow range and are essentially invariant irrespective of the substitution pattern.[22,154,173,174] Thus, average bond torsions (see Appendix B), were used for inter-glycosidic linkages. The 36 disaccharides were then used to build a combinatorial HS hexasaccharide library using an SPL script in an automated manner, following which each sequence was again minimized using glycosidic bond torsion constraints to generate HS sequences with 'average backbone' geometries.[91,128]

Docking of the Comprehensive HS Virtual Sequence Library.

Docking of HS ligand onto the activated form of heparin cofactor II was performed with GOLD v5.1. GOLD is a "soft docking" method that implicitly handles local protein flexibility by allowing a small degree of interpenetration, or van der Waals overlap, of the ligand and protein atoms.[170] GOLD also optimizes the positions of hydrogen-bond donating atoms on Ser, Thr, Tyr, Lys, and Arg residues as part of the docking process. GOLD starts with a population of 100 arbitrarily docked ligand orientations, evaluates them using a scoring function (the GA "fitness" function) and improves their average "fitness" by an iterative optimization procedure that is biased

towards high scores. Docking was driven by $GOLDScore = HB_{EXT} + 1.375 \times VDW_{EXT}$ equation (HB_{EXT} and VDW_{EXT} are the non-bonded intermolecular hydrogen bond and van der Waals terms, respectively) to prioritize different poses, as reported earlier (Raghuraman et al. 2006). As the initial population is selected at random, several such GA runs are required to more reliably predict correct bound conformations. In our study 10 GA runs were used, which are collectively referred to as one docking experiment.

Evaluation of the HS combinatorial library was performed using a two-stage docking protocol (Figure 12), as utilized in our study of the antithrombin-heparin pentasaccharide system.[128] The first stage (the 'affinity' test) involved docking of 46656 HS sequences to HCII to efficiently identify sequences with high affinity for the binding site. To enhance the speed of the search, all sequences were docked using 10,000 iterations (7 – 8X speed up setting) per GA run. Additionally, the GA was set to terminate early if, during the course of docking, the top two ranked solutions were within 2.5 Å RMSD.

For the overall top-ranked docked solution for each of the HS sequences, a modified GOLD score was calculated. Although the GOLD fitness function generally correlates with the observed free energy of binding, a modified form has been found to be more reliable.[175] This modified GOLD score utilizes only the "external" hydrogen-bonding and van der Waals terms of the GOLD fitness function (above equation). The GOLD score, as it is reported in this paper, refers to this modified GOLD scoring function. The top solutions were re-ranked based on the GOLD score, and the top 0.1% were selected for the convergence ('specificity') test.

The ‘specificity’ test consisted of docking the most promising HS sequences from the ‘affinity’ test using the standard GOLD parameter settings (no speed-up; 100,000 GA iterations). The top two solutions of each docking experiment were considered for further analysis. Docking was performed in triplicate to yield a minimum of 6 solutions. A RMSD of less than 2.5 Å among the backbone heavy atoms (pyranose ring atoms and interglycosidic oxygens) of all 6 solutions suggested a high degree of convergence to a ‘unique’ binding geometry. These HS sequences were deemed to be specific.

In both the first and second docking stages, the binding site in heparin cofactor II was comprised of all atoms within 18 Å from the C_γ atom of Lys185 in the D helix. This dimension of the binding site covers a number of basic residues including Lys101, Arg103, Lys173, Arg184, Lys185, Arg189, Arg192, Arg193, Lys220, and Arg464, which are present in the putative heparin-binding domain formed by helices A and D, and part of the *N*-terminus.

3.4.2. Proteins and Chemicals

Human plasma antithrombin (AT), heparin cofactor II (HCII), human thrombin (TH) and human factor Xa (FXa) were purchased from Haematologic Technologies (Essex Junction, VT). AT, HCII, thrombin and FXa were stored in 20 mM sodium phosphate buffer, pH 7.4, containing 25 mM NaCl, 0.1 mM EDTA and 0.1% (w/v) PEG8000 at -20 °C. Spectrozyme FXa (methoxycarbonyl-*D*-cyclohexylglycyl-Gly-Arg-*p*-nitroanilide) and Spectrozyme TH (H-*D*-hexahydrotyrosol-Ala-Arg-*p*-nitroanilide) were obtained from American Diagnostics (Greenwich, CT) and prepared in 20 mM sodium phosphate buffer, pH 7.4, containing 25 mM NaCl, 0.1 mM EDTA and 0.1% (w/v) PEG 8000.

Pooled normal human plasma for coagulation assays was purchased from Affinity Biological (Ancaster, Ontario). Activated partial thromboplastin time reagent containing ellagic acid and 25 mM $CaCl_2$ were obtained from Fisher Diagnostics (Middletown, VA).

3.4.3. Equilibrium Binding Studies using Fluorescence Spectroscopy

The equilibrium dissociation constants of hexasaccharide (HX) – protein complexes were measured using change in fluorescence emission as a function of the concentration of the hexasaccharides in 20 mM sodium phosphate buffer, pH 7.4, containing 25 mM NaCl, 0.1 mM EDTA and 0.1% PEG8000 at 25 °C, as described earlier.[14,156] The experiments were performed using a QM4 fluorometer (Photon Technology International, Birmingham, NJ) in a quartz microcuvette by titrating a 200 μL solution of the protein (100–200 nM) and monitoring the change in the fluorescence at 340 nm (λ_{EX} = 280 nm). Excitation and emission slit width were set to 1.0 mm for each experiment. The saturable change in fluorescence signal was fitted using the quadratic equilibrium binding eq 1 to obtain the K_D of interaction. In this equation, ΔF represents the change in fluorescence at a fixed concentration of HX from the initial fluorescence F_0 and ΔF_{MAX} represents the maximal change in fluorescence following saturation of the protein. $[P]_0$ represents the total concentration of either AT or HCII.

$$\frac{\Delta F}{F_0} = \frac{\Delta F_{max}}{[P]_0} \times \left\{\frac{([P]_0 + [HX]_0 + K_D) - \sqrt{(([P]_0 + [HX]_0 + K_D)^2 - 4[P]_0[HX]_0)}}{2}\right\} \qquad (1)$$

3.4.4. Kinetics of Protease Inhibition in the Presence of HX

The kinetics of inhibition of coagulation proteases TH or FXa by AT or HCII in the presence of HX was measured spectrophotometrically using a microplate reader (FlexStation III, Molecular Devices) under pseudo-first-order conditions, as described

earlier.[82,176] Briefly, a fixed concentration of TH or FXa (~5 nM) was incubated with fixed concentrations of plasma AT or HCII (100 nM) and hexasaccharides (0 – 3200 nM) for **HX1**, (0 – 22 mM) for HX2 and (0 – 10 mM) for **HX3** in 20 mM sodium phosphate buffer, pH 7.4, containing 25 mM NaCl, 0.1 mM EDTA and 0.1% (w/v) PEG 8000 at 25 °C. At regular time intervals, an aliquot of the inhibition reaction was quenched with 100 μL of 125–200 μM chromogenic substrate (Spectrozyme TH or Spectrozyme FXa) in 20 mM sodium phosphate buffer, pH 7.4, containing 25 mM NaCl at 25 °C. To determine the residual protease activity, the initial rate of substrate hydrolysis was measured from the increase in absorbance at 405 nm. The exponential decrease in the initial rate of substrate hydrolysis as a function of time was used to determine the observed pseudo-first-order rate constant of protease inhibition (k_{OBS}). A plot of k_{OBS} at different concentrations of HX–serpin complex could be described by eq 2, in which k_{UNCAT} is the second-order rate constant of protease inhibition by serpin alone and k_{HS} is the second-order rate constant of protein inhibition by serpin-HX complex (HX:P).

$$k_{OBS} = k_{UNCAT}[P]_0 + k_{HX}\,[HX{:}P] \qquad (2)$$

3.4.5. Direct Protease Inhibition in the Presence of HX

Direct inhibition of TH or FXa by hexasaccharides was assessed through a chromogenic substrate hydrolysis assay using a microplate reader (FlexStation III, Molecular Devices), as described earlier.[177] Briefly, each well of the 96-well microplate contained (190–X) μL of the pH 7.4 buffer to which X μL of HX (to give a 500 μM final concentration), or an appropriate reference, was added followed by 5 μL of protease (to give 5 nM final concentration). After 10 min incubation at 25 °C, 5 μL of appropriate chromogenic

substrate (to give 125 mM (Spectrozyme FXa) or 100 mM Spectrozyme TH) was rapidly added and the residual protease activity was measured from the initial rate of increase in A_{405}. Relative residual protease activity at each concentration of HX was calculated from the ratio of the activity in the presence and absence of the inhibitor.

3.4.6. Activated Partial Thromboplastin Time (APTT)

Clotting time was measured in a standard one-stage recalcification assay with a BBL Fibrosystem fibrometer (Becton−Dickinson, Sparles, MD). In the APTT assay, X μL of oligosaccharides (H5 and HX) were mixed with (100 – X) μL of citrated human plasma and 100 μL of prewarmed APTT reagent (0.2% ellagic acid). After incubation for 4 min at 37 °C, clotting was initiated by adding 100 μL of prewarmed 25 mM $CaCl_2$ and the time to clot was noted. The data were fit using a quadratic trend line, from which the concentration of the oligosaccharides (H5 and HX) necessary to double the clotting time was calculated. Clotting time in the absence of an anticoagulant was determined in a similar fashion using 10 μL of deionized water and was found to be 32.1 s on an average for APTT.

CHAPTER 4: DIFFERENTIAL RECOGNITION OF COAGULATION PROTEINS BY HEPARAN SULFATE CONTAINING 2-O-SULFATED GLUCURONIC ACID

4.1 Introduction

Sulfated glycosaminoglycans (GAGs), natural linear co-polymers of hexuronic acid and hexosamine residues, represent nature's bounty of chemical biology tools. Yet, the current state-of-art displays minimal exploitation of this promise. Few GAG-based therapeutic agents have been discovered other than naturally occurring heparin, dermatan sulfate and chondroitin sulfate. A major challenge in realizing the pharmacologic potential of GAGs is the structural diversity inherent in every natural GAG preparation. The variations introduced by incomplete sulfation, deacetylation, and epimerization reactions during their biosynthesis,[124,178-180] coupled with postsynthetic fine tuning of GAG structure by sulfatases,[181] generates millions of distinct sequences that defy resolution and analysis at high homogeneity levels.

Despite this challenge, sulfated GAGs are attractive. The presence of sulfate (—OSO_3^-) groups on a GAG chain induces recognition and modulation of most proteins, especially those that display a collection of Arg/Lys residues on their surface. This gives rise to GAG modulation of a large number of physiological and pathological responses such as growth and cancer, cell renewal and differentiation, hemostasis and fibrinolysis, inflammation and immune response, and microbial invasion and defense.[120,124,182-185] It is

likely that individual proteins bind to only a subset of GAG sequences from the natural repertoire of millions. A classic example of this high selectivity is the heparin pentasaccharide sequence, containing a rare 3-*O*-sulfate glucosamine (GlcN*p*) residue, which binds to antithrombin (AT), a serpin involved in regulation of hemostasis and coagulation, with an affinity of ~50 nM.[14] Another example suggested in the literature is that of a dermatan sulfate hexasaccharide that binds heparin cofactor II (HCII), another plasma serpin, with high selectivity and an affinity of 20 μM.[92] Although both AT and HCII possess considerable three-dimensional similarity,[186] they prefer completely different GAG sequences.[91] Thus, the possibility is high that distinct GAG sequences may modulate proteins in a selective manner.

How can such distinct GAG sequences be identified and studied as chemical biology tools? An often utilized approach is computational study of individual GAG–protein interactions.[187] Examples of such studies include the prediction of GAG binding sites on enzymes (e.g., cathepsin S[188] and heparanase[189]), enzyme inhibitors (e.g., antithrombin,[128] heparin cofactor II[91] and alpha-1-proteinase inhibitor[190]), membrane or cell surface proteins (e.g., αvβ3 integrin,[191] growth factor receptor[192] and human papillomavirus major capsid protein L1),[193] cellular or extracellular proteins (e.g., bone morphogenetic proteins[194] and growth factors),[195,196] and matrix proteins (e.g., thrombospondin-1).[197] Despite this voluminous effort, the number of GAG sequences that exhibit selective targeting of proteins has remained low.

We reasoned that a simple approach to identify selective GAG sequences is to consider rare sequences. Sequences that are rarely present in natural GAGs are most

probably biosynthesized for a specific reason and likely to exhibit selective modulation of target proteins, as exemplified by the 3-*O*-sulfated GlcN*p* residue.[14,128] In addition to its presence in the high affinity AT binding heparin pentasaccharide, it is also part of the heparin octasaccharide that binds glycoprotein D of the herpes simplex virus.[198] No other rare GAG residue has been discovered to date as equally interesting from the chemical biology perspective.

A rare GAG residue of significance could be 2-*O*-sulfated glucuronic acid (GlcA*p*2S). This residue can be biosynthesized by the action of 2-*O*-sulfotransferase (2OST) on GlcA*p*, present in a growing heparan sulfate (HS) chain, that has escaped epimerization reaction with the C-5 epimerase (C5E).[178,199,200] Under normal biosynthetic conditions, the growing HS chain acted upon by *N*-deacetylase/*N*-sulfotransferase (NDST) to produce GlcN*p*2S and GlcA*p* containing sequences, majority of which are further modified to IdoA*p* by C5E.[149,178] 2OST then acts upon IdoA*p* to produce IdoA*p*2S, which eventually gives the most common disaccharide sequence, IdoA*p*2S(1→4)GlcN*p*2S6S, in heparin.[201] Once in a while, C5E could skip epimerization of GlcA*p* resulting in the formation of a rare GlcA*p*2S following 2OST action.[199,200]

This begged the question: What biological consequences would ensue if the GlcA*p*2S residue was more abundant? We used a genetic algorithm-based computational approach to study GlcA*p*2S containing hexasaccharides binding to AT and discovered elements of highly selective recognition. The HS polymer labeled as HS_{2S2S} and containing only GlcA*p*2S and GlcN*p*2S residues was prepared using recombinant biosynthetic enzymes and found to potently bind and activate AT for inhibition of factor

Xa. In addition, HS_{2S2S} targets HCII and thrombin, but not factor Xa, which is corroborated by computational modeling studies. The results convey the potential of HS_{2S2S} in understanding differential recognition of proteins of the coagulation cascade, while also highlighting the significance of studying distinct GAG sequences for pharmacological purposes.

4.2 Results

4.2.1 Rationale for Studying HS sequences containing GlcA*p*2S

As discussed above, the GlcA*p*2S residue is rare in natural HS.[199,202] Yet, it is enhanced 2–3-fold in the cerebral cortex as compared to other tissues suggesting the possibility of its role in an as-yet-undetermined physiologic process.[200] Surprisingly, GlcA*p*2S is biosynthesized by the same enzyme that generates IdoA*p*2S, the predominant uronic acid of heparin, and only one isoform of this critical enzyme, 2-*O*-sulfotransferase (2OST), has been identified to date, which implies that regulation of HS fine structure containing GlcA*p*2S is likely to be an exquisitely fine-tuned process. Additionally, a 3-*O*-sulfotranferase isoform (3OST-2) appears to demonstrate selectivity for sequences containing GlcA*p*2S.[203] This 3OST isoform is expressed more in the brain,[204] which is also the place where GlcA*p*2S proportion is higher.[200]

Apart from the biosynthesis, distribution and possible physiologic relevance perspective, GlcA*p*2S residue is also attractive in the context of HS structure. A HS chain containing GlcA*p*2S can be easily synthesized in only two steps. Treatment of the *E. coli* K5 capsular polysaccharide with *N*-deacetylase/*N*-sulfotransferase (NDST) followed by 2OST treatment gives a HS preparation enriched in →4)GlcA*p*2S(1→4)GlcN*p*2S(1→,

which retains the heterogeneity of HS, *albeit* at a lower level, because of incomplete reactions with NDST and 2OST. This disaccharide sequence, and its counterpart →4)GlcN*p*2S(1→4)GlcA*p*2S(1→, display significantly different electrostatic and hydrophobic surfaces in comparison to that observed for naturally occurring H/HS disaccharides. Nearly 50% of naturally occurring disaccharides possess a higher polar surface area than HS_{2S2S} (Figure 26A). 76.3% of the AT binding heparin pentasaccharide's solvent accessible surface area is polar, which is comparable to HS_{2S2S}'s 75.3%. However, the pentasaccharide displays almost 7 negative charges per 1000 $Å^2$ in comparison to 4.6 for the HS_{2S2S} disaccharide (Figure 26B), giving it a significantly higher charge density. Thus, HS_{2S2S} possesses distinct topological characteristics when compared to the known bioactive HS pentasaccharide sequence. We have previously reported small molecule GAG mimics that target hydrophobic sites on the HBS of antithrombin, thrombin and factor XIa.[82,103,177,205-207] We hypothesized that HS_{2S2S}'s distinct topology may also allow similar hydrophobic interactions with antithrombin's HBS.

4.2.2 HS containing GlcA*p*2S and GlcN*p*2S may Exhibit Promising AT Targeting Capability

To assess whether GlcA*p*2S and GlcN*p*2S residues introduce novel protein recognition features, we utilized a computational workflow that helps sort 'specific' and 'nonspecific' GAG interactions.[91,128] The workflow involved a 'steady state with no duplicates' genetic algorithm (GA) to place HS_{2S2S} sequence containing hexasaccharides onto the heparin-binding site (HBS) of AT. A GA is an artificial intelligence program that explores the 3-

dimensional space around a binding site and attempts to find optimal position(s) for a ligand through an iterative process of natural selection, or alternately 'survival-of-the-fittest' rules. For studying the library of HS_{2S2S} hexasaccharides binding to AT, we utilized GOLD[208] as the GA and assessed the tendency of GlcA*p*2S and GlcN*p*2S monosaccharides to localize to specific sites on AT. The tendencies were quantified using a grid-based approach as shown in Figure 27. Interestingly, both monosaccharides displayed statistically significant enrichment ($p < 2.2e^{-16}$) in the regions that compare favorably with D (GlcN*p*2S6S) and E (GlcA*p*) residues of the heparin pentasaccharide sequence known to bind AT with high affinity (Figure 26). It may be noted that the D and E residues have previously been shown as predominantly responsible for affinity with antithrombin.[14] Significant enrichment at these locales suggested excellent probability of favorable and selective recognition of AT.

To evaluate the predicted interactions more quantitatively, the poses of each monosaccharide were parsed into two groups using k-means clustering to differentiate between specifically interacting and randomly interacting poses, as routinely performed for such studies.[209,210] The average pair-wise RMSD for each group was then calculated. Interestingly, GlcA*p*2S and GlcN*p*2S were found to exhibit low RMSDs of 1.2 and 1.0 Å respectively (Table 9), which suggest a strong possibility of specific interaction with AT at this locale (Figure 26C and D). It is important to note that we typically use a RMSD cut-off 2.5 Å to differentiate 'specific' from 'nonspecific' interactions[91,128] and both of these monosaccharides appear to exhibit a clear preference for HBS of AT.

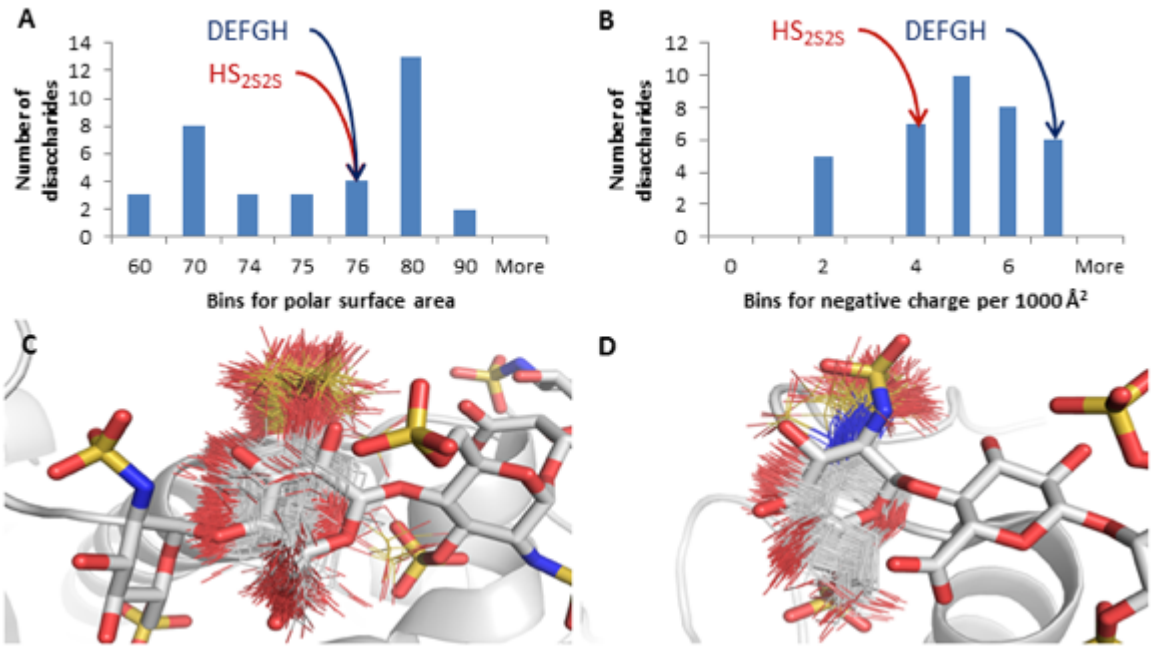

Figure 26. Computational studies with the HS_{2S2S} sequence. (A) Almost 50% of naturally occurring disaccharides possess a higher polar surface area (PSA) than the HS_{2S2S} disaccharide, but the antithrombin binding heparin pentasaccharide (DEFGH) possesses a similar PSA. (B) However, DEFGH possesses significantly higher negative charge density. Thus, HS_{2S2S} is a relatively hydrophobic molecule. Computation predicts specific interactions formed between antithrombin and HS_{2S2S} monosaccharides (C) GlcA*p*2S, corresponding to the D monosaccharide of DEFGH (GlcA*p*2S6S), and (D) GlcN*p*2S, corresponding to E (GlcA*p*). These interactions were identified using a grid-based procedure to monitor locales for monosaccharides placed by a genetic algorithm[208] used previously[14, 18] to study GAG-protein interactions.

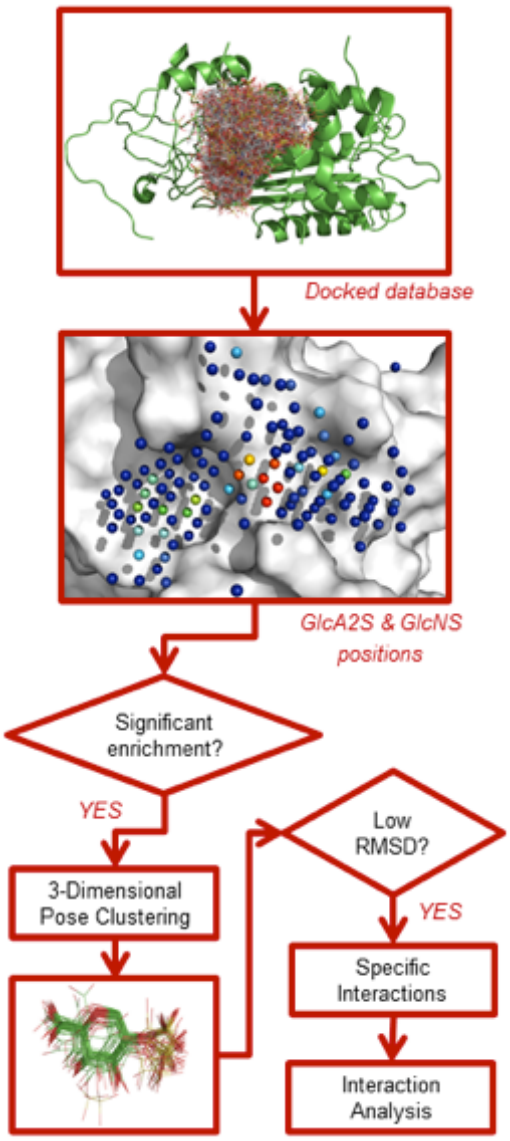

Figure 27. Grid-based identification of preferred locations for GlcA*p*2S and GlcN*p*2S in genetic algorithm-based docked poses. 2S2S sequences were docked into antithrombin's HBS and preferences of the HS_{2S2S} monosaccharides were identified using a grid-based approach. A high resolution (1Å) grid was placed around the docked hexasaccharide poses. Any instances of GlcA*p*2S and GlcN*p*2S, the center of whose pyranosyl ring was closest to a grid point, was recorded as being placed at that grid point. The relative frequency with which a monosaccharide was placed at a grid point – compared to other grid points – reflects the probability that it will prefer binding there, which was significantly high ($p<2.2e^{-16}$).

Table 9: Data for preferred locations of GlcA*p*2S and GlcN*p*2S.

Residue	GlcA*p*2S			GlcN*p*2S		
Protein	**% poses[a]**	**p-value**	**RMSD[b]**	**% poses[a]**	**p-value**	**RMSD[b]**
Antithrombin	16.9%	$<2.2e^{-16}$	1.2	15.7%	$<2.2e^{-16}$	1.0

[a]: Percent instances (poses) of respective residue at highest density location.
[b]: Average RMSD per pyranosyl ring heavy atom (in Å) within cluster (see Experimental Section). Smaller values denote highly conserved interactions.

4.2.3 Digestive Analysis of HS_{2S2S} using RPIP UPLC-MS

In order to identify the structural composition of the HS_{2S2S} polymer, an enzymatic digestion was followed using two UPLC-MS methods to analyze heparin oligosaccharides (Method 1) and disaccharides (Method 2).[211-213] After 5 hours of digestion, no oligosaccharides were observed. However, after 24 hours several tetrasaccharide peaks were observed (Figure 28A). The mass spectra of these peaks led to the identification of tetrasaccharides with 2,3 or 4 sulfate groups (T-2S, T-3S and T-4S respectively) (Figure 28B). At 24 hours some polymeric ions were observed indicating an incomplete digestion. In comparison, a control batch of unfractionated heparin showed almost complete digestion within this time (Figure 29). The UV profiles for the sample demonstrated that the majority sample consisted of tetrasaccharide with 4 sulfate groups (data not shown). At 48 hours complete digestion to disaccharide level was observed (Figure 30). The disaccharide analysis (Method 2) identified that the sample of HS_{2S2S} consisted of mainly disulfated disaccharide with some traces of monosulfated disaccharides (Figure 30). This was as expected from the observations in method 1. Furthermore, based on the elution times, the monosulfated disaccharide is possibly

sulfated at the N-position of the glucosamine similar to heparin disaccharide standard IVS, while the disulfated disaccharide most likely has a sulfation pattern similar to heparin disaccharide standard IIIS and is the major peak in the sample.

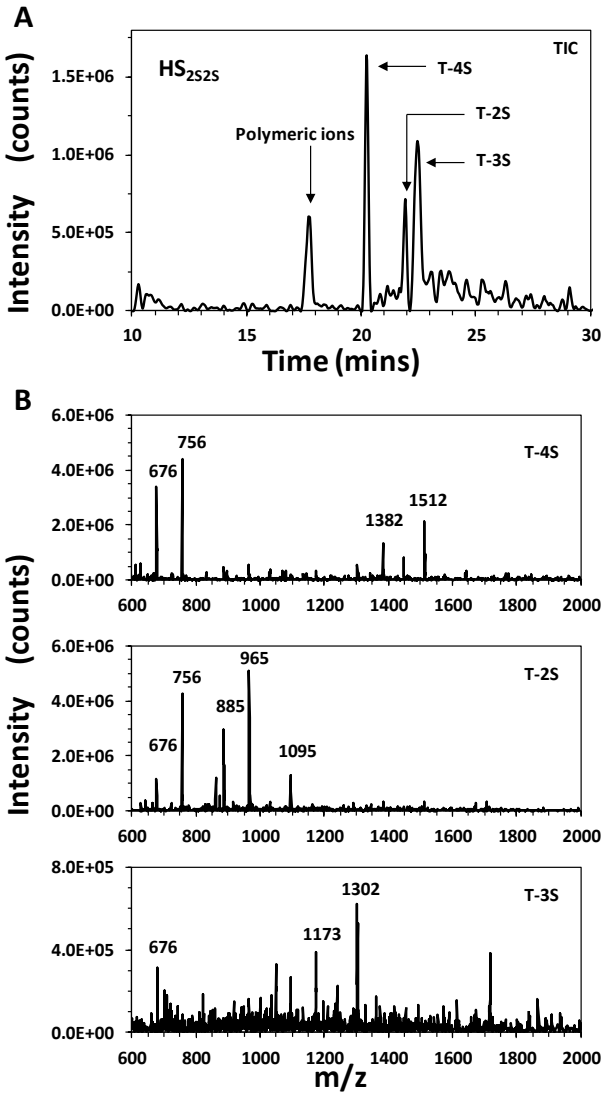

Figure 28. Reversed Phase Ion Pairing (RPIP) UPLC-MS total ion chromatogram (TIC) obtained after 24 hours digestion of HS_{2S2S} using heparanase I, II and III. The chromatogram shows the presence of tetrasaccharides with 2, 3 and 4 sulfate groups (T-2S, T-3S, and T-4S respectively) while also showing undigested polymeric ions. **(B)** The mass spectra in positive mode for the different tetrasaccharides showing the loss of ion-pairing agent: octylamine (130*m/z*) while also showing the fragmented core of tetrasaccharide (*m/z* = 676).

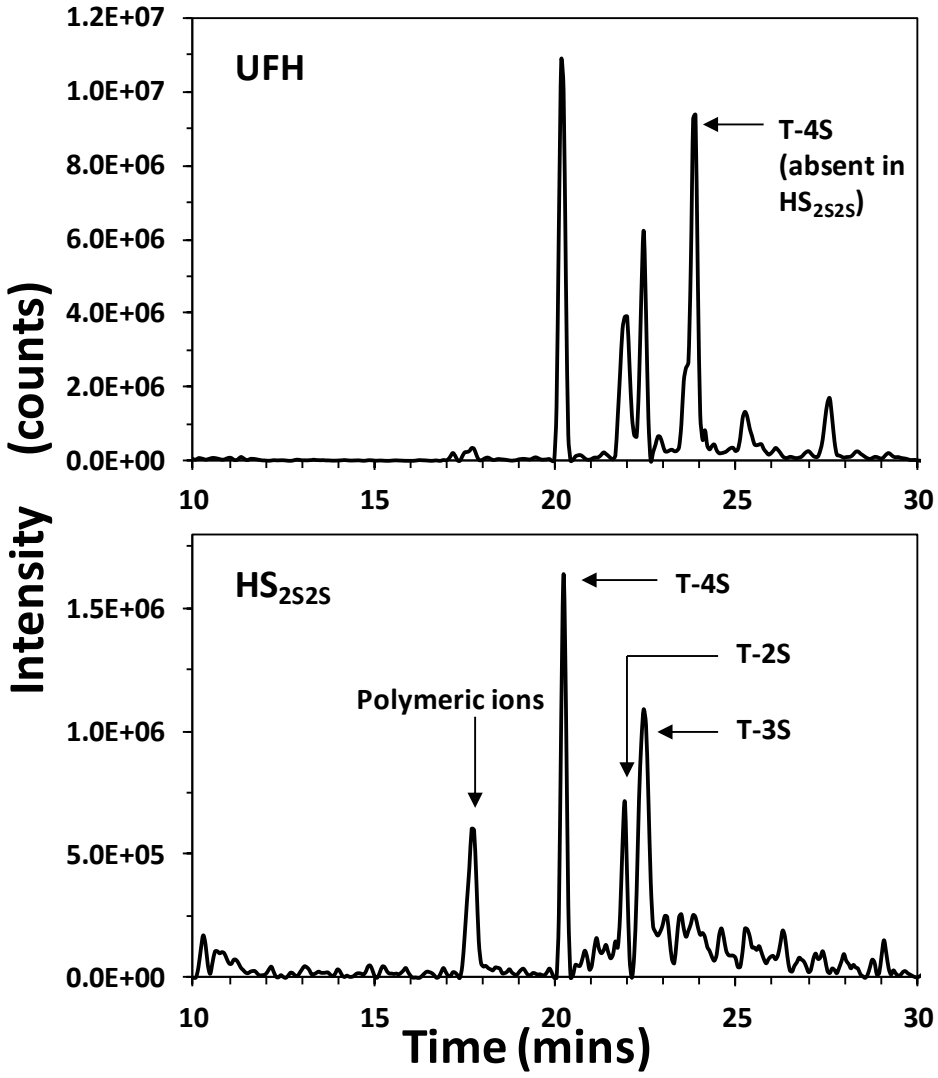

Figure 29. Total ion chromatograms using Method 1 of RPIP-UPLC-MS for unfractionated heparin (UFH) and HS_{2S2S} after 24 hours. While, HS_{2S2S} shows the presence of polymeric ions, UFH shows almost complete digestion to tetrasaccharide level. Additionally UFH shows the presence of a tetrasaccharide with 4 sulfate groups which is absent in HS_{2S2S}.

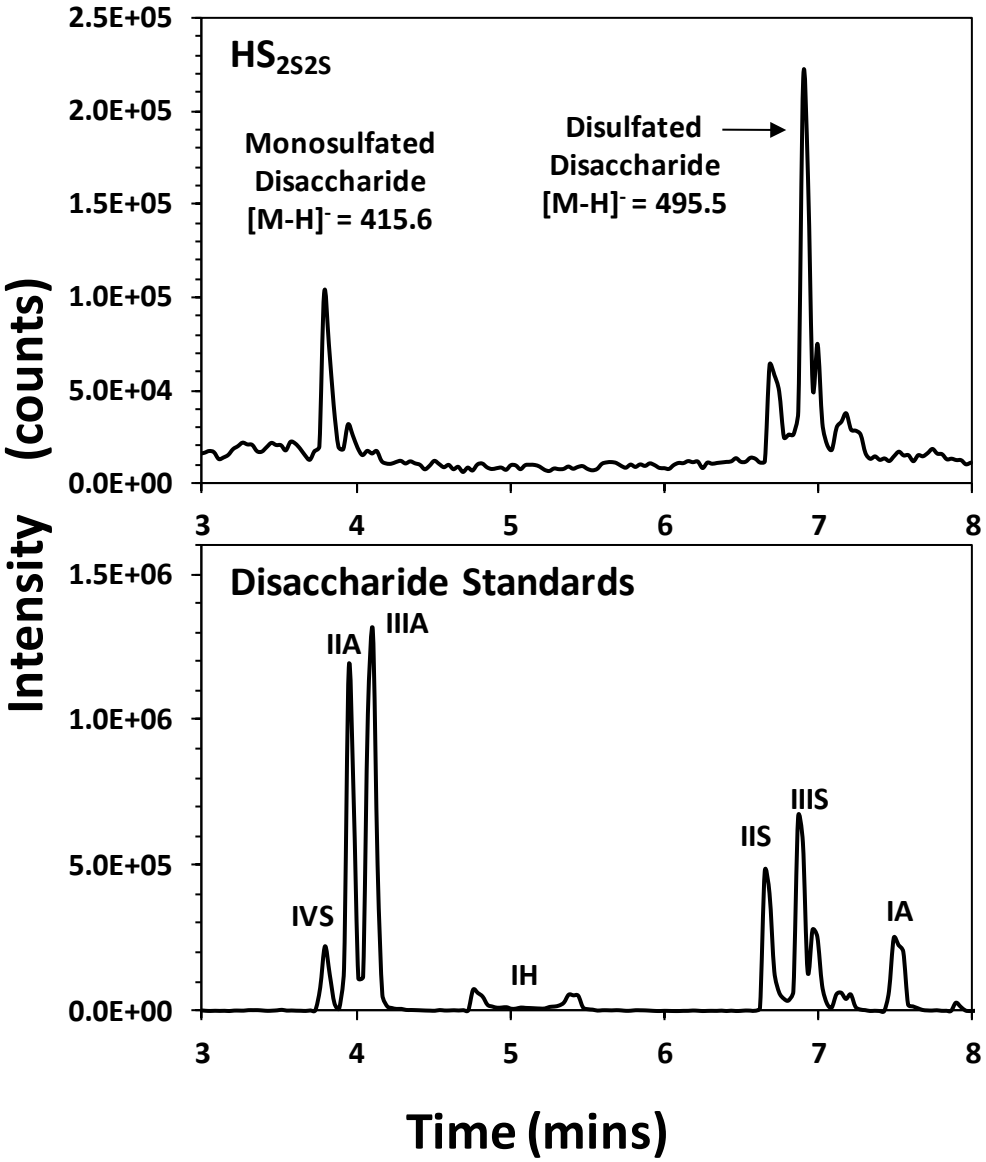

Figure 30. Comparison of disaccharide composition of HS_{2S2S} with known heparin disaccharide standards. The major peak HS_{2S2S} is the disulfated disaccharide which correlates well with the 2-sulfated and N-sulfated heparin disaccharide standard IIIS. HS_{2S2S} also shows the presence of a monosulfated disaccharide, which correlates well with the N-sulfated heparin disaccharide standard IVS.

4.2.4 HS_{2S2S} Potently Interacts with AT

To put the computational prediction of HS_{2S2S}–AT interaction to test, we measured the affinity of the HS variant for antithrombin. The interaction of HS_{2S2S} with AT was

followed using intrinsic tryptophan fluorescence following literature reports.[156] A characteristic decrease followed by gradual saturation was observed for fluorescence emission at 340 nm (λ_{EX} = 280 nm) under pH 7.0, *I* 0.06, 25 ºC conditions, which could be analyzed using the standard quadratic binding eq 3 to yield an AT binding affinity of ~90 nM (Figure 31, Table 10). In comparison, the affinity of full length unfractionated heparin (UFH) and homogenous heparin pentasaccharide (H5) for AT under pH 7.4, *I* 0.15, 25 ºC conditions have been measured to be ~10 and ~50 nM.[14,57] This implies that HS_{2S2S} binds AT with lower affinity than UFH and H5. However, considering the complete absence of the critical GlcN*p*2S3S6S residue in HS_{2S2S} (plus the absence of the adjacent residues that enhance the affinity of H5), the affinity is high. For polymeric heparin devoid of the GlcN*p*2S3S6S residue, an antithrombin affinity of 19 mM has been measured at pH 7.4, *I* 0.15, 25 ºC, which supports the conclusion that HS_{2S2S} potently binds AT.

Table 10: Equilibrium dissociation constant (K_D) and maximal fluorescence change (ΔF_{MAX}) for HS_{2S2S} – coagulation proteins complexes.[a]

Human Protein	ΔF_{MAX}	K_D
	(%)	*(μM)*
Antithrombin	-21±2[b]	0.09±0.03
Heparin co-factor II	-29±2	2.16±0.27
Thrombin	-37±2	0.49±0.09
Factor Xa	N/A[c]	>>100

[a]Measured using intrinsic (Trp) or extrinsic (fluoresceinylated protein) fluorescence in 20 mM Sodium phosphate buffer, pH 7.0, containing 25 mM NaCl, 0.1mM EDTA, 0.1% w/v Peg 8000 at 25 °C. See Experimental Section for additional details. [b]Error represents ±1 S.E. [c]not applicable

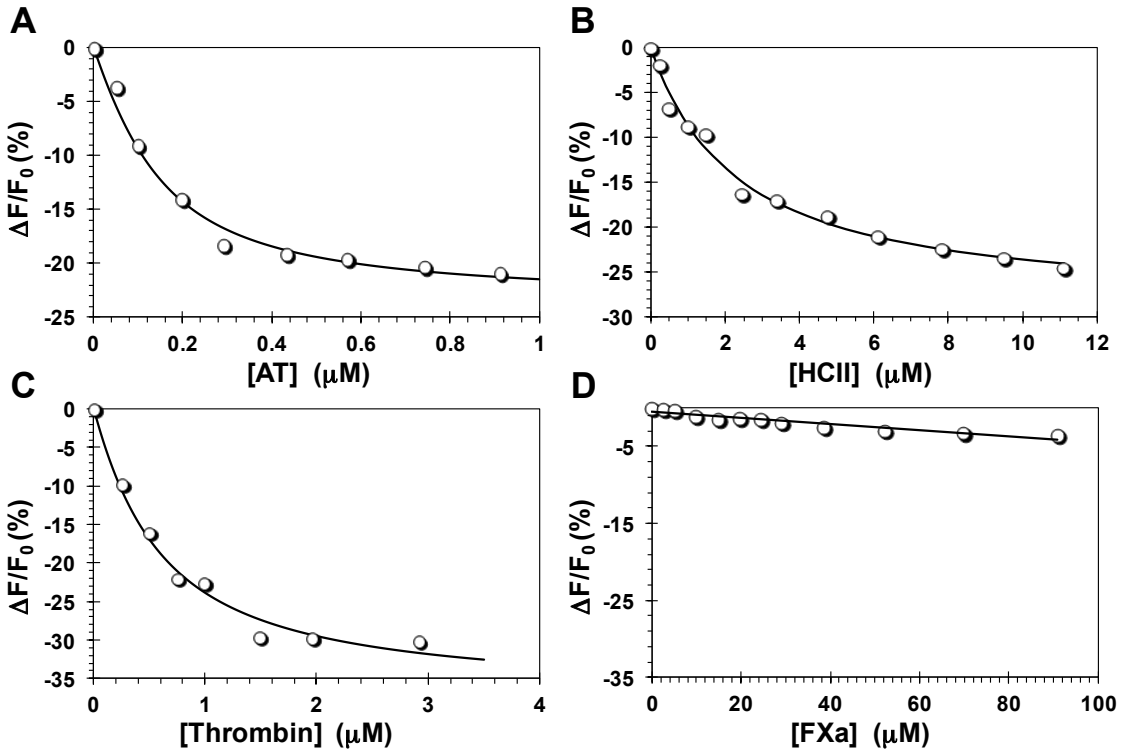

Figure 31. Affinity of HS_{2S2S} for antithrombin (A), heparin cofactor II (B), thrombin (C) and factor Xa (D). Interaction of HS_{2S2S} with the proteins was studied by following the proportional change in fluorescence ($\Delta F/F_0$) as a function of concentration in 20 mM sodium phosphate buffer, pH 7.0, containing 25 mM NaCl at 25 °C. The saturable decrease in Trp (for AT, λ_{EX} = 280 nm, λ_{EM} = 340 nm), TNS (for HCII, λ_{EX} = 330 nm, λ_{EM} = 448 nm) or fluorescein (Thr, λ_{EX} = 490 nm, λ_{EM} = 520 nm) fluorescence was fitted using quadratic eq 3 (solid line) to derive the maximal fluorescence change (DF_{MAX}) and equilibrium dissociation constant (K_D). Essentially no change in fluorescein fluorescence was noted for factor Xa (D). See 'Experimental Section' for additional details.

4.2.5 HS_{2S2S} Accelerates AT Inhibition of FXa really well

To assess the influence of HS_{2S2S} on the ability of AT to inhibit its two primary enzyme targets, we studied the kinetics of inhibition of FXa in a discontinuous assay at pH 7.4, *I* 0.06, 25 ºC, as described earlier. The exponential decrease in residual FXa activity as a function of time was used to derive the observed pseudo-first order rate constant (k_{OBS}) (Figure 32). The profile k_{OBS} versus the concentration of HS_{2S2S}–AT complex was found

to be linear (Figure 32), as expected, which could be fitted by eq 2 to obtain the second-order rate constant for the uncatalyzed inhibition (k_{UNCAT}) from the intercept and HS_{2S2S} catalyzed inhibition of FXa from the slope (k_{HS}).

The k_{UNCAT} was found to be 1490 $M^{-1}s^{-1}$, which is ~1.5-fold lower than that measured at pH 7.4, *I* 0.15, 25 ºC[57] and in line with the expectations arising from the reduced activity of the serine proteinase at the lower pH of the experiment. The k_{HS} was measured to be 323,300 $M^{-1}s^{-1}$, which translates to an increase of ~217-fold in the rate of FXa inhibition in the presence of saturating levels of HS_{2S2S}. This is a major acceleration in the efficacy of AT inhibition of FXa and compares favorably with an acceleration of ~300-fold brought about by H5[14] or ~600-fold induced by UFH.[57] In contrast, full length heparin devoid of the GlcN*p*2S3S6S residue accelerates AT inhibition of FXa by only about 70-fold. This implies that HS_{2S2S} induces AT activation through the conformational mechanism.

The kinetics of AT inhibition of TH in the presence of HS_{2S2S} was also studied in a similar manner at pH 7.0, *I* 0.06, 25 ºC (Figure 32). The k_{UNCAT} and k_{HS} were found to be 1,060 and 80,600 $M^{-1}s^{-1}$, respectively, which implies an acceleration of ~76-fold in the rate of TH inhibition in the presence of saturating levels of HS_{2S2S}. In comparison, UFH accelerates TH inhibition by AT nearly 1000-fold and absence of GlcN*p*2S3S6S in the full-length chain does not introduce any defect in this acceleration.[45] H5, on the other hand, induces only 1.7-fold increase in rate constant.[43] These results suggest that HS_{2S2S} activation of AT for inhibiting TH is not the traditional bridging mechanism, although the chain length of HS_{2S2S} is similar to that of UFH. This aspect is further discussed below.

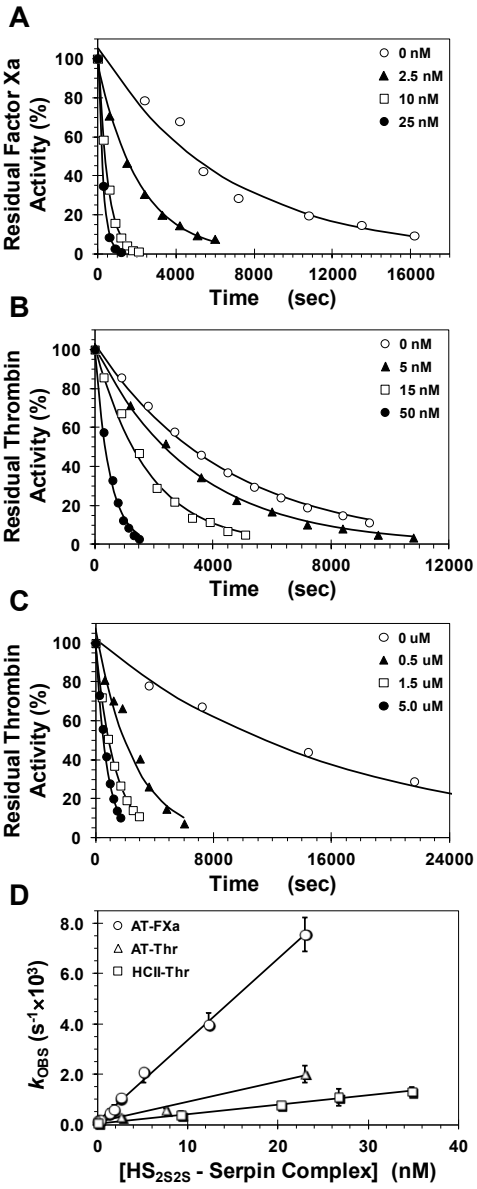

Figure 32. Kinetics of serpin (AT or HCII) inhibition of coagulation enzymes (TH or FXa) in the presence of HS_{2S2S} in 20 mM sodium phosphate buffer, pH 7.0, containing 25 mM NaCl at 25 °C. The residual protease activity was measured from the initial rate of Spectrozyme FXa (A) or Spectrozyme TH (B and C) hydrolysis under pseudo-first-order conditions as a function of time in the presence of different concentrations of HS_{2S2S} and fixed concentrations of AT (A) and HCII (B and C). The profile of the observed pseudo-first order rate constant of inhibition (k_{OBS}) at each HS_{2S2S} concentration was analyzed using linear eq 4 to calculate the uncatalyzed (k_{UNCAT}) and catalyzed (k_{HS}) rate constant of inhibition from the intercept and slope of the fitted lines (solid lines). See 'Experimental Section' for additional details.

4.2.6 Specificity of HS_{2S2S} Interaction with Coagulation Proteins

To assess whether HS_{2S2S} targets proteins related and relevant to the AT system, we studied its interaction with HCII, TH and FXa using spectrofluorometry at pH 7.0, *I* 0.06, 25 ºC. Unfortunately, the change in intrinsic tryptophan fluorescence could not be used for these three proteins because of a small signal. Hence, extrinsic fluorophores were utilized including TNS for HCII and fluorescein for TH and dansyl for FXa, which have been utilized earlier.[155,205] A saturable decrease in extrinsic fluorescence was found for HCII and TH suggesting that HS_{2S2S} binds with an affinity of 2.2 and 0.5 μM, respectively (Figure 31, Table 10). In contrast, essentially no change in fluorescence was observed for HS_{2S2S}–FXa system suggesting minimal interaction (>>100 mM). The results suggest that HS_{2S2S} binds to both HCII as well as TH with fairly high affinity, although it prefers AT by at least 5.5-fold. The dermatan sulfate–HCII and UFH–TH systems have been reasonably well studied and display affinities in the range of 0.5–50 μM at pH 7.4.[155] Likewise, the affinity of a high affinity dermatan sulfate hexasaccharide for HCII has been reported to be 20 μM.[92] Thus, although a direct comparison of the affinities is not possible because of differences in conditions, HS_{2S2S} binds to HCII and TH with affinities either comparable to or better than other GAGs.

4.2.7 HS_{2S2S} accelerates HCII inhibition of TH

To assess whether the dual interaction of HS_{2S2S} is an aid or barrier to HCII inhibition of TH, we studied the kinetics of inhibition (Figure 32). The second-order rate constant of HCII inhibition of TH was measured in a manner similar to that for AT through discontinuous measurement of pseudo-first order rate constants at varying HS_{2S2S}

concentrations. HCII inhibition of TH was also accelerated ~38-fold by HS_{2S2S} (Table 11). In comparison, full-length heparin and dermatan sulfate are known to accelerate this reaction greater than 2000-fold predominantly through a conformational change mechanism.[155] The literature reports that HCII–UFH system is a non-specific system,[155] which implies that even if HS_{2S2S} was binding to HCII in a non-specifically manner, an activation significantly higher than 38-fold should have been observed. This implies that most probably favorable binding to TH in addition to HCII is most probably limiting full activation potential of HS_{2S2S}.

Table 11: Acceleration in serpin inhibition of coagulation enzymes brought about by HS_{2S2S}.[a]

Serpin – Enzyme System	k_{UNCAT}	k_{HS}	Acceleration[b]
	$(M^{-1}s^{-1})$	$(M^{-1}s^{-1})$	
AT – FXa	1490±200[c]	323,300±7,560	217±34
AT – Thr	1060±100	80,600±8,200	76±15
HCII – Thr	1090±100	36,800±1,320	34±4

[a]Measured using discontinuous enzyme inhibition assay in 20 mM Sodium phosphate buffer, pH 7.0, containing 25 mM NaCl, 0.1mM EDTA, 0.1% w/v Peg 8000 at 25 °C. See 'Experimental Section' for additional details. [b]Refers to the ratio of catalyzed and uncatalyzed rate constants. [c]Error represents ±1 S.E.

4.2.8 HS_{2S2S} Directly Inhibits TH, but not FXa

To assess whether HS_{2S2S} directly inhibits target proteases, TH and FXa, we measured their residual activity in the presence of HS_{2S2S} using chromogenic substrate hydrolysis assay, as described earlier.[207] Interestingly, TH activity decreased as a function of HS_{2S2S} concentration, which could be fitted using the logistic dose-response eq 3 to obtain an IC_{50} of 4.3±0.3 μM (Figure 33) and an efficacy of 40±1.3 %. In contrast, FXa activity

remained[214,215] essentially unaffected even at 100 μM HS_{2S2S}.[47, 48] Although a number of studies report GAG binding to thrombin,[134,216] this is the first demonstration of direct TH inhibition. We have previously reported a group of polymeric sulfated GAG mimetics as potent direct inhibitors of TH (and also of FXa). These sulfated GAG mimetics were significantly more hydrophobic than GAGs and were found to bind to exosite II of thrombin and induce allosteric inhibition. In a similar manner, we hypothesize that HS_{2S2S} also exhibits allosteric inhibition of thrombin. This implies that HS_{2S2S} is able to exploit a major difference in heparin-binding sites of two highly similar serine proteases.

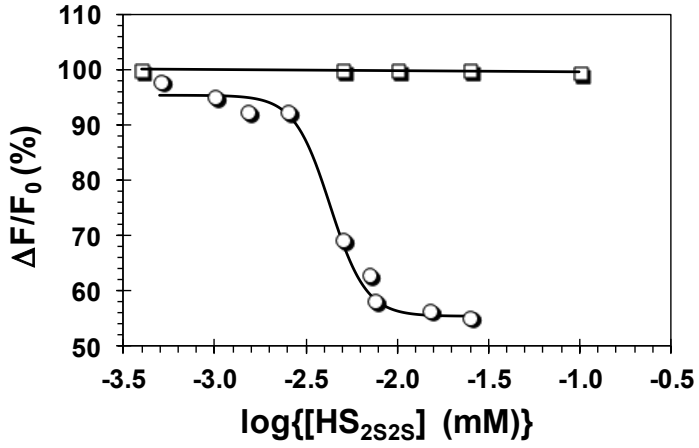

Figure 33. Studies on direct inhibition of thrombin (❍) and factor Xa (❑) by HS_{2S2S}. Protease inhibition was measured spectrophotometrically through chromogenic substrate hydrolysis assay in 20 mM sodium phosphate, pH 7.0, containing 25 mM NaCl at 25 °C. Solid lines represent sigmoidal fits to the data using eq 3 to obtain IC_{50}, Y_M and Y_0. See 'See experimental Section' for additional details.

4.3 Discussion

4.3.1 Rare Saccharide Sequences as a means to Identify Novel Interactions

The strategy of utilizing rare saccharide sequence have been fruitful in the identification of novel interactions and can serve as an efficient tool. Numerous reported examples showcase the importance of other rare sequence like the *3-O* sulfate glucosamine residue among similar examples. The *2-O* sulfate glucuronic acid we studied is another such rare sequence and is interesting from the chemical biology perspective especially in unearthing novel interaction with known coagulation systems.

4.3.2 Differential Affinity and Specificity of HS_{2S2S} allows Probing of Coagulation Cascade Pathways

The accelerated inhibition of thrombin by antithrombin occurs mainly by a bridging mechanism, where the main driving force is co-localization of antithrombin and thrombin on the surface of heparin, which requires high-affinity, high-specificity antithrombin-heparin and low-affinity, low-specificity thrombin-heparin interactions.[43] Discovery of the HS_{2S2S} polymer is a unique event because it possesses high affinity (≤ 500 nM) for both, antithrombin and thrombin. This enables us to deduce the effects of high affinity on coagulation pathways. As observed, HS_{2S2S} accelerates inhibition of thrombin by antithrombin only by 76-fold (Table 11), compared to ~2,400-fold, as observed previously.[43] On the other hand, HS_{2S2S} accelerates inhibition of FXa by antithrombin 217-fold, which is similar to previous observations.[46,217] The reason for this reduced thrombin-inhibition compared to unchanged FXa-inhibition by antithrombin lies in the mechanism of action exerted by the participating GAG. Antithrombin-mediated FXa

inhibition is mainly due to conformational change induced by heparin, which is clearly also exerted by HS_{2S2S}, and is perhaps caused by specific electrostatic interactions. However, previous studies for the antithrombin-heparin-thrombin interaction comprehends a ~1.7-fold conformational and ~2400-fold bridging mechanism attributed to the acceleration.[43] The antithrombin-HS_{2S2S}-thrombin system possibly maintains the conformational aspect however, due to the increased affinity towards TH, loses the bridging mechanism and accounting for the vast loss of acceleration.

The HCII-heparin-thrombin system shows a ~2400-fold activation of the serpin with ~7-fold attributed to bridging and ~2400-fold attributed towards conformational activation. The low 34-fold acceleration seen in the presence of the HS_{2S2S} polymer thus indicates a lower specificity of interaction incapable of replicating a similar level of conformational activation as heparin. However, a miniscule level of activation is observed, serving as a proof of the concept that affinity need not necessarily translate into high specificity.

4.3.3 Direct Inhibition of Heparin is a Previously Unknown Effect

Thrombin-heparin interactions have been widely reported to be non-specific. Heparin is known to bind to the exosite II of thrombin, but does not produce any direct inhibition of thrombin. Thus, the direct inhibition of thrombin observed here is a novel effect. The mode of action here perhaps cannot be described by the model employed here to assess specificity of interactions between thrombin and HS_{2S2S} because heparin is not known to manifest a similar inhibition by binding at this site. This also lays stress on the study of rare disaccharides in glycobiology.

4.3.4 Computational Studies can Predict Protein-GAG Specificity and Affinity

Our work provides a good platform to showcase the utilization of computational tools in understanding complex systems and designing agents by a systematic approach to allow for more predictable outcomes. Heparin and heparan sulfate are notoriously heterogeneous systems with a variety of saccharide compilations and sulfation patterns making it a difficult system to work with in an experimental setting. Utilizing the computational resources at our disposal we have attempted to decipher specific non-natural monosaccharides/disaccharides present in the abundant H/HS library. The *in vitro* results thus obtained were expected, based on our design strategy. Thus, this serves as platform to further utilize computational design strategies to provide prediction in the outcomes when dealing with such complex mixtures.

4.4 Experimental Section

4.4.1 Computational Methods

Preparation of a Library of HS Hexasaccharides for Computational Studies

Ten HS disaccharide sequences containing GlcA*p*2S or GlcN*p* were constructed using SybylX v. 2.0. The sequences incorporated all the known natural variations at the 2-, 3- and 6-positions of the two residues. These disaccharides were then used to construct a combinatorial library in which oligomerization at the C-4 and C-1 positions was performed by deletion of appropriate atom(s) and addition of a desired disaccharide sequence. The operations were repeated in an automated manner to produce a library of 9918 hexasaccharide sequences containing at least one

→4)GlcA*p*2Sβ(1→4)GlcN*p*2S(1→ or →4)GlcN*p*2Sα(1→4)GlcA*p*2S(1→ disaccharide sequence.

Docking of HS_{2S2S}-containing Hexasaccharide Library onto AT

The AT structure used in these studies was 1TB6[134] and was prepared using Sybyl's "prepare protein" option. Hydrogens were added and minimized using the Tripos force field and Gasteiger-Hückel charges. The library of 9918 HS_{2S2S} sequences was docked into the heparin-binding site of AT using GOLD,[208] which uses a genetic algorithm to place ligands into the binding site. Each hexasaccharide sequence was docked using 100 GA runs, each consisting of 100,000 iterations. A 16 Å docking radius around the NZ atom of Lys125 was used, which is approximately in the center of the heparin-binding site of AT. The inter-glycosidic linkages of the hexasaccharides were maintained rigid at the average phi and psi values derived from the literature.[18] The GA runs were allowed to terminate early if the top three solutions had an RMSD of 2.5 Å or lower, of which the two best poses were stored and analyzed at the end of the docking experiment. GoldScore was used to assess the fitness of the docked poses.

Grid-based Screening of Protein-monosaccharide Interactions

The overall scheme describing assessment of specific and high-affinity protein-monosaccharide interactions is described in Figure 27. In-house python scripts that incorporated the Openeye OEChem toolkit[218] were used to investigate the residence tendencies of monosaccharides on protein HBSs. A grid was generated around the docked 2S2S-containing hexasaccharides to analyze preferences in location of monosaccharides. A density map was obtained by counting the number of times a

monosaccharide resided closest to a grid point. Statistical significance of monosaccharide enrichment at its highest-density location compared to other locations on the grid was analyzed using a proportionality test in the R statistical programming environment.

Clustering and Statistical Evaluation

A k-means clustering algorithm for comparison of molecular positions was generated in-house using the Openeye OEChem toolkit.[218] The algorithm was specifically asked to search for 2 clusters amongst a group of monosaccharide positions, maximizing the distance between the cluster centers. This enabled identification of the "tightest" cluster, i.e. showing least deviation in atomic positions of the pyranose ring, as measured by the RMSD metric. All statistical analysis was conducted using the R statistical environment.[304]

4.4.2 Proteins and Chemicals

Human plasma AT, HCII, thrombin (TH), fluorescein tagged TH (FFPRCK-TH) and fluorescein tagged human FXa (FXa-DEGR) were purchased from Haematologic Technologies (Essex Junction, VT) and used as such. The proteins were stored in 20 mM sodium phosphate buffer, pH 7.0, containing 25 mM NaCl, 0.1 mM EDTA and 0.1% (w/v) PEG8000 at -80 °C. Spectrozyme FXa and thrombin were obtained from American Diagnostics (Greenwich, CT). TNS ((2-(*p*-toluidino)naphthalene-6-sulfonic acid) was purchased from Sigma Aldrich (Milwaukee, WI). Anhydrous CH_3CN and, NH_4OAc, acetic acid were purchased from Fisher scientific (Pittsburgh, PA) and used as such. Tributylamine (TrBA), octylamine (OTA) were purchased from Acros organics (New Jersey, NY). All these reagents were of a high purity LC/MS grade quality. Heparin

standards (1,1,1,3,3,3-Hexafluoro-2-propanol) were obtained from Galen labs (Middletown, CT) whereas, the unfractionated heparin was purchased from Sigma Aldrich (Milwaukee, WI).

4.4.3 Mass Spectrometry Studies

Enzymatic Digestion

An enzymatic digestion on 320 μg of HS_{2S2S} or porcine unfractionated heparin (UFH) was performed in 40 μL volume. The sample was treated with heparinase I, II and III (5 mIU each/ 1mg substrate). The mixture was incubated in the Acquity H-Class UPLC sample's manager (Waters) for 75 h at 37 °C. Direct sampling of 5μL from the reaction mixture was performed and injected into the UPLC-MS after 5, 26, 48 and 75 h using the following technique of reversed-phase ion-pairing (RPIP).

RPIP UPLC-MS

All analyses were carried out with Waters Acquity H-Class UPLC system coupled to Waters Acquity TQD detector (Milford, MA). There are several UPLC-MS techniques in the literature for analysis of GAGs oligosaccharides and disaccharides.[43-45] We performed a time-based digestion of HS_{2S2S} and unfractionated heparin (as control) using heparinases I, II, and III. The initial formation of oligosaccharides was monitored using Method 1, while the disaccharide composition upon complete digestion was examined using Method 2.

Method 1

For analysis of oligosaccharides during the initial stages of digestion (5 and 26h), we adopted the UPLC separation method and MS parameters described by Robert J. Linhardt

et al. and Cynthia K. Larive et al. with some modifications.[213] The reversed phase separation was performed by injecting 5μL of the digestion mixture onto an Acquity UPLC BEH C18 1.7 μm (2.1 x 150 mm) column with a guard column. The temperature of the column was maintained at 40 °C. A gradient of 100% solvent A was maintained at a flow rate 0.1ml/min for 2 min and raised to 100% of solvent B over 45 min. Solvent A consisted of Water:ACN (95:5, v/v), and solvent B was (15:85, v/v). Both solvents A and B contained 15 mM octylamine (OTA) as an ion-pairing reagent and 100 mM HFIP as organic modifier. The outlet from the column was passed through an Acquity PDA detector and directly infused into the mass spectrometer. The ESI-MS was performed in positive ionization mode with a capillary voltage of 3.20 KV, extractor voltage of 1V, radio frequency of 0.1V, source temperature of 150 °C, and desolvation temperature of 350 °C. MS scans between 500-2000 m/z were obtained at different cone voltages ranging from 20V-100V in 20V increments so as to monitor in source fragmentation.

Method 2

For disaccharide analysis after complete digestion (>48hrs), we performed a method previously demonstrated for heparin disaccharide analysis.[213] Briefly, the binary solvent system contained the same concentrations of ion pairing agent tributylamine (TrBA) 20 mM, ammonium acetate 2.5 mM and acetic acid 22.2 mM. Solvent A and B consists of Water:ACN (95:5, v/v) and (20:80, v/v), respectively. The pH of the mobile phase was carefully adjusted at 7. An injection of 5μL of the digestion sample or heparin disaccharide standard mixture containing 50μg/ml of each standard was made onto the Acquity UPLC BEH C18 1.7 μm (2.1 x 100 mm) column with a guard column. The

temperature of the column was maintained at 40°C, while the flow rate was maintained at 0.5ml/min. The ESI-MS was set to negative ionization mode using a capillary voltage of 3.0 KV, extractor voltage of 1V, radio frequency of 0.5V, source temperature of 150 °C, desolvation temperature of 350 °C. The cone gas flow of 20L/h worked best on our instrument so as to prevent source contamination. The MS scans were obtained from 250-1000 m/z with 20V, 30V and 40V cone voltage settings. An SIR for the various disaccharides standards was also set up to allow better comparison with quicker scan times.

4.4.4 Equilibrium Binding Studies using Fluorescence Spectroscopy

The dissociation constant of HS_{2S2S}–protein complexes were measured using change in fluorescence emission as a function of the concentration of the GAG in 20 mM sodium phosphate buffer, pH 7.0, containing 25 mM NaCl, 0.1 mM EDTA and 0.1% PEG8000 at 25 °C, as described earlier.[176] The experiments were performed using a QM4 fluorometer (Photon Technology International, Birmingham, NJ) in a quartz microcuvette by titrating it into a 200 μL solution of the protein (100–250 nM) and monitoring the change in the fluorescence at either 340 nm (for AT, λ_{EX} = 280 nm), 520 nm (for TH, λ_{EX} = 490 nm), 448 nm (for HCII, λ_{EX} = 330 nm), or 547 nm (for FXa, λ_{EX} = 345 nm). The concentration of TNS used for measuring affinity of HS_{2S2S} for HCII was 10 mM. Excitation and emission slit width were set to 1.0 mm. The saturable change in fluorescence signal was fitted using the quadratic equilibrium binding eq 3 to obtain the K_D of interaction. In this equation, ΔF represents the change in fluorescence at a fixed concentration of HS_{2S2S} from the initial fluorescence F_0 and ΔF_{MAX} represents the maximal change in

fluorescence following saturation of the protein. $[P]_0$ represents the concentration of either AT, HCII, TH or FXa.

$$\frac{\Delta F}{F_0} = \frac{\Delta F_{max}}{[P]_0} \times \{\frac{([P]_0 + [HS_{2S2S}]_0 + K_D) - \sqrt{(([P]_0 + [HS_{2S2S}]_0 + K_D)^2 - 4[P]_0[HS_{2S2S}]_0)}}{2}\} \quad (3)$$

4.4.5 Kinetics of Protease Inhibition in the Presence of HS_{2S2S}

The kinetics of inhibition of coagulation proteases, TH or FXa, by AT or HCII in the presence of HS_{2S2S} was measured spectrophotometrically using a microplate reader (FlexStation III, Molecular Devices) under pseudo-first-order conditions, as described earlier.[82] Briefly, a fixed concentration of TH or FXa (5 nM) was incubated with fixed concentrations of plasma AT (100 nM) or HCII (50 nM) and HS_{2S2S} (0 – 5000 nM) in 20 mM sodium phosphate buffer, pH 7.0, containing 25 mM NaCl, 0.1 mM EDTA and 0.1% (w/v) PEG8000 at 25 °C. At regular time intervals, an aliquot of the inhibition reaction was quenched with 100 µL of 125 – 200 µM chromogenic substrate (Spectrozyme TH or Spectrozyme FXa) in 20 mM sodium phosphate buffer, pH 7.0, containing 25 mM NaCl at 25 °C. To determine the residual protease activity, the initial rate of substrate hydrolysis was measured from the increase in absorbance at 405 nm. The exponential decrease in the initial rate of substrate hydrolysis as a function of time was used to determine the observed pseudo-first-order rate constant of protease inhibition (k_{OBS}). A plot of k_{OBS} at different concentrations of HS_{2S2S}–serpin complex could be described by eq 4, in which k_{UNCAT} is the second-order rate constant of protease inhibition by serpin alone and k_{HS} is the second-order rate constant of protein inhibition by serpin-HS_{2S2S} complex (HS_{2S2S}:P).

$$k_{OBS} = k_{UNCAT}[P]_0 + k_{HS}\,[HS_{2S2S}{:}P] \quad (4)$$

4.4.6. Direct Protease Inhibition in the Presence of HS_{2S2S}

Direct inhibition of TH or FXa was measured through a chromogenic substrate hydrolysis assay using a microplate reader (FlexStation III, Molecular Devices), as described earlier.[177] Briefly, each well of the 96-well microplate contained 190–X μL of pH 7.0 buffer to which X μL of HS_{2S2S} (to give 0 – 25 μM final concentration), or reference, was added followed by 5 μL of protease (to give 5 nM final concentration). After 10 min incubation at 25 °C, 5 μL of appropriate chromogenic substrate (to give 125 mM (Spectrozyme FXa) or 200 mM Spectrozyme TH) was rapidly added and the residual protease activity was measured from the initial rate of increase in A_{405}. Relative residual protease activity at each concentration of HS_{2S2S} was calculated from the ratio of the activity in the presence and absence of the inhibitor. The dose – response profile was fitted by eq 5 to calculate the potency (IC_{50}) and efficacy ($\Delta Y = Y_M - Y_0$) of inhibition. In this equation, Y is the relative residual protease activity, Y_M and Y_0 are the maximum and minimum values of the relative residual protease activity, IC_{50} is the concentration of HS_{2S2S} that results in 50% inhibition of protease activity and HC is the Hill slope.

$$Y = Y_0 + \frac{Y_m - Y_0}{1+10^{\left(log[HS_{2S2S}]_0 - log\, IC_{50}\right) HC}} \qquad (5)$$

CHAPTER 5: SULFATED QUINAZOLIN-4(3H)-ONES AS ALLOSTERIC MODULATORS TARGETING FXIa.

5.1 Introduction

Advances in the field of anticoagulants have been abundant and continuous over recent years Yet, thromboembolism continues to be a major concern in the clinical set up.[10] The direct inhibitors of FXa and thrombin have progressed considerably with newer drugs being added to this class of inhibitors.[219] Nonetheless, the bleeding risks associated with the older agents have been persistently seen at an alarming rate within the newer generation of anticoagulants as well, making it vital to develop newer strategies to develop safer agents.[220,221] Generally, FXa and thrombin which, belong to the common pathway of the cascade, are known to be essential from the initiation and propagation perspectives. However, proteases belonging to the intrinsic pathway are primarily involved in the amplification of the coagulation signal.[9,11] A hypothesis that is gradually gathering pace involves engaging proteases in the intrinsic pathway.[221] Proteases such as FXIa can be targeted to develop safer antithrombotics compared to FXa and thrombin. Current studies have indicated that depleting FXIa levels reduces thrombotic complications whilst leaving the hemostatic system intact.[9,11,105] Similarly, absence of FXI was found to cause mild bleeding disorders whereas; the occurrence of ischemic stroke was evidently reduced in such patients.[108] Elevated FXI levels were found to

enhance risk of venous thrombosis and cardiovascular diseases in women.[105-107] Consequently, FXIa could serve as a more efficient and safer target.

GAGs including heparin are known to interact with a number of enzymes in the coagulation cascade.[222] A major problem in discovering GAG-based molecules, however, is the rather poor specificity of interaction of these with proteins.[129,222,223] This is generally due to the nature of the forces that are responsible for interactions that are electrostatic in nature and predominantly nondirectional and operational over long distances.[222] This implies that these could, therefore, non-selectively recognize any positively charged domain of a protein severely limiting its selectivity profile. Strategies designed to overcome these problems range from the application of small saccharide units with limited anionic groups (sulfates, phosphates, carboxylates) like the oligosaccharides containing sulfate and phosphate apatamers, sulfated-linked cyclitols, and dendritic polyglycerol sulfates.[133,224-226] Another concept utilizes sulfate decorated small molecules like sulfated flavones, sulfated xanthones and sulfated tetrahydroisoquinolines.[82,176]

5.1.1. Hypothesis

The field suffers from the lack of a generalizable strategy for the rational design of modulator of GAG-protein interactions. Consequently a rational strategy was devised in the Desai laboratory, which involves the utilization of the hydrophobic (hP) domain near the heparin binding sites (HBS) of proteins.[206] This domain has been observed to be different in various proteins and thus we hypothesized that it should be possible to

discover molecules, herein called as sulfated allosteric modulators (SAMs), by exploiting differential recognition of hP patches around the HBS. This strategy is postulated to recognize the binding site in two steps which involves (1) initial attraction of an anionic sulfate group present on a SAM to the one or more electropositive lysine/arginine residues located in the heparin-binding protein (HBP) followed by (2) recognition of an adjacent hP patch on the HBP to form a complex (Figure 34). Thus, if this strategy is valid, enzymes devoid of either the electropositive HBS or the hP domain would not favorably interact with the SAM and thereby lack inhibition. Enzymes possessing both the electropositive HBS and the hP will be targeted by SAM. However, the potency of inhibition is dependent on the complementarity of the SAMs hydrophobic scaffold with the hP domain on the enzyme. Briefly, this strategy revolves around the electronic steering of the small molecule to the HBS of the protein due to nondirectional initial, weak ionic bond followed by filtering and tight locking of an optimal hydrophobic SAM scaffold.[206]

5.1.2. Studies on first generation of quinazolin4-(3H)ones (QAOs) as allosteric inhibitors of FXIa

The dual element hypothesis (Figure 34) was examined by a library of 26 QAOs including 7 monomers and 19 dimers containing 1-4 sulfate groups. This scaffold is a well-known hP scaffold with three-dimensional similarity to flavonoid scaffold studied earlier as heparin binding site (HBS) ligand.[176,227,228] The monomers were synthesized using simple condensation techniques (see experimental section) and then sulfated.[229] Inhibition data however, revealed lack of any activity against fXIa. To further diversify, a

library of 19 dimers was synthesized; each designed to probe specific features of the fXIa-binding site. In general, these could be classified on the basis of the feature probed,

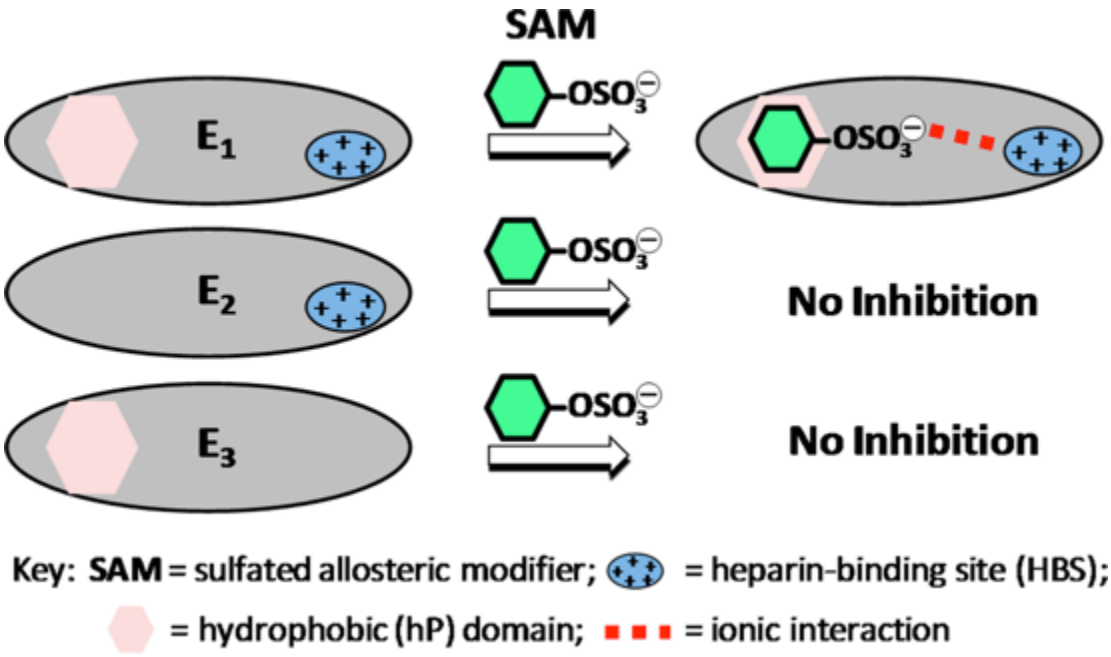

Figure 34. Strategy for the design of a SAM of a GBP exploiting the difference in hydrophobicity (hP, shown as light colored patch) on the periphery of a HBS (shown as blue ellipse with positive charges). A SAM binds an enzyme (shown by red dashed line), e.g., E1, only if it contains both hP and HBS. E2 and E3 do not recognize the SAM because of an absence of either hP or HBS. This generates selectivity of recognition.[206] (Adapted from reference 206).

1) **Number of sulfate groups**- In general, monomers containing a single sulfate group were found to be inactive. Similarly, dimers containing a single sulfate group were not potent either. Only dimers containing two sulfate groups, one sulfate group on each dimer were deemed active (Figure 35A). However, dimers possessing 3 or 4 sulfates displayed a reduced potency towards fXIa.[206]

2) **The core quinazolinone scaffold-** Around 14 compound possessed the quinazolinone scaffold to form the dimer. (Figure 35A), which though not symmetric in the technical terms, were referred to as the homo-dimers due to the incorporation of a quinazolinone scaffold on both the monomers. The activity for such compounds ranged from (50-320 μM). To test the structural dependence of the hP domain, flavonoid-containing dimers were synthesized. These involved the incorporation of a flavonoid scaffold additionally; these were decorated with 4 sulfates and hence the term hetero-dimers (Figure 35C). However, these lacked any activity against fXIa thereby indicating the importance of the quinazolinone scaffold.
3) **The linker length and geometry-** The linker length and geometry were examined through the synthesis of compounds containing varying length (8-11) of intervening atoms. Similarly, the geometric constraints were varied through the use of 1,4- (Figure 35A) or 1,5-triazole (Figure 35D) and the two-triazole linker analogs (Figure 35B). IC_{50} studies with this set indicated increasing potency with increasing linker length; similarly, the 1,4- triazole geometry was found to be more suitable to maintain potency. However, the need to introduce a more extensive search to further understand this domain was deemed to be essential to enhance potency and improve selectivity.
4) **The position of the sulfate groups-** For active dimers decorated with two sulfate groups, the presence of a sulfate group at the para-para position was more favorable as compared to its positioning at the meta-para position and the meta-meta positions.

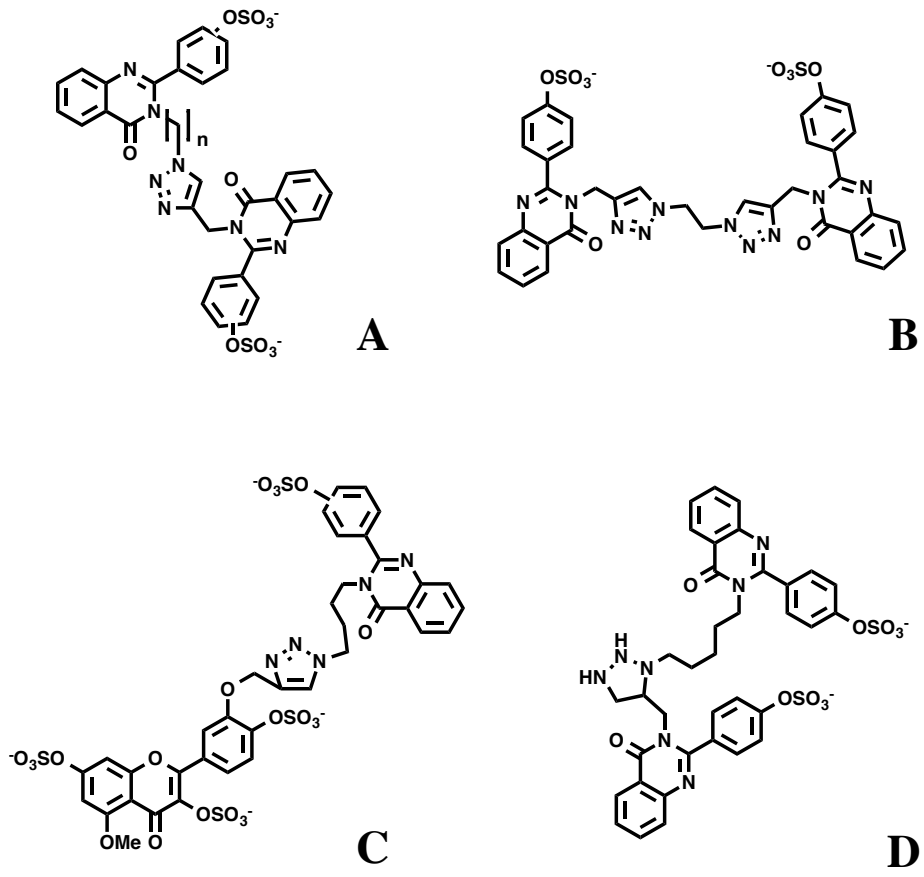

Figure 35: The library of first generation QAO dimers. A. Quinazolinone dimer with a 1,4-triazole linker B. Quinazolinone dimer with a two triazole rings in the linker C. Mixed dimer containing a flavonoid scaffold D. Quinazolinone dimer with a 1,5-triazole linker.

5.1.3. Mechanism of Inhibition of First Generation Sulfated Quinazolinones

Mechanistic studies provided insights into the functioning of these molecules, primarily indicating key features

1. All these molecules indicated a lack of potency against other serine proteases in the coagulation and the digestive system (FXa, thrombin, trypsin and chymotrypsin) indicating the success of the dual element strategy.

2. Michaelis-Menten studies indicated these to be functioning through a non-competitive mechanism, which was a major design goal of the dual element strategy.
3. Mutagenesis studies indicated the location of binding to be around the heparin-binding site within the catalytic domain. Similarly, studies involving neutralization of the charge interaction through the use of an electropositive polymer confirmed the functioning through the hP domain.
4. Fluorescence-based affinity studies shows a sigmoidal profile suggestive of a cooperative binding process, further confirmed by the high Hill coefficient (6.4-9.0).

These extensive studies therefore, laid the foundations for confirming the functioning of the dual element strategy as well as providing insights into the mechanism of action of these agents.

5.1.4. Updated Hypothesis: Second Generation of FXIa Inhibitors

The first generation of allosteric SAMs were beneficial in providing a basic understanding of the dual element strategy and the functioning of this system. Utilizing the important inferences obtained through these studies, we have tried to improve on the general features like the potency and understanding the of the mechanism understanding of this class of molecules. A major domain that we postulated to have large effects on the potency of these molecules was the linker domain. We therefore fragmented the core structure of the first generation library and split it into 3 major domains: 1. **The hydrophobic domain** 2. **The linker domain** 3. **The charged group-containing domain**. (Figure 36)

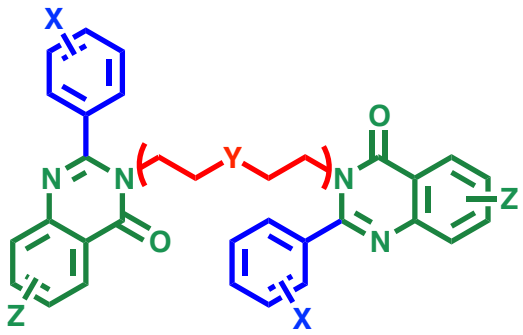

Figure 36. Strategy for the design of more potent and selective set of molecules, by splitting the scaffold into the hydrophobic domain (green), the linker region (red) and the charged group containing domain (blue)

Previous studies had already established the importance of the quinazolinone based hydrophobic domain, with the replacement of a flavonoid conferring a decrease in potency. Similarly, the presence of two sulfates, one on each monomer, is essential to maintain activity. Modifications in the linker domain indicated the most promise for developing newer more potent and selective agents. The linker length and geometry was therefore targeted through a library of molecules with major modifications aimed at this domain. This work describes the utilization of dual element strategy with further modifications in the linker domain and the mechanistic outcomes of these modifications.[206]

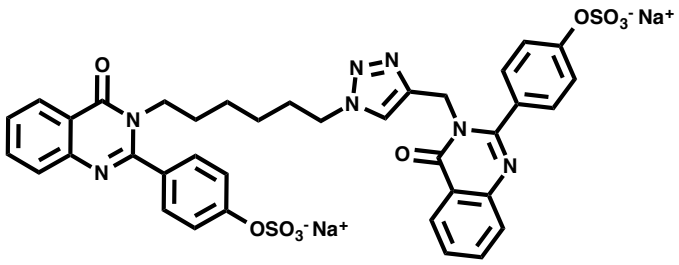

Figure 37. The structure of **16S**, IC_{50} = 52 μM.

5.2. Results and Discussions

5.2.1. Synthesis of the Library of QAOs.

In continuation with our initially reported dual element strategy, we synthesized a total of 18 sulfated dimers. These were synthesized with modifications to our reported lead **16S** (Figure 37).[206] We employed a new approach to synthesize a library of fairly diverse compounds with major modifications targeting the linker domain (Figure 36). The original approach utilized copper-catalyzed azide-alkyne cycloaddition (CuAAC) reaction, which was used to dimerize the quinazolinone dimers incorporating a triazole ring in the linker during the process. The new strategy incorporates a simple aromatic or aliphatic linker by utilizing a simple nucleophilic substitution reaction. Thus, affording a library of 18 diverse compounds **7S-24S**, which could be used to further probe the heparin-binding site in FXIa and obtain a more detailed understanding of the binding site of these QAOs.

The QAO core scaffold was synthesized using a condensation reaction between anthranilamide and suitably substituted benzaldehyde to obtain QAO monomers **2a-2b** containing one phenolic group (Scheme 1). This was followed by protection of the phenolic group through acetylation in the presence of acetic anhydride and DIPEA, thereby preparing it for dimerization using a substitution reaction in the presence of potassium carbonate and the required aryl/alkyl dibromo linker affording a suitable dimer. These dimers were then deprotected and the resulting intermediates were subjected to microwave-assisted sulfation to obtain sulfated QAOs **7S-24S** (Scheme 2). All these compounds contain similar monomer units separated by linkers of varying lengths and could therefore be classified as homodimers. The compounds synthesized

could be broadly classified on the basis of the linker incorporated into the dimers. Compounds **7S-11S** contain an aromatic linker, which could either be *o*, *m* or *p*-xylene based. Each of these orients the quinazolinone rings in a distinct geometry and thereby, could be used to obtain important information on the geometry preferred by the HBS in FXIa. Compounds **12S-24S** incorporate an aliphatic chain that varies in length (4-12) of carbon atoms. Similarly, two compounds which contains a trans but-2-ene linker (**12S)** imparting rigidity and the 1-propoxypropane containing linker **(15S)** were also synthesized to assess geometry and hydrogen bonding capability of linker, respectively.

Scheme 1. Synthesis of QAOs[a]

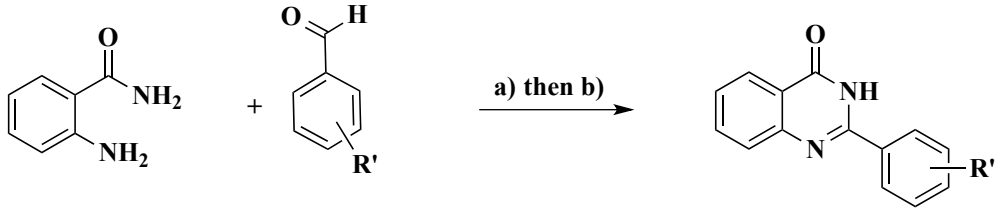

1

2a: R = 3-OH
2b: R = 4-OH

3a: R = 3-OAc
3b: R = 4-OAc

[a]Conditions: (a) $NaHSO_3$, p-toluene sulfonic acid, DMAD, reflux/overnight, 85-90%; (b) Acetic anhydride, DCM, DIPEA, 4-6 h, 85-90%.

Scheme 2. Synthesis of Sulfated QAOs 19S-36S[a]

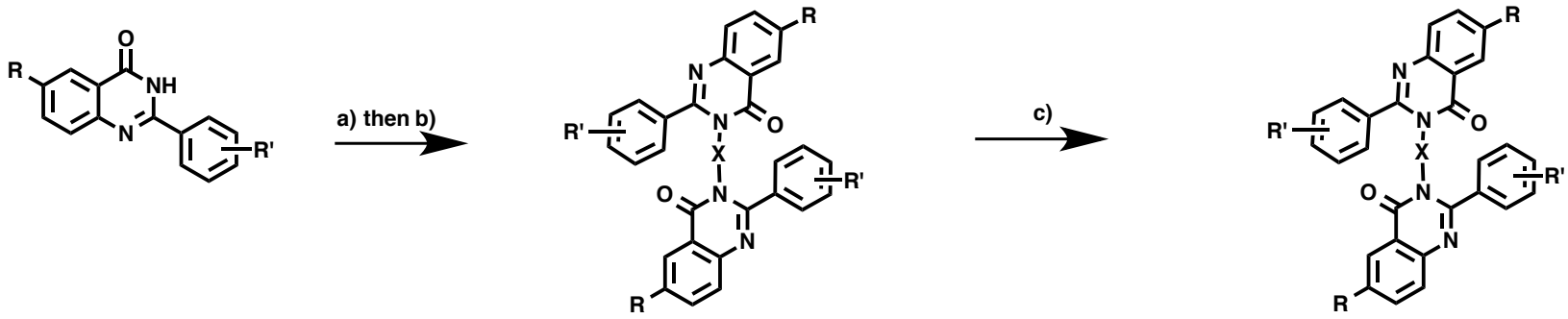

4: R= H; R'=3-OAc
5: R=H, R'=4-OAc
6: R=CH3;R' = 4-OAc

Aromatic linkers
7:R=H; R'=3-OH; X= -p-xylene
8:R=H; R'=3-OH; X= -m-xylene
9:R=H; R'=4-OH; X= -m-xylene
10:R=H; R'=3-OH; X= -o-xylene
11:R=H; R'=4-OH; X= -o-xylene

Aliphatic linkers
12:R=H; R'=3-OH; X= trans-1,4-but-2-ene
13:R=H; R'=3-OH; X= 1,5-pentane
14:R=H; R'=4-OH; X= 1,5-pentane
15:R=H; R'=3-OH; X= 1-propoxypropane
16:R=H; R'=4-OH; X= 1,6-hexane
17:R=H; R'=4-OH; X= 1,6-hexane
18:R=CH3; R'=4-OH; X= 1,6-hexane
19:R=H; R'=4-OH; X= 1,7-heptane
20:R=H; R'=4-OH; X= 1,8-octane
21:R=H; R'=4-OH; X= 1,9-nonane
22:R=H; R'=4-OH; X= 1,10-decane
23:R=H; R'=4-OH; X= 1,11-undecane
24:R=H; R'=4-OH; X= 1,12-dodecane

Aromatic linkers
7S:R=H; R'=3-OSO_3^-; X= -p-xylene
8S:R=H; R'=3-OSO_3^-; X= -m-xylene
9S:R=H; R'=4-OSO_3^-; X= -m-xylene
10S:R=H; R'=3-OSO_3^-; X= -o-xylene
11S:R=H; R'=4-OSO_3^-; X= -o-xylene

Aliphatic linkers
12S:R=H; R'=3-OSO_3^-; X= trans-1,4-but-2-ene
13S:R=H; R'=3-OSO_3^-; X= 1,5-pentane
14S:R=H; R'=4-OSO_3^-; X= 1,5-pentane
15S:R=H; R'=3-OSO_3^-; X= 1-propoxypropane
16S:R=H; R'=4-OSO_3^-; X= 1,6-hexane
17S:R=H; R'=4-OSO_3^-; X= 1,6-hexane
18S:R=CH3; R'=4-OSO_3^-; X= 1,6-hexane
19S:R=H; R'=4-OSO_3^-; X= 1,7-heptane
20S:R=H; R'=4-OSO_3^-; X= 1,8-octane
21S:R=H; R'=4-OSO_3^-; X= 1,9-nonane
22S:R=H; R'=4-OSO_3^-; X= 1,10-decane
23S:R=H; R'=4-OSO_3^-; X= 1,11-undecane
24S:R=H; R'=4-OSO_3^-; X= 1,12-dodecane

[a]Conditions: (a) K_2CO_3, aryl/alkyl dibromide, DMF, rt/overnight, 70–80%; (b) $LiOH.H_2O$, THF, rt/4-6 h, 85–90%; (c) SO_3/Me_3N, TEA, CH_3CN, microwave/30 min, 85−90%.

5.2.2. Inhibition Profile of Sulfated QAOs against Human Factor XIa and Other Similar Proteases in the Coagulation and Digestive System

The library of sulfated QAOs was screened for inhibition of human FXIa and other coagulation enzymes using a chromogenic substrate hydrolysis assay (see Experimental Section). The sigmoidal decrease in the initial rate of protease activity (on a semilog plot) as a function of ligand concentration was fitted using the logistic dose-response equation to calculate the IC_{50} (Table 12). Each of the 18 molecules displayed some activity against FXIa (~6.0–415μM). The library of dimers was built using a simple nucleophilic substitution reaction that provided high yields of the desired compounds. The general theme of the library design revolved around targeting modifications in the linker domain (Figure 35). The first generation incorporated of a triazole-based linker; further studies had highlighted the importance of the linker geometry and length, and these were the two features we decided to target and further probe to obtain more potent inhibitors, while maintaining the selectivity. The library can be thought off in two sets: 1) the aromatic linkers and 2) the aliphatic linkers-containing set.

Aromatic linkers

A set of five dimers were synthesized composed of the xylene-based linkers. Each of these was synthesized to probe into the geometric element of the linkers. In general, the *ortho*, *meta* and *para* -xylene linkers were used, each possessing 4, 5 and 6 intervening atoms, respectively (Table 12). These molecules, however, displayed a progressively lower potency ranging from 57 to 248 μM. Surprisingly, the shorter ortho (n =4), where 'n' is the number of intervening atoms in the linker, and meta (n = 5) linker containing

dimers displayed a better potency compared to the para (n = 6) xylene linkers. The positioning of the sulfate group indicating maximal potency was not consistent, with either the 3-OSO_3^- or the 4-OSO_3^- variably preferred. We attribute this to the variable geometry in each of these molecules. However, these did help us play down the importance of the triazole ring, which was evidently not required considering the same level of potency displayed by **11S** (Table12).

Aliphatic Linkers

On the basis of our initial study with aromatic linkers we synthesized dimers containing the 4-6 intervening atoms. To continue with the placement of a rigid structure, **12S** (IC_{50} = 415 μM) was synthesized consisting of an unsaturated trans-but-2-ene linker, however this was found to lack potency. Our subsequent approach was to use a saturated aliphatic linker containing 5 carbons. Both the 3-OSO_3^- (**13S**) (IC_{50} = 88.5 μM) and the 4-OSO_3^- (**14S**) derivatives were synthesized. This approach produced drastic improvement in potency (Table 12) with (**14S**) (IC_{50} = 49.3 μM), the 4-OSO_3^- derivative being more potent. Another feature that we probed was the probability of unearthing hydrophilic interactions around the linker domain that could be targeted. In view of this strategy, we introduced a 1-propoxypropane linker containing 5 intervening atoms. This, however, confirmed the lack of any hydrogen bond like interactions with the linker domain, illustrated by the lack of potency of **15S** (IC_{50} = 401 μM). Surprisingly, a flexible aliphatic saturated linker was the one preferred. The result suggests that an extended linker probably serves to place the two QAO scaffolds better within two hydrophobic regions of FXIa. We therefore, then focused on the length of the linker, which was altered

from (5 to 12) intervening atoms. The general trend seen within this library indicated that increasing the length produced a consistent improvement in the potency from 34.3 to 6.1 μM. However, as the length was increased the selectivity profile faltered with maximum selectivity achieved when the length was 9 atoms. Further increase in linker length produced an increased potency against other enzymes like FXa and trypsin. Thus indicating the maximum length required to maintain the potency and selectivity.

Table 12. Inhibition of human factor XIa by sulfated QAOs 7S–24S[a]

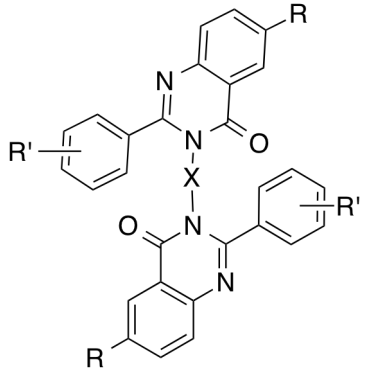

Aromatic linkers

Inhibitor	R	R'	X	n	IC_{50} *μM*	ΔY %
7S	H	3-OSO_3^-	*p*-xylene	6	248±2.6[b]	100.2±3
8S	H	3-OSO_3^-	*m*-xylene	5	59.7±1.1	92.4±5
9S	H	4-OSO_3^-	*m*-xylene	5	76.3±1.2	95.8±6

10S	H	3-OSO_3^-	*o*-xylene	4	94.3±2.2	92.6±3.6
11S	H	4-OSO_3^-	*o*-xylene	4	57.1±1.7	86.7±3.3
			Aliphatic linkers			
12S	H	3-OSO_3^-	Trans-1,4-but-2-ene	4	415±10.3	96.2±7.2
13S	H	3-OSO_3^-	1,5-pentane	5	88.5±1.1	96±2.15
14S	H	4-OSO_3^-	1,5-pentane	5	49.3±0.8	92.3±2.6
15S	H	3-OSO_3^-	1-propoxypropane	5	401±22	94.4±15.8
16S	H	3-OSO_3^-	1,6-hexane	6	53.4±0.9	95.9±4.9
17S	H	4-OSO_3^-	1,6-hexane	6	34.3±1.9	87±2.6
18S	-OCH3	4-OSO_3^-	1,6-hexane	6	34.8±0.8	95.1±2.5
19S	H	4-OSO_3^-	1,7-heptane	7	23±0.84	96.4±4
20S	H	4-OSO_3^-	1,8-octane	8	19.6±0.5	80.9±2.4
21S	H	4-OSO_3^-	1,9-nonane	9	8.2±0.5	101±7.8
22S	H	4-OSO_3^-	1,10-decane	10	16.6±0.3	94.5±2
23S	H	4-OSO_3^-	1,11-undecane	11	14.5±0.8	96±5.8
24S	H	4-OSO_3^-	1,12-dodecane	12	6.1±0.4	90.3±5

[a]The IC_{50}, HS and Y values were obtained following nonlinear regression analysis of direct inhibition of factor XIa. Inhibition was monitored by spectrophotometric measurements of residual proteases activity (see Experimental section). [b]Errors represent ±1 SE.

5.2.3. Inhibition Potency of Sulfated QAOs in Human Plasma.

To assess whether the chromogenic substrate-based inhibition of human factor XIa by sulfated QAOs translates into activity against macromolecular substrates, we studied anticoagulant activity in human plasma. The activated partial thromboplastin time (APTT) assays is typically utilized to identify an inhibitor's ability to retard the intrinsic pathway. For the compounds tested (**19S-24S**) the dose dependent prolongation of about 15 to 20–fold less active in comparison to the potency in buffer was detected. This is typical of many anticoagulants and could be attributed to interactions with serum albumin.

Table 13: Effect of Sulfated QAOs on human plasma clotting times.[a]

Inhibitor	**2 x APTT** ***μM***
19S	824
20S	684
21S	813
22S	963
23S	793
24S	891

[a]Prolongation of clotting time as a function of concentration of sulfated quinazolinones for the activated partial thromboplastin time assay (APTT). Clotting assays were performed in triplicates (SE ≤ 10%) as described in the experimental section.

5.2.4. Mechanism of Inhibition of Sulfated QAOs.

These molecules were designed to function allosterically and therefore these should possess inherent non-competitive or uncompetitive mechanism of inhibition. To assess this, the kinetics of chromogenic substrate S2366 hydrolysis by factor XIa in the presence of **21S** was studied. The plot of the initial rate as a function of Spectrozyme FXIa concentration displayed a characteristic hyperbolic profile (Figure 38), which was fitted using the standard Michaelis–Menten equation to derive the K_M and V_{max} of factor XIa activity. The K_M for Spectrozyme FXIa was found to be 0.27±0.01 mM, which did not change much as the concentration of **21S** increased to 200 μM (0.26±0.32 mM) (Table 14). In contrast, the Vmax decreased from 36.9±1.5 to 9.7±0.37 mAU/min as the concentration of **21S** increased from 0 to 200 μM (Figure 38) (Table 14). Thus, while the affinity of the small chromogenic substrate remains unaffected by **21S** binding, the proteolytic activity decreases. This is characteristic of a noncompetitive mechanism of factor XIa inhibition, and most H/HS mimetics[230] reported in the literature to date, and more importantly our previous set of QAOs have exhibited a similar mechanism.[206]

Table 14. **Michaelis-Menten Kinetics of S2366 hydrolysis by human factor XIa in the presence of sulfated QAOs**.

[21]	V_{max}	K_M
μM	***mAU/min***	***mM***
0	36.9[a]±0.6	0.23[a]±0.01
10	36±1.5	0.28±0.04
20	32.1±2	0.31±0.06
50	21±0.7	0.26±0.03
120	17.2±0.6	0.28±0.03
200	9.7±0.4	0.26±0.03

[a]Calculated from the rate of hydrolysis at various substrate concentrations measured spectrophotometrically in 50 mM Tris-HCl buffer, pH 7.4 containing 150 mM NaCl and 0.1% PEG 8000 at 37° C. The V_{max} and K_M were obtained by nonlinear regression fit of the data by eq 7 Error = ± SE.

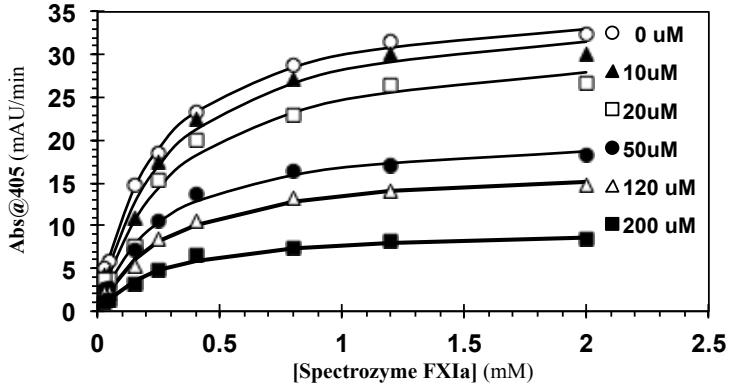

Figure 38. Michaelis-Menten kinetics of S2366 hydrolysis by human factor XIa in the presence of sulfated QAO **21S**. The initial rate of hydrolysis at various substrate concentrations was measured spectrophotometrically in pH 7.4 buffer at 37°C. Solid lines represent nonlinear regressional fits to the data by the standard Michaelis-Menten equation to yield K_M and V_{max}.

5.2.5. Affinity Studies.

The fluorescence of FXIa–DEGR was monitored as a function of sulfated QAO concentration. Figure 39 shows the profiles of the titrations for the most potent sulfated QAOs **19S–24S**. The profiles reveal a characteristic sigmoidal dependence on the concentration of sulfated QAO. This confirms the cooperative binding process observed in the first generation agents. The profile can be fitted well by the standard, three parameter Hill equation (eq 8), which gives the maximal fluorescence change (ΔF_{max}), the Hill coefficient (n), and the apparent dissociation constant (K_D) of binding (Table 15). By using this equation, the three sulfated QAOs were found to bind with an affinity of ~20 μM, which compare favorably with IC_{50} measured above (Table 12). The Hill coefficients were calculated to be in the range of (3.6–5), through which the fluorescence-based study demonstrates that sulfated QAOs bind to FXIa through a classic, allosteric interaction process.

Table 15. Binding of Sulfated QAOs to human FXIa [a]

Inhibitor	**ΔF_{max}**	**n**	**K_D**
	%		***μM***
19S	130±2	3.6±0.56	20±0.8
20S	87.1±1.4	4.3±0.5	20.2±0.7
21S	265±3.1	5.0±0.4	19.9±0.5

Titrations were performed by adding aliquots of a solution of sulfated QAOs (**19S–21S**) to 250nM FXIa–DEGR in 50mM Tris–HCl buffer of pH 7.4 containing 150mM NaCl and 0.1% PEG8000 at 37°C and monitoring the change in fluorescence of FXIa–DEGR at 547nm (λex = 345nm). The ΔF_{max}, the Hill coefficient "n", and K_D were obtained by nonlinear regressional fit of the data by eq 8 Error = ± SE.

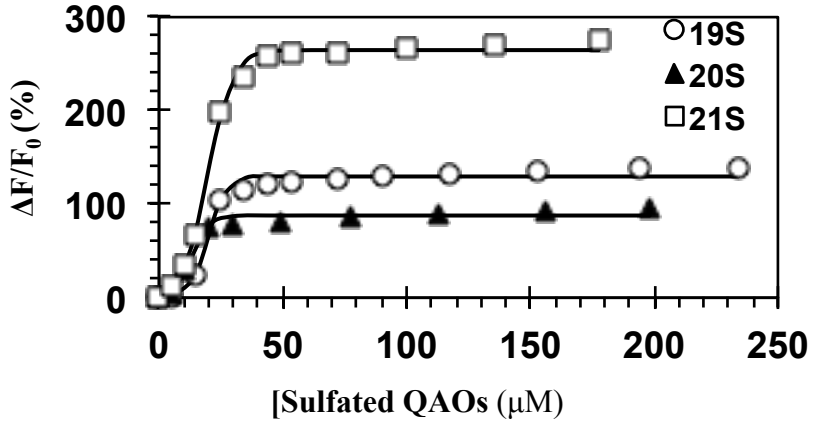

Figure 39. Fractional change in fluorescence of FXIa-DEGR at 547nm (λex = 345nm) as a function of the concentration of sulfated QAOs (**19S–21S**). These were recorded in 50mM Tris–HCl buffer of pH 7.4 containing 150mM NaCl and 0.1% PEG8000 at 37°C. Solid lines represents nonlinear regressional fit to the data using the standard Hill eq 8 to obtain the ΔF_{max}, Hill coefficient "n", and K_D of binding.

5.2.6. Analytical Ultracentrifugation of FXIa and FXIa-21S Complex.

Analytical ultracentrifugation (AUC) was performed to observe the oligomerization properties of FXIa and the effect of the QAO (**21S**) on the oligomerization. In general FXIa is predominantly observed as a dimer (s = 6.6S), whereas miniscule amounts of monomer-dimer equilibrium peak (s = 4.9S, ~13%) were also observed for the apoenzyme. The FXIa-21S complex also exhibits the presence of a dimer (s = 6.5S) however, results in an increased detection of monomer-dimer equilibrium (s = ~4.6S, ~19%). This indicates that the QAOs could be targeting FXIa with a unique mechanism that suggestively destabilizes the FXIa dimer. Literature reports indicate a covalent disulfide bond between the two monomers[100]. Additionally, non-covalent interactions help stabilize the functional dimer form of FXIa.[120] The presence of the equilibrium state is suggestive of **21S** interfering with these non-covalent interactions destabilizing the

stable dimeric form of fXIa.

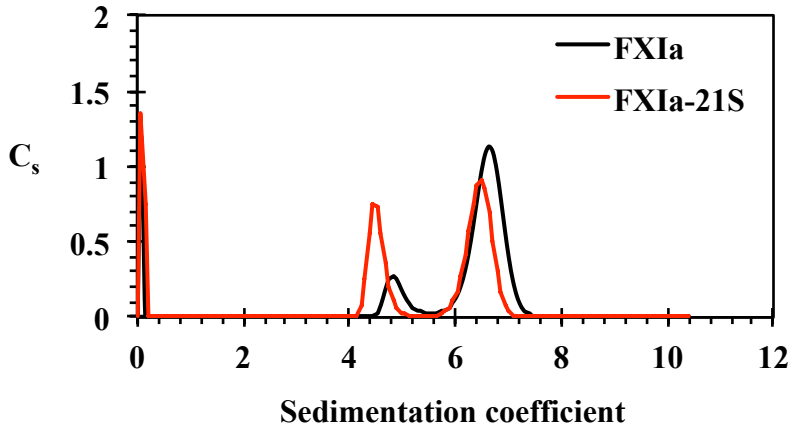

Figure 40. Sedimentation velocity profile showing molecular species of FXIa−ligand complex. **C(s)** is the relative concentration of each species: black for unliganded fXIa, red for the fXIa-**21S** complex.

5.3. Experimental Procedures

5.3.1. Chemicals, Reagents and Analytical Chemistry

Anhydrous CH_2Cl_2, THF, CH_3CN, DMF, DMA and acetone were purchased from Sigma-Aldrich (Milwaukee, WI) or Fisher (Pittsburgh, PA) and used as such. Other solvents used were of reagent gradient and used unmodified. Analytical TLC was performed using UNIPLATE^{TM} silica gel GHLF 250 µm pre-coated plates (ANALTECH, Newark, DE). Column chromatography was performed using silica gel (200-400 mesh, 60 Å) from Sigma-Aldrich. Chemical reactions sensitive to air or moisture were carried out under nitrogen atmosphere in oven-dried glassware. Reagent solutions, unless otherwise noted, were handled under a nitrogen atmosphere using syringe techniques. Flash chromatography was performed using Teledyne ISCO (Lincoln, NE) Combiflash RF system and disposable normal silica cartridges of 30–50 µ particle size, 230–400 mesh size and 60 Å pore size. The flow rate of the mobile phase

was in the range of 18 to 35 ml/min and mobile phase gradients of ethyl acetate/hexanes and CH_2Cl_2/CH_3OH were used to elute compounds.

5.3.2. Proteins and Chromogenic Substrates

Human plasma proteases including thrombin, factor Xa, factor IXa, and factor XIa were obtained from Haematologic Technologies (Essex Junction, VT). Active sited labeled FXIa, i.e., FXIa-DEGR, was obtained from US Biological (Marblehead, MA). Bovine α-chymotrypsin and bovine trypsin were obtained from Sigma-Aldrich (St. Louis, MO). Stock solutions of factor XIa, thrombin, trypsin, and chymotrypsin were prepared in 50 mM Tris-HCl buffer, pH 7.4, containing 150 mM NaCl, 0.1% PEG8000, and 0.02% Tween80. Stock solutions of factor Xa was prepared in 20 mM Tris-HCl buffer, pH 7.4, containing 100 mM NaCl, 2.5 mM $CaCl_2$, 0.1% PEG8000, and 0.02% Tween80. Chromogenic substrates, Spectrozyme TH (H-*D*-hexahydrotyrosol-Ala-Arg-*p*-nitroanilide), Spectrozyme factor Xa (Methoxycarbonyl-*D*-cyclohexylglycyl-Gly-Arg-*p*-nitroanilide), and Spectrozyme CTY were obtained from American Diagnostica (Greenwich, CT). Factor XIa chromogenic substrate (S-2366, H-*D*-Val-Leu-Arg-*p*-nitroanilide.2HCl) and trypsin substrate (S-2222, Benzyl-Ile-Glu(–OH and $–OCH_3$)-Gly-Arg-*p*-nitroanilide·HCl) were obtained from Diapharma (West Chester, OH). Pooled normal human plasma for coagulation assays was purchased from Valley Biomedical (Winchester, VA). Activated partial thromboplastin time reagent containing ellagic acid, thromboplastin-D, and 25 mM $CaCl_2$ were obtained from Fisher Diagnostics (Middletown, VA).

5.3.3. Chemical Characterization of Compounds

^{1}H and ^{13}C NMR were recorded on Bruker-400 MHz spectrometer in either $CDCl_3$, CD_3OD, acetone-d_6, DMSO-D_6, or D_2O. Signals, in part per million (ppm), are either relative to the internal standard or to the residual peak of the solvent. The NMR data are reported as chemical shift (ppm), multiplicity of signal (s= singlet, d= doublet, t= triplet, q= quartet, dd= doublet of doublet, m= multiplet), coupling constants (Hz), and integration. ESI-MS of compounds were recorded using Waters Acquity TQD MS spectrometer in positive or negative ion mode. Samples were dissolved in methanol and infused at a rate of 20 μL/min. The purity of each final compound was greater than 95% as determined by UPLC-MS.

5.3.4. Synthetic Procedures

General Procedure for Synthesis of Quinazolin-4(3H)-ones

The quinazolinone core structure was synthesized using a condensation reaction between anthranilamide and suitably substituted benzaldehyde in presence of sodium hydrogen sulfite and catalytic amounts of *p*-toluenesulfonic acid. This is a well-established thermal cyclodehydration reaction.[229] To a solution of anthranilamide (1 equiv) in *N,N*-dimethylacetamide (DMAD) (10mL) 3- or 4-hydroxybenzaldehyde (**1 or 2)** (1 equiv) was added followed by the addition of sodium hydrogen sulphate (1.2 equiv) and *p*-toluenesulfonic acid (0.1equiv) into a single neck flask attached with a condenser and the mixture was stirred at 150 °C for 3 hrs. The reaction was cooled by the addition of (100 mL) of ice water to form a white precipitate that was filtered off washed with water and a small amount of methanol and dried in vacuo to obtain a white colored powder.

Depending on the substitution on the benzaldehyde, two monomers viz. **3a** and **3b** were synthesized. The products were formed in 85-90% yields and characterized using NMR.

General Procedure for Protection of Quinazolinone Core Structure

3a and 3b were then acetylated to protect the free hydroxyl group(s). This was done by solubilizing in dichloromethane followed by addition of *N*, *N*-Diisopropylethylamine DIPEA (2.0 equiv per hydroxyl group) and acetic anhydride (1.0 equiv per hydroxyl group). This was vigorously stirred at room temperature and after 10 hours extracted using acidified water and dichloromethane. The organic layer was dried (Na_2SO_4), concentrated *in vacuo* and purified using flash chromatography on silica gel (10-50% ethyl acetate in hexanes) to give **3a and 3b** in 90% yields.

General Procedure for Dimerization of Quinazolinone Monomers using Nucleophilic Substitution Reaction

Dimer formation was achieved through a simple substitution reaction. To a solution of **3a or 3b** in *N, N*-dimethyl formamide was added to potassium carbonate K_2CO_3 (2.5 equiv) and stirred for two minutes. This was followed by addition of the respective aryl/alkyl dibromide (0.5 equiv) followed by vigorous stirring for 12 hours. After the reaction completed and confirmed by TLC, the reaction mixture was extracted using acidified water and ethyl acetate. The organic layer was dried over Na_2SO_4, concentrated *in vacuo* and purified using flash chromatography on silica gel (10-50% ethyl acetate in hexanes) to give the acetylated dimers in 70-80% yield.

General Procedure for the Deprotection of the Acetylated Dimers.

To obtain the hydroxyl dimers, acetylated dimers were solubilized in THF, followed by

the addition of LiOH.H_20 (4 equiv). Vigorous stirring at room temperature for 4-6 hours afforded the final hydroxyl product. After complete deprotection of acetyl groups confirmed using TLC, the reaction mixture was extracted using acidified water and ethyl acetate. The organic layer was separated and dried over Na_2SO_4, concentrated *in vacuo* and purified using flash chromatography on silica gel (20-70% ethyl acetate in hexanes) to give the deacetylated dimers **7-24** in 70-80% yields.

General Procedure for Synthesis of Sulfated Quinazolin-4(3H)-ones dimers.

Sulfation of phenolic precursors was achieved using microwave assisted chemical sulfation as described earlier.[206,231,232] Briefly, to a stirred solution of polyphenol in anhydrous CH_3CN (1 – 5 mL) at room temperature Et_3N (10 equvi per –OH group) and $Me_3N{:}SO_3$ complex (6 equvi per –OH) was added. The reaction vessel was sealed and micro-waved (CEM Discover, Cary, NC) for 30 min at 90 °C. The reaction mixture was cooled and transferred to a round bottom flask and volume reduced as much as possible under low-pressure conditions at 25 °C. The reaction mixture was then directly loaded on to a flash chromatography column and purified using dichloromethane and methanol solvent system (5-20%) to obtain the sulfated QAOs. The samples were concentrated and re-loaded onto a SP Sephadex C-25 column for sodium exchange. Appropriate fractions were pooled, concentrated in *vacuo*, and lyophilized to obtain a white powder. Spectral characteristics of all the sulfated compounds **7S-24S** are listed below.

(7S). ^{1}H NMR ($DMSOd_6$, 400MHz): 8.37(s, 2H), 8.3(d, J = 7.7Hz, 2H), 8.22(d, J = 7.96Hz, 2H), 8.01-7.94(m, 4H), 7.7(s, 4H), 7.67-7.63(m, 2H), 7.51-7.4(m, 2H), 7.37-7.36(m, 2H), 5.83(s, 4H). ^{13}C NMR (DMSOd6, 100MHz): 165.92, 158.93, 157.57,

151.25, 138.66, 136.36, 134.3, 129.53, 128.37, 127.6, 127.16, 123.3, 119.06, 117.93, 114.76, 114.55, 67.70. MS (ESI) calculated for $C_{36}H_{24}N_4Na_2O_{10}S_2$ $[(M - Na)]^-$, *m/z* 759.71, found $[(M - 2Na)]^{2-}$, *m/z* 367.899.

(8S). ^{1}H NMR ($DMSOd_6$, 400MHz): 8.38(s, 2H), 8.29(d, J = 7.8Hz, 2H), 8.18(d, J = 7.9Hz, 2H), 8.02-7.95(m, 5H), 7.68-7.60(m, 4H), 7.53-7.44(m, 3H), 7.37(d, J = 7.56Hz, 2H). ^{13}C NMR (DMSOd6, 100MHz): 165.99, 158.70, 153.92, 151.23, 138.26, 136.74, 134.31, 128.86, 128.8, 127.66, 127.21, 123.28, 123.04, 120.37, 114.57, 67.89. MS (ESI) calculated for $C_{36}H_{24}N_4Na_2O_{10}S_2$ $[(M - Na)]^-$, *m/z* 759.71, found $[(M - 2Na)]^{2-}$, *m/z* 367.931.

(9S). ^{1}H NMR ($DMSOd_6$, 400MHz): 8.5(d, J = 8.65Hz, 4H), 8.14 (d, J = 8.12Hz, 2H), 7.97-7.90(m, 5H), 7.66-7.61(m, 5H), 7.36(d, J = 8.64, 4H), 5.87(s, 4H). ^{13}C NMR (DMSOd6, 100MHz): 165.89, 158.80, 156.13, 136.91, 134.23, 131.79, 129.03, 128.75, 127.80, 127.48, 127.32, 126.86, 123.20, 119.81, 114.32, 67.82. MS (ESI) calculated for $C_{36}H_{24}N_4Na_2O_{10}S_2$ $[(M - Na)]^-$, *m/z* 759.71, found $[(M - 2Na)]^{2-}$, *m/z* 367.931.

(10S). ^{1}H NMR ($DMSOd_6$, 400MHz): 8.34(s, 2H), 8.17(d, J = 4.6Hz, 2H), 8.0-7.83(m, 6H, (m, 2H), 8.0-7.9(m, 8H), 7.8-7.4(m, 8H), 6.08(s, 4H). ^{13}C NMR (DMSOd6, 100MHz): 165.8, 158.57, 153.84, 151.11, 138.2, 135.12, 134.1, 130.37, 128.73, 127.5, 126.97, 123.16, 122.96, 120.35, 114.37, 66.64. MS (ESI) calculated for $C_{36}H_{24}N_4Na_2O_{10}S_2$ $[(M - Na)]^-$, *m/z* 782.71, found $[(M - 2Na)]^{2-}$, *m/z* 367.963.

(11S). ^{1}H NMR ($DMSOd_6$, 400MHz): 8.3(d, J = 8.8Hz, 4H), 7.93(d, J = 8Hz, 2H), 7.8-7.7(m, 6H), 7.43-7.41(m, 2H), 7.32-7.27(m, 2H), 7.21(d, J = 8.8Hz, 4H), 5.98(s, 4H). ^{13}C NMR (DMSOd6, 100MHz): 165.74, 158.67, 156.05, 151.25, 135.18, 134.07, 131.71,

130.06, 128.92, 128.60, 127.4, 126.60, 122.91, 119.70, 114.14, 66.6. MS (ESI) calculated for $C_{36}H_{24}N_4Na_2O_{10}S_2$ $[(M - Na)]^-$, *m/z* 782.71, found $[(M - 2Na)]^{2-}$, *m/z* 367.889.

(12S). ^1H NMR ($DMSOd_6$, 400MHz): 8.35-8.20(m, 6H), 7.9(s, 4H), 7.64(s, 2H), 7.43(m, 5H), 6.5(s, 2H), 5.4(s, 4H). ^{13}C NMR (DMSOd6, 100MHz): 165.8, 153.9, 151.2, 138.3, 134.3, 128.84, 128.5, 127.62, 127.2, 123.2, 123.03, 120.4, 114.52, 66.29, 52.77. MS (ESI) calculated for $C_{32}H_{22}N_4Na_2O_{10}S_2$ $[(M - Na)]^-$, *m/z* 732.65, found $[(M - 2Na)]^{2-}$, *m/z* 342.908.

(13S). ^1H NMR ($DMSOd_6$, 400MHz): 8.24(s, 2H), 8.17(d, J = 7.68Hz, 2H), 8.06(d, J = 7.64Hz, 2H), 7.91-7.84(m, 4H), 7.53-7.52(m, 2H), 7.38-7.28(m, 4H), 4.72(t, J = 6.3Hz, 4H), 2.04-1.97(m, 4H), 1.8-1.73(m, 2H). ^{13}C NMR (DMSOd6, 100MHz): 166.3, 158.8, 153.89, 151.13, 138.4, 134.12, 128.79, 127.60, 127.02, 123.18, 122.94, 120.40, 114.62, 66.67, 52.75, 27.94, 22.32, 13.56. MS (ESI) calculated for $C_{33}H_{26}N_4Na_2O_{10}S_2$ $[(M - Na)]^-$, *m/z* 748.69, found $[(M - 2Na)]^{2-}$, *m/z* 350.940.

(14S). ^1H NMR ($DMSOd_6$, 400MHz): 8.38(d, J = 8.8, 4H), 8.04(d, J = 8.0, 2H), 7.88(m, 4H), 7.51-7.47(m, 2H), 7.27(d, J = 8.8, 4H), 4.71(s, 4H). ^{13}C NMR (DMSOd6, 100MHz): 166.2, 158.90, 156.08, 151.26, 134.04, 131.92, 128.92, 127.45, 126.64, 123.12, 119.8, 66.59, 52.75, 27.95, 22.34. MS (ESI) calculated for $C_{33}H_{26}N_4Na_2O_{10}S_2$ $[(M - Na)]^-$, *m/z* 748.69, found $[(M - 2Na)]^{2-}$, *m/z* 351.004.

(15S). ^1H NMR ($DMSOd_6$, 400MHz): 8.4(d, J = 8.76Hz, 4H), 8.02(d, J = 8.12Hz, 4H), 7.92-7.85(m, 4H), 7.47(t, J = 7.96Hz, 2H), 7.33(d, J = 8.73Hz, 4H), 4.89(s, 4H). ^{13}C NMR (DMSOd6, 100MHz): 165.8, 153.9, 151.2, 138.3, 134.3, 128.84, 128.5, 127.62,

127.2, 123.2, 123.03, 120.4, 114.52, 66.29, 52.77. MS (ESI) calculated for $C_{32}H_{24}N_4Na_2O_{11}S_2$ $[(M - Na)]^-$, *m/z* 750.66, found $[(M - 2Na)]^{2-}$, *m/z* 351.861.

(16S). ^{1}H NMR ($DMSOd_6$, 400MHz): 8.3(s, 2H), 8.25(d, J = 7.36Hz, 2H), 8.14(d, J = 8Hz, 2H), 7.98-7.93(m, 4H), 7.58-7.37(m, 6H), 4.76(s, 4H), 2.0(s, 4H), 1.7(s, 4H). ^{13}C NMR (DMSOd6, 100MHz): 166.29, 158.77, 153.88, 151.11, 138.41, 134.12, 128.81, 127.59, 127.03, 123.189, 122.95, 120.42, 114.6, 66.77, 28.14, 25.4. MS (ESI) calculated for $C_{34}H_{28}N_4Na_2O_{10}S_2$ $[(M - Na)]^-$, *m/z* 739.72, found $[(M - 2Na)]^{2-}$, *m/z* 357.915.

(17S). ^{1}H NMR ($DMSOd_6$, 400MHz): 8.4(d, J = 8.8, 4H), 8.1(d, J = 7.97Hz, 2H), 7.93-7.89(m, 4H), 7.56-7.52(m, 2H), 7.34(d, J = 8.8, 4H), 4.74(t, J = 6.32Hz, 4H), 2.0(s, 4H), 1.7(s, 4H). ^{13}C NMR (DMSOd6, 100MHz): 166.29, 158.77, 153.88, 151.11, 138.41, 134.12, 128.81, 127.59, 127.03, 123.189, 122.95, 120.42, 114.6, 66.77, 28.14, 25.4. MS (ESI) calculated for $C_{33}H_{26}N_4Na_2O_{10}S_2$ $[(M - Na)]^-$, *m/z* 762.72, found $[(M - 2Na)]^{2-}$, *m/z* 357.947.

(18S). ^{1}H NMR ($DMSOd_6$, 400MHz): 8.40(d, J = 8.6Hz, 4H), 7.8(d, J = 9.1Hz, 2H), 7.51-7.48(m, 2H), 7.33-7.31(m, 6H), 4.73(t, J = 6.4Hz), 3.8(s, 6H), 2.0(s, 4H), 1.7(s, 4H) ^{13}C NMR (DMSOd6, 100MHz): 165.30, 157.34, 156.86, 146.78, 132.13, 129.13, 128.5, 125.4, 119.8, 114.93, 101.39, 66.55, 55.48, 28.11, 25.34. MS (ESI) calculated for $C_{36}H_{32}N_4Na_2O_{10}S_2$ $[(M - Na)]^-$, *m/z* 822.77, found $[(M - 2Na)]^{2-}$, *m/z* 387.962.

(19S). ^{1}H NMR ($DMSOd_6$, 400MHz): 8.4(d, J = 8.7Hz, 4H), 8.06(d, J = 8.16Hz, 2H), 7.85-7.81(m, 4H), 7.53-7.5(m, 2H), 7.3(d, J = 8.7Hz, 4H), 4.65(t, J = 6.4Hz, 4H), 3.0(s, 4H), 1.16(s, 1H), 1.08-1.0(m, 6H). ^{13}C NMR (DMSOd6, 100MHz): 166.2, 158.88, 156.07, 151.25, 134.04, 131.92, 128.92, 127.44, 126.68, 123.18, 119.81, 114.39, 66.73,

52.75, 28.58, 28.16, 25.57. MS (ESI) calculated for $C_{35}H_{30}N_4Na_2O_{10}S_2$ $[(M - Na)]^-$, *m/z* 776.74, found $[(M - 2Na)]^{2-}$, *m/z* 364.987.

(20S). ^1H NMR ($DMSOd_6$, 400MHz): 8.4(d, J = 8.8Hz, 4H), 8.13(d, J = 7.93Hz, 2H), 7.94-7.88(m, 4H), 7.61-7.54(m, 2H), 7.34(d, J = 8.8Hz, 4H), 4.71(t, J = 6.4Hz, 4H), 2.09-1.89(m, 4H), 1.56-1.47(m, 4H), 1.08(t, J = 7.2Hz, 4H). ^{13}C NMR (DMSOd6, 100MHz): 166.19, 158.89, 156.09, 151.25, 134.02, 131.91, 128.91, 127.44, 126.65, 123.16, 119.80, 114.39, 66.72, 52.75, 28.69, 28.16, 25.52. MS (ESI) calculated for $C_{36}H_{32}N_4Na_2O_{10}S_2$ $[(M - Na)]^-$, *m/z* 790.77, found $[(M - 2Na)]^{2-}$, *m/z* 371.962.

(21S). ^1H NMR ($DMSOd_6$, 400MHz): 8.4(d, J = 8.8Hz, 4H), 8.13(d, J = 8.24Hz, 2H), 7.95-7.89(m, 4H), 7.62-7.58(m, 2H), 7.34(d, J = 8.8Hz, 4H), 4.71(t, J = 6.4Hz, 4H), 2.1-1.87(m, 4H), 1.54(s, 4H), 1.4(s, 6H). ^{13}C NMR (DMSOd6, 100MHz): 166.22, 158.89, 156.13, 151.15, 134.05, 131.83, 129.9, 128.93, 127.37, 126.68, 123.19, 119.80, 115.30, 114.39, 66.76, 52.74, 28.86, 28.70, 28.64, 28.17, 25.55. MS (ESI) calculated for $C_{37}H_{34}N_4Na_2O_{10}S_2$ $[(M - Na)]^-$, *m/z* 804.80, found $[(M - 2Na)]^{2-}$, *m/z* 379.034.

(22S). ^1H NMR ($DMSOd_6$, 400MHz): 8.4(d, J = 8.8Hz, 4H), 8.14(d, J = 8.3Hz, 2H), 7.96-7.90(m, 4H), 7.63-7.60(m, 2H), 7.4(d, J = 8.8Hz, 4H), 4.71(t, 6.52Hz, 4H), 1.93-1.86(m, 4H), 1.54-1.49(m, 4H), 1.4-1.34(m, 8H). ^{13}C NMR (DMSOd6, 100MHz): 166.22, 159.1, 134.16, 130.03, 128.99, 126.71, 126.50, 123.21, 119.80, 115.36, 114.17, 66.81, 28.77, 28.61, 28.10, 25.44. MS (ESI) calculated for $C_{38}H_{36}N_4Na_2O_{10}S_2$ $[(M - Na)]^-$, *m/z* 818.82, found $[(M - 2Na)]^{2-}$, *m/z* 386.042.

(23S). ^1H NMR ($DMSOd_6$, 400MHz): 8.4(d, J = 8.8Hz, 4H), 8.13(d, J = 8.0Hz, 2H), 7.94-7.88(m, 4H), 7.6(t, J = 1.6, 2H), 7.34(d, J = 8.8Hz, 4H), 4.7(t, J = 6.4Hz, 4H), 1.93-

1.87(m, 4H), 1.53-1.48(m, 4H), 1.38-1.31(m, 10H). ^{13}C NMR (DMSOd6, 100MHz): 166.19, 158.89, 156.09, 151.26, 134.02, 131.90, 128.90, 127.45, 126.64, 123.16, 119.79, 114.39, 66.72, 28.89, 28.85, 28.71, 28.55, 28.33, 28.15, 25.53. MS (ESI) calculated for $C_{39}H_{38}N_4Na_2O_{10}S_2$ $[(M - Na)]^-$, *m/z* 832.85, found $[(M - 2Na)]^{2-}$, *m/z* 392.986.

(24S). ^{1}H NMR ($DMSOd_6$, 400MHz): 8.4(d, J = 8.8Hz, 4H), 8.14(d, J = 8.0Hz, 2H), 7.97-7.91(m, 4H), 7.64-7.60(m, 2H), 7.35(d, J = 8.8Hz, 4H), 4.71(t, J = 6.5Hz, 4H), 1.91-1.88(m, 4H), 1.53-1.49(m, 4H), 1.37-1.23(m, 12H). ^{13}C NMR (DMSOd6, 100MHz): 166.29, 159.08, 158.87, 134.20, 130.06, 128.99, 126.45, 123.22, 119.80, 115.36, 114.35, 114.15, 66.78, 28.60, 28.08, 25.42. MS (ESI) calculated for $C_{40}H_{40}N_4Na_2O_{10}S_2$ $[(M - Na)]^-$, *m/z* 846.88, found $[(M - 2Na)]^{2-}$, *m/z* 399.962.

5.3.5. Direct Inhibition of Factor XIa by Sulfated QAOs.

A chromogenic substrate hydrolysis assay using a microplate reader (FlexStation III, Molecular Devices) was used to measure direct inhibition of FXIa, as described earlier.[206,233] Generally, each well of the 96-well microplate had 85 µL of pH 7.4 buffer (50 mM TrisHCl, 150 mM NaCl, 0.1% PEG8000, and 0.02% Tween80) to which 5 µL of a potential FXIa inhibitor (or solvent reference) was added followed by 5 µL of FXIa to give 0.765 nM in the well. After 10 min incubation at 37 °C, 5 µL FXIa substrate S2366 (345 µM in the well) was rapidly added and the residual FXIa activity was measured from the initial rate of increase in absorbance at 405 nm. Stocks of FXIa inhibitors were 20 mM, which were then serially diluted to give twelve different aliquots in the plate wells. Relative residual FXIa activity at each concentration of the inhibitor was calculated from the ratio of FXIa activity in the presence and absence of the inhibitor. Eq

6 was used to fit the dose–dependence of residual proteinases activity to obtain the potency (IC_{50}) and efficacy (ΔY) of inhibition. In this equation, Y is the ratio of residual factor XIa activity in the presence of inhibitor to that in its absence (fractional residual activity), Y_M and Y_0 are the maximum and minimum possible values of the fractional residual proteinase activity, IC_{50} is the concentration of the inhibitor that results in 50% inhibition of enzyme activity, and HS is the Hill slope. Nonlinear curve fitting resulted in Y_M, Y_0, IC_{50} and HS values.

$$Y = Y_0 + \frac{Y_M - Y_0}{1 + 10^{(log[I]_0 - log\ IC_{50}) \times HS}} \qquad (6)$$

5.3.6. Inhibition of Proteases of the Coagulation and Digestive Systems.

The inhibition potential of 500 μM of **7S to 24S** against coagulation enzymes including thrombin, factor IXa and factor Xa and digestive enzymes including trypsin and chymotrypsin was evaluated using chromogenic substrate hydrolysis assays reported in the literature. These assays were performed using substrates appropriate for the enzyme being studied under conditions closest to the physiological condition (37 °C and pH 7.4), except for thrombin, which was performed at 25 ºC and pH 7.4. The concentrations of enzymes and substrates in microplate wells, respectively, were: 6 nM and 50 mM for thrombin; 1.09 nM and 125 mM for factor Xa, 2.5 ng/ml and 80 mM for bovine trypsin; and 500 ng/ml and 240 mM for bovine chymotrypsin and 89 nM and 425 mM for FIXa. The ratio of the proteolytic activity of an enzyme in the presence of the sulfated QAO to that in its absence was used to calculate percent inhibition (%).

5.3.7. Michaelis–Menten Kinetics of Substrate Hydrolysis in Presence of 21S.

The initial rate of S2366 hydrolysis by FXIa was obtained from the linear increase in absorbance at 405 nM corresponding to less than 10% consumption of S2366. The initial rate was measured as a function of various concentrations of the substrate (0.03–2 mM) in the presence of fixed concentration of **21S** in 50 mM TrisHCl buffer, pH 7.4, containing 150 mM NaCl, 0.1% PEG8000, and 0.02% Tween80 at 37 ^{O}C. The data was fitted using the standard Michaelis–Menten eq 7 to determine the K_M and V_{MAX}.

$$V = \frac{V_{MAX}\,[S]}{K_M + [S]} \qquad (\mathbf{7})$$

5.3.8. Equilibrium dissociation constant (K_D) of Sulfated QAOs Binding to Human Factor XIa.

Fluorescence experiments were performed using a QM4 spectrofluorometer (Photon Technology International, Birmingham, NJ) in 50 mM Tris-HCl buffer of pH 7.4 containing 150 mM NaCl and 0.1% PEG8000 at 37 °C. The equilibrium dissociation constant (K_D) of sulfated QAOs – FXIa complex was measured using the change in the fluorescence of the active site dansyl group due to binding. Titrations were performed by adding aliquots of a solution of sulfated QAOs (**19S**, **20S** and **21S**) in the above buffer to a fixed concentration of FXIa–DEGR (250 nM) and monitoring the change in the fluorescence of FXIa-DEGR at 547 nm (λ_{EX} = 345 nm). The slit widths on the excitation and emission side were 1mm each. The change in fluorescence at 547 nm was fitted using the standard Hill equation for ligand binding eq 8 for co-operative binding to obtain the apparent dissociation constant ($K_{D,app}$) of binding. In this equation, ΔF represents the

change in fluorescence following addition of sulfated QAO from the initial fluorescence (F_0), while ΔF_{MAX} represents the maximal change in fluorescence. Hill coefficient '*n'* is a measure of the cooperativity of binding.

$$\frac{\Delta F}{F_0} = \Delta F_{MAX} \times \frac{[sulfated\ QAQ]^n}{(K_{D,app})^n + [sulfated\ QAQ]^n} \qquad (\mathbf{8})$$

5.3.9. Activated Partial ThromboplastinTime (APTT)

Intrinsic clotting time was measured in a standard one–stage recalcification assay with a BBL Fibrosystem fibrometer (Becton-Dickinson, Sparles, MD). For the aPTT assay, x µL of same molecules was mixed with (100-x) µL of citrated human plasma and 100 µL of prewarmed APTT reagent (0.2% ellagic acid). After incubation for 4 min at 37 ^{O}C, clotting was initiated by adding 100 µL of pre-warmed 25 mM $CaCl_2$ and time to clot noted. The data were fit to a quadratic trend line, which was used to determine the concentration of the inhibitor necessary to double the clotting time. Clotting time in the absence of an anticoagulant was determined in similar fashion using 10 µL of deionized water and/or appropriate organic vehicle and was found to be 34.8 s for APT.

5.3.10. Analytical Ultracentrifugation of FXIa and FXIa-21S complex.

FXIa-DEGR was diluted to 0.2 mg/mL in 50 mM Tris-HCl buffer of pH 7.4 containing 150 mM NaCl and 0.1% PEG8000 at 20 °C. Samples (420 **µ**L) of FXIa alone and FXIa with 100 µM **21S**, with a buffer sample were run at 25000 rpm overnight at 20° C in a Beckman Coulter Proteome Lab XL-I analytical ultracentrifuge. Absorbance (λ = 345nm) and interference scans were recorded until the boundary moved to the bottom of the cell. The continuous distribution **c**(**S**) distribution analysis was performed using SEDFIT (https://sedfitsedphat.nibib.nih.gov).

CHAPTER 6: SIGNIFICANCE OF CURRENT WORK AND FUTURE DIRECTIONS

6.1. Novel Hexasaccharide Based Activators of Heparin co-factor II and Antithrombin

Antithrombin activation has been the primary indirect mechanism of anticoagulation by heparin and its analogs. Structural studies, however, have revealed the specificity of interaction involved in this mechanism, shedding light on the fact that a similar system could exist for related serpins like HCII. Reports did suggest the lack of specificity in the HCII system primarily due to the lack of structural homogeneity in the sequences known to activate it and to the lack of any structural knowledge. The utilization of computational resources to solve this difficult puzzle could offer an alternative. The computational techniques we utilized did predict highly specific structures for both the HCII and the AT system. This lays the foundation for utilization of similar techniques on other unknown protein-GAG systems to predictively identify sequences. **HX1** was identified as one of the first heparin based hexasaccharide sequences to potently target both AT and HCII. This property has the added advantage that this sequence is capable of targeting both venous and arterial thrombosis. Targeting HCII introduces the capability of inhibiting both free and bound thrombin.

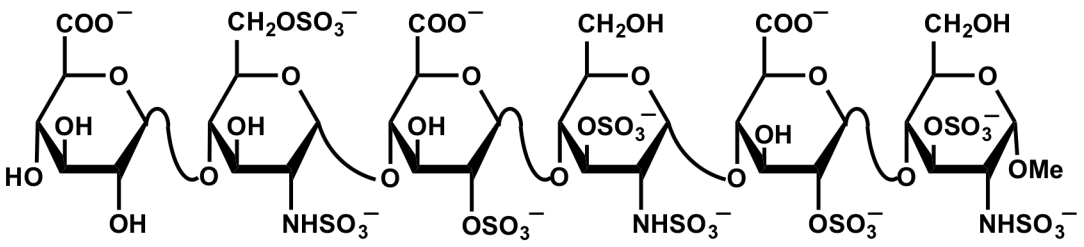

HX1

A major problem with heparin-based anticoagulants has been the occurrence of thrombocytopenia and bleeding complications. The problem of heparin-induced thrombocytopenia was diminished through the utilization of the smaller and homogeneous heparin pentasaccaharide; the hexasaccharide thus synthesized could also be postulated to possess a similar advantage. Other bleeding complication are generally attributed to the potent affinity of heparin pentasaccharide, however the moderate affinity observed with the hexasaccharide without the loss of activation potential could reduce the bleeding complications observed with simple measures like dialysis or the utilization of an antidote.

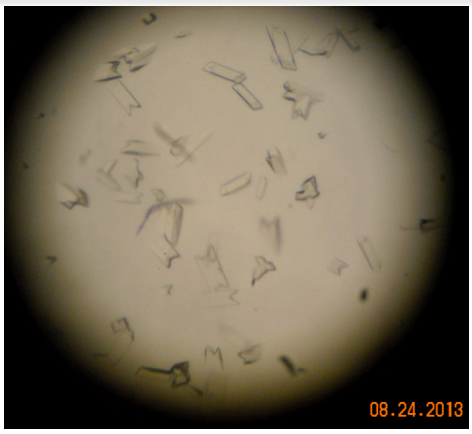

Antithrombin crystals

The study thus performed is an initial step toward further understanding the complex HCII system. However, the utilization of our computational approach could have implications for this system. Experimental data brings to light the structural aspect

of these hexasaccharides. However, mechanistic understanding needs to be clarified. Some of the mechanistic studies that we are already in the process of undertaking include the salt dependent studies to recognize ionic component of the interaction of these sequences with HCII and AT. Structural elucidation through the utilization of X-ray crystallography could serve as important tool to gain a more comprehensive understanding. These have already been undertaken with numerous AT crystals being soaked with the potent **HX1**. However, efforts to obtain the structure and the site of binding have failed. Similarly, the promise these offer warrants animal studies, which we plan to undertake through the help of our collaborators.

6.2. Differential Recognition of Coagulation Proteins by a Heparan sulfate containing 2-*O*-sulfated Glucuronic acid

GAGs are highly heterogeneous structures decorated by an array of sulfates (—OSO_3^-), the placement of which induces recognition and modulation of proteins that possess surfaces draped with positively charged Arg/Lys residues. The interaction patterns involved dictate the type of function modulated which range from physiological modulation of growth to pathophysiological ones like cancer and microbial invasion. The emphasis is on the structure of the GAG interacting with the protein.

Our work involves recognizing such a rare sequence in the form of HS_{2S2S}, which was found to be unique in many ways. Its natural occurrence and the possibility of it being used to unearth newer interaction profiles caught our attention. Our experimental findings suggest a novel profile with it targeting usual serpins like AT and HCII. However, the direct inhibition of thrombin is a feature not generally seen in heparin-

based polymers. Further, the correlation of these results with our computational predictions suggests the importance of studying such rare sequences through the use of a more predictable model.

Our study lays the foundation for similar studies to be performed to unearth novel interactions of GAGs with the variety of proteins these are known to interact. The computational resources we utilized thus offer an avenue to predictively study such systems.

6.3. Sulfated Quinazolin-4(3H)-ones as Allosteric Modulators Targeting FXIa

Numerous studies have signified the benefits of directly targeting upstream coagulation proteases like FXIa. Targeting FXIa does not produce any bleeding complications, subsequently without altering the normal hemostasis. Additionally, the lack of FXIa does not produce significant problems in individual carriers of the mutation with it. Animal studies have revealed similar trends with no complications observed. Altogether these features make it a potentially attractive target.

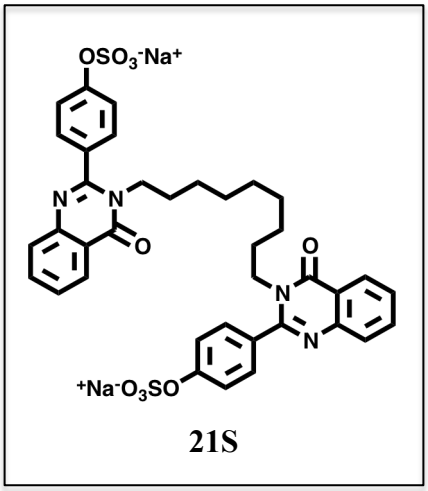

21S

The dual element strategy, was successfully incorporated to develop the initial QAOs[206], and similarly used to design allosteric inhibitor for thrombin.[177] These initial QAOs were the first group of allosteric inhibitors of FXIa. Sulfated pentagalloyl glucoside are the other structurally diverse allosteric inhibitors of FXIa, which were reportedly found to function by a different allosteric mechanism. The present study extends our structural and mechanistic understanding of

the QAOs based inhibitors. The second generation of compounds has stretched the potency by 9-fold (**21S**) while maintaining a similar selectivity profile. This generation primarily focused on the linker domain, thus unearthing important features required in this domain especially in terms of its geometry and length, additionally the positioning of the sulfate group has also been deciphered. Mechanistically, the analytical ultracentrifugation studies have thrown light into the interference with the non-covalent dimer forming interactions as a possible route of inhibition, further confirming a non-competitive mechanism of action. This study validates on the utilization of the dual element strategy and its extension to gain a reasonable structure-activity understanding of the binding site in addition to the mechanistic knowledge gained.

Literature Cited

Literature Cited

(1) Nussinov, R.; Tsai, C. J. Allostery in disease and in drug discovery. *Cell* **2013,** *153*, 293-305.

(2) Monod, J.; Wyman, J.; Changeux, J. P. On the Nature of Allosteric Transitions: A Plausible Model. *J. Mol. Biol.* **1965,** *12*, 88-118.

(3) Peracchi, A.; Mozzarelli, A. Exploring and exploiting allostery: Models, evolution, and drug targeting. *Biochim. Biophys. Acta* **2011,** *1814*, 922-933.

(4) Maksay, G. Allostery in pharmacology: thermodynamics, evolution and design. *Prog. Biophys. Mol. Biol.* **2011,** *106*, 463-473.

(5) Huang, Z.; Mou, L.; Shen, Q.; Lu, S.; Li, C.; Liu, X.; Wang, G.; Li, S.; Geng, L.; Liu, Y.; Wu, J.; Chen, G.; Zhang, J. ASD v2.0: updated content and novel features focusing on allosteric regulation. *Nucleic Acids Res.* **2014,** *42*, D510-516.

(6) Huang, Z.; Zhu, L.; Cao, Y.; Wu, G.; Liu, X.; Chen, Y.; Wang, Q.; Shi, T.; Zhao, Y.; Wang, Y.; Li, W.; Li, Y.; Chen, H.; Chen, G.; Zhang, J. ASD: a comprehensive database of allosteric proteins and modulators. *Nucleic Acids Res.* **2011,** *39*, D663-669.

(7) Stassen, J. M.; Arnout, J.; Deckmyn, H. The hemostatic system. *Curr. Med. Chem.* **2004,** *11*, 2245-2260.

(8) Riddel, J. P., Jr.; Aouizerat, B. E.; Miaskowski, C.; Lillicrap, D. P. Theories of blood coagulation. *J. Pediatr. Oncol. Nurs.* **2007,** *24*, 123-131.

(9) Davie, E. W. A brief historical review of the waterfall/cascade of blood coagulation. *J. Biol. Chem.* **2003,** *278*, 50819-50832.

(10) Brian, L. H.; Umesh, R. D. Anticoagulants. In *Burgers Medicinal Chemistry and Drug discovery*; 7 ed.; Abraham, D. J.; Rotella, D. P., Eds.; John Wiley and sons: Newyork, 2010.

(11) Adams, R. L.; Bird, R. J. Review article: Coagulation cascade and therapeutics update: relevance to nephrology. Part 1: Overview of coagulation, thrombophilias and history of anticoagulants. *Nephrology* **2009,** *14*, 462-470.

(12) Straub, A.; Roehrig, S.; Hillisch, A. Oral, direct thrombin and factor Xa inhibitors: the replacement for warfarin, leeches, and pig intestines? *Angew. Chem. Int. Ed. Engl.* **2011,** *50*, 4574-4590.

(13) Lechtenberg, B. C.; Freund, S. M.; Huntington, J. A. An ensemble view of thrombin allostery. *Biol. Chem.* **2012,** *393*, 889-898.

(14) Desai, U. R.; Petitou, M.; Bjork, I.; Olson, S. T. Mechanism of heparin activation of antithrombin. Role of individual residues of the pentasaccharide activating sequence in the recognition of native and activated states of antithrombin. *J. Biol. Chem.* **1998,** *273*, 7478-7487.

(15) Desai, U. R. New antithrombin-based anticoagulants. *Med. Res. Rev.* **2004,** *24*, 151-181.

(16) Petitou, M.; van Boeckel, C. A. A synthetic antithrombin III binding pentasaccharide is now a drug! What comes next? *Angew. Chem. Int. Ed. Engl.* **2004,** *43*, 3118-3133.
(17) Petitou, M.; Barzu, T.; Herault, J. P.; Herbert, J. M. A unique trisaccharide sequence in heparin mediates the early step of antithrombin III activation. *Glycobiology* **1997,** *7*, 323-327.
(18) Hirsh, J. Current anticoagulant therapy--unmet clinical needs. *Thromb. Res.* **2003,** *109 Suppl 1*, S1-8.
(19) Ruef, J.; Katus, H. A. New antithrombotic drugs on the horizon. *Expert Opin Investig Drugs* **2003,** *12*, 781-797.
(20) Rosenberg, R. D.; Damus, P. S. The purification and mechanism of action of human antithrombin-heparin cofactor. *J. Biol. Chem.* **1973,** *248*, 6490-6505.
(21) Blajchman, M. A. An overview of the mechanism of action of antithrombin and its inherited deficiency states. *Blood Coagul. Fibrinolysis* **1994,** *5 Suppl 1*, S5-11; discussion S59-64.
(22) Jin, L.; Abrahams, J. P.; Skinner, R.; Petitou, M.; Pike, R. N.; Carrell, R. W. The anticoagulant activation of antithrombin by heparin. *Proc. Natl. Acad. Sci. U. S. A.* **1997,** *94*, 14683-14688.
(23) Carrell, R. W.; Stein, P. E.; Fermi, G.; Wardell, M. R. Biological implications of a 3 A structure of dimeric antithrombin. *Structure* **1994,** *2*, 257-270.
(24) Schreuder, H. A.; de Boer, B.; Dijkema, R.; Mulders, J.; Theunissen, H. J.; Grootenhuis, P. D.; Hol, W. G. The intact and cleaved human antithrombin III complex as a model for serpin-proteinase interactions. *Nat. Struct. Biol.* **1994,** *1*, 48-54.
(25) Skinner, R.; Abrahams, J. P.; Whisstock, J. C.; Lesk, A. M.; Carrell, R. W.; Wardell, M. R. The 2.6 A structure of antithrombin indicates a conformational change at the heparin binding site. *J. Mol. Biol.* **1997,** *266*, 601-609.
(26) Gettins, P. G. Serpin structure, mechanism, and function. *Chem. Rev.* **2002,** *102*, 4751-4804.
(27) Wright, H. T. The structural puzzle of how serpin serine proteinase inhibitors work. *Bioessays* **1996,** *18*, 453-464.
(28) Wright, H. T.; Scarsdale, J. N. Structural basis for serpin inhibitor activity. *Proteins* **1995,** *22*, 210-225.
(29) Baglin, T. P.; Carrell, R. W.; Church, F. C.; Esmon, C. T.; Huntington, J. A. Crystal structures of native and thrombin-complexed heparin cofactor II reveal a multistep allosteric mechanism. *Proc. Natl. Acad. Sci. U. S. A.* **2002,** *99*, 11079-11084.
(30) Bruch, M.; Weiss, V.; Engel, J. Plasma serine proteinase inhibitors (serpins) exhibit major conformational changes and a large increase in conformational stability upon cleavage at their reactive sites. *J. Biol. Chem.* **1988,** *263*, 16626-16630.
(31) Kaslik, G.; Kardos, J.; Szabo, E.; Szilagyi, L.; Zavodszky, P.; Westler, W. M.; Markley, J. L.; Graf, L. Effects of serpin binding on the target proteinase: global

stabilization, localized increased structural flexibility, and conserved hydrogen bonding at the active site. *Biochemistry* **1997,** *36*, 5455-5464.
(32) Bjork, I.; Olson, S. T. Antithrombin. A bloody important serpin. *Adv. Exp. Med. Biol.* **1997,** *425*, 17-33.
(33) Calugaru, S. V.; Swanson, R.; Olson, S. T. The pH dependence of serpin-proteinase complex dissociation reveals a mechanism of complex stabilization involving inactive and active conformational states of the proteinase which are perturbable by calcium. *J. Biol. Chem.* **2001,** *276*, 32446-32455.
(34) Huntington, J. A.; Read, R. J.; Carrell, R. W. Structure of a serpin-protease complex shows inhibition by deformation. *Nature* **2000,** *407*, 923-926.
(35) Plotnick, M. I.; Mayne, L.; Schechter, N. M.; Rubin, H. Distortion of the active site of chymotrypsin complexed with a serpin. *Biochemistry* **1996,** *35*, 7586-7590.
(36) Latallo, Z. S.; Jackson, C. M. Reaction of thrombins with human antithrombin III: II. Dependence of rate of inhibition on molecular form and origin of thrombin. *Thromb. Res.* **1986,** *43*, 523-537.
(37) Olson, S. T.; Shore, J. D. Demonstration of a two-step reaction mechanism for inhibition of alpha-thrombin by antithrombin III and identification of the step affected by heparin. *J. Biol. Chem.* **1982,** *257*, 14891-14895.
(38) Wong, R. F.; Windwer, S. R.; Feinman, R. D. Interaction of thrombin and antithrombin. Reaction observed by intrinsic fluorescence measurements. *Biochemistry* **1983,** *22*, 3994-3999.
(39) Craig, P. A.; Olson, S. T.; Shore, J. D. Transient kinetics of heparin-catalyzed protease inactivation by antithrombin III. Characterization of assembly, product formation, and heparin dissociation steps in the factor Xa reaction. *J. Biol. Chem.* **1989,** *264*, 5452-5461.
(40) Pike, R. N.; Potempa, J.; Skinner, R.; Fitton, H. L.; McGraw, W. T.; Travis, J.; Owen, M.; Jin, L.; Carrell, R. W. Heparin-dependent modification of the reactive center arginine of antithrombin and consequent increase in heparin binding affinity. *J. Biol. Chem.* **1997,** *272*, 19652-19655.
(41) Mc, L. J. The discovery of heparin. *Circulation* **1959,** *19*, 75-78.
(42) Chuang, Y. J.; Swanson, R.; Raja, S. M.; Olson, S. T. Heparin enhances the specificity of antithrombin for thrombin and factor Xa independent of the reactive center loop sequence. Evidence for an exosite determinant of factor Xa specificity in heparin-activated antithrombin. *J. Biol. Chem.* **2001,** *276*, 14961-14971.
(43) Olson, S. T.; Bjork, I. Predominant contribution of surface approximation to the mechanism of heparin acceleration of the antithrombin-thrombin reaction. Elucidation from salt concentration effects. *J. Biol. Chem.* **1991,** *266*, 6353-6364.
(44) Duchaussoy, P.; Jaurand, G.; Driguez, P. A.; Lederman, I.; Ceccato, M. L.; Gourvenec, F.; Strassel, J. M.; Sizun, P.; Petitou, M.; Herbert, J. M. Assessment through chemical synthesis of the size of the heparin sequence involved in thrombin inhibition. *Carbohydr. Res.* **1999,** *317*, 85-99.
(45) Petitou, M.; Herault, J. P.; Bernat, A.; Driguez, P. A.; Duchaussoy, P.; Lormeau, J. C.; Herbert, J. M. Synthesis of thrombin-inhibiting heparin mimetics without side effects. *Nature* **1999,** *398*, 417-422.

(46) Rezaie, A. R. Calcium enhances heparin catalysis of the antithrombin-factor Xa reaction by a template mechanism. Evidence that calcium alleviates Gla domain antagonism of heparin binding to factor Xa. *J. Biol. Chem.* **1998,** *273*, 16824-16827.
(47) Arocas, V.; Bock, S. C.; Raja, S.; Olson, S. T.; Bjork, I. Lysine 114 of antithrombin is of crucial importance for the affinity and kinetics of heparin pentasaccharide binding. *J. Biol. Chem.* **2001,** *276*, 43809-43817.
(48) Desai, U.; Swanson, R.; Bock, S. C.; Bjork, I.; Olson, S. T. Role of arginine 129 in heparin binding and activation of antithrombin. *J. Biol. Chem.* **2000,** *275*, 18976-18984.
(49) Ersdal-Badju, E.; Lu, A.; Zuo, Y.; Picard, V.; Bock, S. C. Identification of the antithrombin III heparin binding site. *J. Biol. Chem.* **1997,** *272*, 19393-19400.
(50) Schedin-Weiss, S.; Desai, U. R.; Bock, S. C.; Gettins, P. G.; Olson, S. T.; Bjork, I. Importance of lysine 125 for heparin binding and activation of antithrombin. *Biochemistry* **2002,** *41*, 4779-4788.
(51) Schedin-Weiss, S.; Arocas, V.; Bock, S. C.; Olson, S. T.; Bjork, I. Specificity of the basic side chains of Lys114, Lys125, and Arg129 of antithrombin in heparin binding. *Biochemistry* **2002,** *41*, 12369-12376.
(52) Chuang, Y. J.; Swanson, R.; Raja, S. M.; Bock, S. C.; Olson, S. T. The antithrombin P1 residue is important for target proteinase specificity but not for heparin activation of the serpin. Characterization of P1 antithrombin variants with altered proteinase specificity but normal heparin activation. *Biochemistry* **2001,** *40*, 6670-6679.
(53) Olson, S. T.; Bjork, I.; Shore, J. D. Kinetic characterization of heparin-catalyzed and uncatalyzed inhibition of blood coagulation proteinases by antithrombin. *Methods Enzymol.* **1993,** *222*, 525-559.
(54) Atha, D. H.; Lormeau, J. C.; Petitou, M.; Rosenberg, R. D.; Choay, J. Contribution of monosaccharide residues in heparin binding to antithrombin III. *Biochemistry* **1985,** *24*, 6723-6729.
(55) Atha, D. H.; Stephens, A. W.; Rimon, A.; Rosenberg, R. D. Sequence variation in heparin octasaccharides with high affinity for antithrombin III. *Biochemistry* **1984,** *23*, 5801-5812.
(56) Lindahl, U.; Backstrom, G.; Thunberg, L.; Leder, I. G. Evidence for a 3-O-sulfated D-glucosamine residue in the antithrombin-binding sequence of heparin. *Proc. Natl. Acad. Sci. U. S. A.* **1980,** *77*, 6551-6555.
(57) Lindahl, U.; Thunberg, L.; Backstrom, G.; Riesenfeld, J.; Nordling, K.; Bjork, I. Extension and structural variability of the antithrombin-binding sequence in heparin. *J. Biol. Chem.* **1984,** *259*, 12368-12376.
(58) Cosmi, B.; Hirsh, J. Low molecular weight heparins. *Curr. Opin. Cardiol.* **1994,** *9*, 612-618.
(59) Hirsh, J.; Levine, M. N. Low molecular weight heparin. *Blood* **1992,** *79*, 1-17.
(60) Alban, S.; Franz, G. Characterization of the anticoagulant actions of a semisynthetic curdlan sulfate. *Thromb. Res.* **2000,** *99*, 377-388.

(61) Alban, S.; Jeske, W.; Welzel, D.; Franz, G.; Fareed, J. Anticoagulant and antithrombotic actions of a semisynthetic beta-1,3-glucan sulfate. *Thromb. Res.* **1995,** *78*, 201-210.
(62) Drozd, N. N.; Sher, A. I.; Makarov, V. A.; Galbraikh, L. S.; Vikhoreva, G. A.; Gorbachiova, I. N. Comparison of antithrombin activity of the polysulphate chitosan derivatives in in vivo and in vitro system. *Thromb. Res.* **2001,** *102*, 445-455.
(63) Logeart-Avramoglou, D.; Jozefonvicz, J. Carboxymethyl benzylamide sulfonate dextrans (CMDBS), a family of biospecific polymers endowed with numerous biological properties: a review. *J. Biomed. Mater. Res.* **1999,** *48*, 578-590.
(64) Muzzarelli, R. A.; Tanfani, F.; Emanuelli, M.; Pace, D. P.; Chiurazzi, E.; Piani, M. Sulfated N-(carboxymethyl)chitosans: novel blood anticoagulants. *Carbohydr. Res.* **1984,** *126*, 225-231.
(65) Boneu, B. Low molecular weight heparins: are they superior to unfractionated heparins to prevent and to treat deep vein thrombosis? *Thromb. Res.* **2000,** *100*, V113-120.
(66) Cohen, M. The role of low-molecular-weight heparins in arterial diseases: optimizing antithrombotic therapy. *Thromb. Res.* **2000,** *100*, V131-139.
(67) Hirsh, J.; Warkentin, T. E.; Raschke, R.; Granger, C.; Ohman, E. M.; Dalen, J. E. Heparin and low-molecular-weight heparin: mechanisms of action, pharmacokinetics, dosing considerations, monitoring, efficacy, and safety. *Chest* **1998,** *114*, 489S-510S.
(68) Theroux, P.; Waters, D.; Lam, J.; Juneau, M.; McCans, J. Reactivation of unstable angina after the discontinuation of heparin. *N. Engl. J. Med.* **1992,** *327*, 141-145.
(69) Warkentin, T. E.; Chong, B. H.; Greinacher, A. Heparin-induced thrombocytopenia: towards consensus. *Thromb. Haemost.* **1998,** *79*, 1-7.
(70) Young, E.; Podor, T. J.; Venner, T.; Hirsh, J. Induction of the acute-phase reaction increases heparin-binding proteins in plasma. *Arterioscler. Thromb. Vasc. Biol.* **1997,** *17*, 1568-1574.
(71) Leizorovicz, A.; Haugh, M. C.; Chapuis, F. R.; Samama, M. M.; Boissel, J. P. Low molecular weight heparin in prevention of perioperative thrombosis. *BMJ* **1992,** *305*, 913-920.
(72) Nurmohamed, M. T.; ten Cate, H.; ten Cate, J. W. Low molecular weight heparin(oid)s. Clinical investigations and practical recommendations. *Drugs* **1997,** *53*, 736-751.
(73) Shriver, Z.; Sundaram, M.; Venkataraman, G.; Fareed, J.; Linhardt, R.; Biemann, K.; Sasisekharan, R. Cleavage of the antithrombin III binding site in heparin by heparinases and its implication in the generation of low molecular weight heparin. *Proc. Natl. Acad. Sci. U. S. A.* **2000,** *97*, 10365-10370.
(74) Thomas, D. P. Does low molecular weight heparin cause less bleeding? *Thromb. Haemost.* **1997,** *78*, 1422-1425.
(75) Turpie, A. G. Anticoagulants in acute coronary syndromes. *Am. J. Cardiol.* **1999,** *84*, 2M-6M.

(76) Yu, G.; LeBrun, L.; Gunay, N. S.; Hoppensteadt, D.; Walenga, J. M.; Fareed, J.; Linhardt, R. J. Heparinase I acts on a synthetic heparin pentasaccharide corresponding to the antithrombin III binding site. *Thromb. Res.* **2000,** *100*, 549-556.
(77) Ampofo, S. A.; Wang, H. M.; Linhardt, R. J. Disaccharide compositional analysis of heparin and heparan sulfate using capillary zone electrophoresis. *Anal. Biochem.* **1991,** *199*, 249-255.
(78) Desai, U. R.; Wang, H.; Ampofo, S. A.; Linhardt, R. J. Oligosaccharide composition of heparin and low-molecular-weight heparins by capillary electrophoresis. *Anal. Biochem.* **1993,** *213*, 120-127.
(79) Desai, U. R.; Wang, H. M.; Linhardt, R. J. Substrate specificity of the heparin lyases from Flavobacterium heparinum. *Arch. Biochem. Biophys.* **1993,** *306*, 461-468.
(80) Lovely, R. S.; Moaddel, M.; Farrell, D. H. Fibrinogen gamma' chain binds thrombin exosite II. *J. Thromb. Haemost.* **2003,** *1*, 124-131.
(81) Venkataraman, G.; Shriver, Z.; Raman, R.; Sasisekharan, R. Sequencing complex polysaccharides. *Science* **1999,** *286*, 537-542.
(82) Al-Horani, R. A.; Liang, A.; Desai, U. R. Designing nonsaccharide, allosteric activators of antithrombin for accelerated inhibition of factor Xa. *J. Med. Chem.* **2011,** *54*, 6125-6138.
(83) Briginshaw, G. F.; Shanberge, J. N. Identification of two distinct heparin cofactors in human plasma. II. Inhibition of thrombin and activated factor X. *Thromb. Res.* **1974,** *4*, 463-477.
(84) Briginshaw, G. F.; Shanberge, J. N. Identification of two distinct heparin cofactors in human plasma. Separation and partial purification. *Arch. Biochem. Biophys.* **1974,** *161*, 683-690.
(85) Tollefsen, D. M.; Majerus, D. W.; Blank, M. K. Heparin cofactor II. Purification and properties of a heparin-dependent inhibitor of thrombin in human plasma. *J. Biol. Chem.* **1982,** *257*, 2162-2169.
(86) Aihara, K.; Azuma, H.; Takamori, N.; Kanagawa, Y.; Akaike, M.; Fujimura, M.; Yoshida, T.; Hashizume, S.; Kato, M.; Yamaguchi, H.; Kato, S.; Ikeda, Y.; Arase, T.; Kondo, A.; Matsumoto, T. Heparin cofactor II is a novel protective factor against carotid atherosclerosis in elderly individuals. *Circulation* **2004,** *109*, 2761-2765.
(87) He, L.; Vicente, C. P.; Westrick, R. J.; Eitzman, D. T.; Tollefsen, D. M. Heparin cofactor II inhibits arterial thrombosis after endothelial injury. *J. Clin. Invest.* **2002,** *109*, 213-219.
(88) Huang, P. H.; Leu, H. B.; Chen, J. W.; Wu, T. C.; Lu, T. M.; Yu-An Ding, P.; Lin, S. J. Decreased heparin cofactor II activity is associated with impaired endothelial function determined by brachial ultrasonography and predicts cardiovascular events. *Int. J. Cardiol.* **2007,** *114*, 152-158.
(89) Takamori, N.; Azuma, H.; Kato, M.; Hashizume, S.; Aihara, K.; Akaike, M.; Tamura, K.; Matsumoto, T. High plasma heparin cofactor II activity is associated

with reduced incidence of in-stent restenosis after percutaneous coronary intervention. *Circulation* **2004,** *109*, 481-486.
(90) Rau, J. C.; Mitchell, J. W.; Fortenberry, Y. M.; Church, F. C. Heparin cofactor II: discovery, properties, and role in controlling vascular homeostasis. *Semin. Thromb. Hemost.* **2011,** *37*, 339-348.
(91) Raghuraman, A.; Mosier, P. D.; Desai, U. R. Understanding Dermatan Sulfate-Heparin Cofactor II Interaction through Virtual Library Screening. *ACS Med. Chem. Lett.* **2010,** *1*, 281-285.
(92) Maimone, M. M.; Tollefsen, D. M. Structure of a dermatan sulfate hexasaccharide that binds to heparin cofactor II with high affinity. *J. Biol. Chem.* **1990,** *265*, 18263-18271.
(93) Sarilla, S.; Habib, S. Y.; Kravtsov, D. V.; Matafonov, A.; Gailani, D.; Verhamme, I. M. Sucrose octasulfate selectively accelerates thrombin inactivation by heparin cofactor II. *J. Biol. Chem.* **2010,** *285*, 8278-8289.
(94) Ansell, J. Factor Xa or thrombin: is factor Xa a better target? *J. Thromb. Haemost.* **2007,** *5 Suppl 1*, 60-64.
(95) Mann, K. G.; Brummel, K.; Butenas, S. What is all that thrombin for? *J. Thromb. Haemost.* **2003,** *1*, 1504-1514.
(96) Gulseth, M. P.; Michaud, J.; Nutescu, E. A. Rivaroxaban: an oral direct inhibitor of factor Xa. *Am. J. Health Syst. Pharm.* **2008,** *65*, 1520-1529.
(97) Harenberg, J.; Wehling, M. Current and future prospects for anticoagulant therapy: inhibitors of factor Xa and factor IIa. *Semin. Thromb. Hemost.* **2008,** *34*, 39-57.
(98) Piccini, J. P.; Patel, M. R.; Mahaffey, K. W.; Fox, K. A.; Califf, R. M. Rivaroxaban, an oral direct factor Xa inhibitor. *Expert Opin Investig Drugs* **2008,** *17*, 925-937.
(99) Weinz, C.; Schwarz, T.; Kubitza, D.; Mueck, W.; Lang, D. Metabolism and excretion of rivaroxaban, an oral, direct factor Xa inhibitor, in rats, dogs, and humans. *Drug Metab. Dispos.* **2009,** *37*, 1056-1064.
(100) Emsley, J.; McEwan, P. A.; Gailani, D. Structure and function of factor XI. *Blood* **2010,** *115*, 2569-2577.
(101) Jin, L.; Pandey, P.; Babine, R. E.; Gorga, J. C.; Seidl, K. J.; Gelfand, E.; Weaver, D. T.; Abdel-Meguid, S. S.; Strickler, J. E. Crystal structures of the FXIa catalytic domain in complex with ecotin mutants reveal substrate-like interactions. *J. Biol. Chem.* **2005,** *280*, 4704-4712.
(102) Papagrigoriou, E.; McEwan, P. A.; Walsh, P. N.; Emsley, J. Crystal structure of the factor XI zymogen reveals a pathway for transactivation. *Nat. Struct. Mol. Biol.* **2006,** *13*, 557-558.
(103) Al-Horani, R. A.; Ponnusamy, P.; Mehta, A. Y.; Gailani, D.; Desai, U. R. Sulfated pentagalloylglucoside is a potent, allosteric, and selective inhibitor of factor XIa. *J. Med. Chem.* **2013,** *56*, 867-878.
(104) Schumacher, W. A.; Seiler, S. E.; Steinbacher, T. E.; Stewart, A. B.; Bostwick, J. S.; Hartl, K. S.; Liu, E. C.; Ogletree, M. L. Antithrombotic and hemostatic effects of a small molecule factor XIa inhibitor in rats. *Eur. J. Pharmacol.* **2007,** *570*, 167-174.

(105) Duga, S.; Salomon, O. Factor XI Deficiency. *Semin. Thromb. Hemost.* **2009,** *35*, 416-425.
(106) Gomez, K.; Bolton-Maggs, P. Factor XI deficiency. *Haemophilia* **2008,** *14*, 1183-1189.
(107) Seligsohn, U. Factor XI deficiency in humans. *J. Thromb. Haemost.* **2009,** *7 Suppl 1*, 84-87.
(108) Salomon, O.; Steinberg, D. M.; Koren-Morag, N.; Tanne, D.; Seligsohn, U. Reduced incidence of ischemic stroke in patients with severe factor XI deficiency. *Blood* **2008,** *111*, 4113-4117.
(109) Rosen, E. D.; Gailani, D.; Castellino, F. J. FXI is essential for thrombus formation following FeCl3-induced injury of the carotid artery in the mouse. *Thromb. Haemost.* **2002,** *87*, 774-776.
(110) Buchanan, M. S.; Carroll, A. R.; Wessling, D.; Jobling, M.; Avery, V. M.; Davis, R. A.; Feng, Y.; Xue, Y.; Oster, L.; Fex, T.; Deinum, J.; Hooper, J. N.; Quinn, R. J. Clavatadine A, a natural product with selective recognition and irreversible inhibition of factor XIa. *J. Med. Chem.* **2008,** *51*, 3583-3587.
(111) Deng, H.; Bannister, T. D.; Jin, L.; Babine, R. E.; Quinn, J.; Nagafuji, P.; Celatka, C. A.; Lin, J.; Lazarova, T. I.; Rynkiewicz, M. J.; Bibbins, F.; Pandey, P.; Gorga, J.; Meyers, H. V.; Abdel-Meguid, S. S.; Strickler, J. E. Synthesis, SAR exploration, and X-ray crystal structures of factor XIa inhibitors containing an alpha-ketothiazole arginine. *Bioorg. Med. Chem. Lett.* **2006,** *16*, 3049-3054.
(112) Hanessian, S.; Larsson, A.; Fex, T.; Knecht, W.; Blomberg, N. Design and synthesis of macrocyclic indoles targeting blood coagulation cascade Factor XIa. *Bioorg. Med. Chem. Lett.* **2010,** *20*, 6925-6928.
(113) Lazarova, T. I.; Jin, L.; Rynkiewicz, M.; Gorga, J. C.; Bibbins, F.; Meyers, H. V.; Babine, R.; Strickler, J. Synthesis and in vitro biological evaluation of aryl boronic acids as potential inhibitors of factor XIa. *Bioorg. Med. Chem. Lett.* **2006,** *16*, 5022-5027.
(114) Lin, J.; Deng, H.; Jin, L.; Pandey, P.; Quinn, J.; Cantin, S.; Rynkiewicz, M. J.; Gorga, J. C.; Bibbins, F.; Celatka, C. A.; Nagafuji, P.; Bannister, T. D.; Meyers, H. V.; Babine, R. E.; Hayward, N. J.; Weaver, D.; Benjamin, H.; Stassen, F.; Abdel-Meguid, S. S.; Strickler, J. E. Design, synthesis, and biological evaluation of peptidomimetic inhibitors of factor XIa as novel anticoagulants. *J. Med. Chem.* **2006,** *49*, 7781-7791.
(115) Wong, P. C.; Crain, E. J.; Watson, C. A.; Schumacher, W. A. A small-molecule factor XIa inhibitor produces antithrombotic efficacy with minimal bleeding time prolongation in rabbits. *J. Thromb. Thrombolysis* **2011,** *32*, 129-137.
(116) Badellino, K. O.; Walsh, P. N. Localization of a heparin binding site in the catalytic domain of factor XIa. *Biochemistry* **2001,** *40*, 7569-7580.
(117) Sinha, D.; Badellino, K. O.; Marcinkiewicz, M.; Walsh, P. N. Allosteric modification of factor XIa functional activity upon binding to polyanions. *Biochemistry* **2004,** *43*, 7593-7600.
(118) Kraushaar, D. C.; Dalton, S.; Wang, L. Heparan sulfate: a key regulator of embryonic stem cell fate. *Biol. Chem.* **2013,** *394*, 741-751.

(119) Yamada, S.; Morimoto, H.; Fujisawa, T.; Sugahara, K. Glycosaminoglycans in Hydra magnipapillata (Hydrozoa, Cnidaria): demonstration of chondroitin in the developing nematocyst, the sting organelle, and structural characterization of glycosaminoglycans. *Glycobiology* **2007,** *17*, 886-894.
(120) Gandhi, N. S.; Mancera, R. L. The structure of glycosaminoglycans and their interactions with proteins. *Chem. Biol. Drug Des.* **2008,** *72*, 455-482.
(121) Sarrazin, S.; Lamanna, W. C.; Esko, J. D. Heparan sulfate proteoglycans. *Cold Spring Harb. Perspect. Biol.* **2011,** *3*.
(122) Coombe, D. R.; Kett, W. C. Heparan sulfate-protein interactions: therapeutic potential through structure-function insights. *Cell. Mol. Life Sci.* **2005,** *62*, 410-424.
(123) Raman, R.; Sasisekharan, V.; Sasisekharan, R. Structural insights into biological roles of protein-glycosaminoglycan interactions. *Chem. Biol.* **2005,** *12*, 267-277.
(124) Esko, J. D.; Selleck, S. B. Order out of chaos: assembly of ligand binding sites in heparan sulfate. *Annu. Rev. Biochem.* **2002,** *71*, 435-471.
(125) Desai, U. R. The promise of sulfated synthetic small molecules as modulators of glycosaminoglycan function. *Future Med. Chem.* **2013,** *5*, 1363-1366.
(126) Mulloy, B.; Forster, M. J. Conformation and dynamics of heparin and heparan sulfate. *Glycobiology* **2000,** *10*, 1147-1156.
(127) Grootenhuis, P. D. v. B., C. A. A. Constructing a molecular model of the interaction betweeen antithrombin III and a potent heparin analog. *J. Am. Chem. Soc.* **1991,** *113*, 2743-2747.
(128) Raghuraman, A.; Mosier, P. D.; Desai, U. R. Finding a needle in a haystack: development of a combinatorial virtual screening approach for identifying high specificity heparin/heparan sulfate sequence(s). *J. Med. Chem.* **2006,** *49*, 3553-3562.
(129) Mosier, P. D.; Krishnasamy, C.; Kellogg, G. E.; Desai, U. R. On the specificity of heparin/heparan sulfate binding to proteins. Anion-binding sites on antithrombin and thrombin are fundamentally different. *PLoS One* **2012,** *7*, e48632.
(130) Maimone, M. M.; Tollefsen, D. M. Activation of heparin cofactor II by heparin oligosaccharides. *Biochem. Biophys. Res. Commun.* **1988,** *152*, 1056-1061.
(131) Duchaussoy, P. L., P. S.; Petitou, M.; Sinay, P.; Lormeau, J. C.; Choay, J. The first total synthesis of the antithrombin III binding site of porcine mucosa heparin. *Bioorg. Med. Chem. Lett.* **1991,** *2*, 99-102.
(132) Petitou, M.; Duchaussoy, P.; Jaurand, G.; Gourvenec, F.; Lederman, I.; Strassel, J. M.; Barzu, T.; Crepon, B.; Herault, J. P.; Lormeau, J. C.; Bernat, A.; Herbert, J. M. Synthesis and pharmacological properties of a close analogue of an antithrombotic pentasaccharide (SR 90107A/ORG 31540). *J. Med. Chem.* **1997,** *40*, 1600-1607.
(133) Petitou, M.; Nancy-Portebois, V.; Dubreucq, G.; Motte, V.; Meuleman, D.; de Kort, M.; van Boeckel, C. A.; Vogel, G. M.; Wisse, J. A. From heparin to EP217609: the long way to a new pentasaccharide-based neutralisable anticoagulant with an unprecedented pharmacological profile. *Thromb. Haemost.* **2009,** *102*, 804-810.

(134) Li, W.; Johnson, D. J.; Esmon, C. T.; Huntington, J. A. Structure of the antithrombin-thrombin-heparin ternary complex reveals the antithrombotic mechanism of heparin. *Nat. Struct. Mol. Biol.* **2004,** *11*, 857-862.
(135) Izaguirre, G.; Olson, S. T. Residues Tyr253 and Glu255 in strand 3 of beta-sheet C of antithrombin are key determinants of an exosite made accessible by heparin activation to promote rapid inhibition of factors Xa and IXa. *J. Biol. Chem.* **2006,** *281*, 13424-13432.
(136) Faham, S.; Hileman, R. E.; Fromm, J. R.; Linhardt, R. J.; Rees, D. C. Heparin structure and interactions with basic fibroblast growth factor. *Science,* **1996,** *271*, 1116-1120.
(137) Carter, W. J.; Cama, E.; Huntington, J. A. Crystal structure of thrombin bound to heparin. *J. Biol. Chem.* **2005,** *280*, 2745-2749.
(138) Pellegrini, L.; Burke, D. F.; von Delft, F.; Mulloy, B.; Blundell, T. L. Crystal structure of fibroblast growth factor receptor ectodomain bound to ligand and heparin. *Nature* **2000,** *407*, 1029-1034.
(139) Schlessinger, J.; Plotnikov, A. N.; Ibrahimi, O. A.; Eliseenkova, A. V.; Yeh, B. K.; Yayon, A.; Linhardt, R. J.; Mohammadi, M. Crystal structure of a ternary FGF-FGFR-heparin complex reveals a dual role for heparin in FGFR binding and dimerization. *Molecular cell* **2000,** *6*, 743-750.
(140) Capila, I.; Hernaiz, M. J.; Mo, Y. D.; Mealy, T. R.; Campos, B.; Dedman, J. R.; Linhardt, R. J.; Seaton, B. A. Annexin V--heparin oligosaccharide complex suggests heparan sulfate--mediated assembly on cell surfaces. *Structure,* **2001,** *9*, 57-64.
(141) Moon, A. F.; Edavettal, S. C.; Krahn, J. M.; Munoz, E. M.; Negishi, M.; Linhardt, R. J.; Liu, J.; Pedersen, L. C. Structural analysis of the sulfotransferase (3-o-sulfotransferase isoform 3) involved in the biosynthesis of an entry receptor for herpes simplex virus 1. *J. Biol. Chem.* **2004,** *279*, 45185-45193.
(142) Shaw, J. P.; Johnson, Z.; Borlat, F.; Zwahlen, C.; Kungl, A.; Roulin, K.; Harrenga, A.; Wells, T. N.; Proudfoot, A. E. The X-ray structure of RANTES: heparin-derived disaccharides allows the rational design of chemokine inhibitors. *Structure* **2004,** *12*, 2081-2093.
(143) Ragazzi, M.; Ferro, D. R.; Perly, B.; Sinay, P.; Petitou, M.; Choay, J. Conformation of the pentasaccharide corresponding to the binding site of heparin for antithrombin III. *Carbohydr. Res.* **1990,** *195*, 169-185.
(144) Verhamme, I. M.; Bock, P. E.; Jackson, C. M. The preferred pathway of glycosaminoglycan-accelerated inactivation of thrombin by heparin cofactor II. *J. Biol. Chem.* **2004,** *279*, 9785-9795.
(145) Liaw, P. C.; Becker, D. L.; Stafford, A. R.; Fredenburgh, J. C.; Weitz, J. I. Molecular basis for the susceptibility of fibrin-bound thrombin to inactivation by heparin cofactor ii in the presence of dermatan sulfate but not heparin. *J. Biol. Chem.* **2001,** *276*, 20959-20965.
(146) Warda, M.; Gouda, E. M.; Toida, T.; Chi, L.; Linhardt, R. J. Isolation and characterization of raw heparin from dromedary intestine: evaluation of a new

source of pharmaceutical heparin. *Comp. Biochem. Physiol. C. Toxicol. Pharmacol.* **2003,** *136*, 357-365.
(147) Warda, M.; Linhardt, R. J. Dromedary glycosaminoglycans: molecular characterization of camel lung and liver heparan sulfate. *Comp. Biochem. Physiol. B, Biochem. Mol Biology* **2006,** *143*, 37-43.
(148) Vongchan, P.; Warda, M.; Toyoda, H.; Toida, T.; Marks, R. M.; Linhardt, R. J. Structural characterization of human liver heparan sulfate. *Biochim. Biophys. Acta.* **2005,** *1721*, 1-8.
(149) Rabenstein, D. L. Heparin and heparan sulfate: structure and function. *Nat. Prod. Rep.* **2002,** *19*, 312-331.
(150) Sharp, A. M.; Stein, P. E.; Pannu, N. S.; Carrell, R. W.; Berkenpas, M. B.; Ginsburg, D.; Lawrence, D. A.; Read, R. J. The active conformation of plasminogen activator inhibitor 1, a target for drugs to control fibrinolysis and cell adhesion. *Structure* **1999,** *7*, 111-118.
(151) Li, W.; Huntington, J. A. The heparin binding site of protein C inhibitor is protease-dependent. *The Journal of biological chemistry* **2008,** *283*, 36039-36045.
(152) Li, W.; Huntington, J. A. Crystal structures of protease nexin-1 in complex with heparin and thrombin suggest a 2-step recognition mechanism. *Blood* **2012,** *120*, 459-467.
(153) Johnson, D. J.; Langdown, J.; Huntington, J. A. Molecular basis of factor IXa recognition by heparin-activated antithrombin revealed by a 1.7-A structure of the ternary complex. *Proct. Natl. Acad. Sci. of the U. S. A.* **2010,** *107*, 645-650.
(154) Johnson, D. J.; Li, W.; Adams, T. E.; Huntington, J. A. Antithrombin-S195A factor Xa-heparin structure reveals the allosteric mechanism of antithrombin activation. *EMBO J.* **2006,** *25*, 2029-2037.
(155) Liaw, P. C.; Austin, R. C.; Fredenburgh, J. C.; Stafford, A. R.; Weitz, J. I. Comparison of heparin- and dermatan sulfate-mediated catalysis of thrombin inactivation by heparin cofactor II. *J. Biol. Chem.* **1999,** *274*, 27597-27604.
(156) Meagher, J. L.; Beechem, J. M.; Olson, S. T.; Gettins, P. G. Deconvolution of the fluorescence emission spectrum of human antithrombin and identification of the tryptophan residues that are responsive to heparin binding. *J. Biol. Chem.* **1998,** *273*, 23283-23289.
(157) Herbert, J. M.; Herault, J. P.; Bernat, A.; van Amsterdam, R. G.; Lormeau, J. C.; Petitou, M.; van Boeckel, C.; Hoffmann, P.; Meuleman, D. G. Biochemical and pharmacological properties of SANORG 34006, a potent and long-acting synthetic pentasaccharide. *Blood* **1998,** *91*, 4197-4205.
(158) Herbert, J. M.; Herault, J. P.; Bernat, A.; van Amsterdam, R. G.; Vogel, G. M.; Lormeau, J. C.; Petitou, M.; Meuleman, D. G. Biochemical and pharmacological properties of SANORG 32701. Comparison with the "synthetic pentasaccharide' (SR 90107/ORG 31540) and standard heparin. *Circ. Res.* **1996,** *79*, 590-600.
(159) Fareed, J.; Hoppensteadt, D. A.; Bick, R. L. An update on heparins at the beginning of the new millennium. *Semin. Thromb. Hemost.* **2000,** *26 Suppl 1*, 5-21.

(160) van Boeckel, C. A. A. P., M. . The unique antithrombin II binding domain of heparin : A lead to new synthetic antithrombotics. *Angew. Chem. Int. Ed. Engl.* **1993,** *32*, 1671-1818.
(161) O'Keeffe, D.; Olson, S. T.; Gasiunas, N.; Gallagher, J.; Baglin, T. P.; Huntington, J. A. The heparin binding properties of heparin cofactor II suggest an antithrombin-like activation mechanism. *J. Biol. Chem.* **2004,** *279*, 50267-50273.
(162) Suwan, J.; Zhang, Z.; Li, B.; Vongchan, P.; Meepowpan, P.; Zhang, F.; Mousa, S. A.; Mousa, S.; Premanode, B.; Kongtawelert, P.; Linhardt, R. J. Sulfonation of papain-treated chitosan and its mechanism for anticoagulant activity. *Carbohydr. Res.* **2009,** *344*, 1190-1196.
(163) Zhu, Z.; Zhang, Q.; Chen, L.; Ren, S.; Xu, P.; Tang, Y.; Luo, D. Higher specificity of the activity of low molecular weight fucoidan for thrombin-induced platelet aggregation. *Thromb. Res.* **2010,** *125*, 419-426.
(164) Fonseca, R. J.; Mourao, P. A. Fucosylated chondroitin sulfate as a new oral antithrombotic agent. *Thromb. Haemost.* **2006,** *96*, 822-829.
(165) Goto, F. O., T. Synthesis of a dermatan sulfate hexasaccharide that activates heparin cofactor II. *Bioorg. Med. Chem. Lett.* **1994,** *4*, 619.
(166) Petitou, M.; Lormeau, J. C.; Perly, B.; Berthault, P.; Bossennec, V.; Sie, P.; Choay, J. Is there a unique sequence in heparin for interaction with heparin cofactor II? Structural and biological studies of heparin-derived oligosaccharides. *J. Biol. Chem.* **1988,** *263*, 8685-8690.
(167) Linhardt, R. J.; Rice, K. G.; Merchant, Z. M.; Kim, Y. S.; Lohse, D. L. Structure and activity of a unique heparin-derived hexasaccharide. *J. Biol. Chem.* **1986,** *261*, 14448-14454.
(168) Desai, B. J.; Boothello, R. S.; Mehta, A. Y.; Scarsdale, J. N.; Wright, H. T.; Desai, U. R. Interaction of thrombin with sucrose octasulfate. *Biochemistry* **2011,** *50*, 6973-6982.
(169) Seeberger, P. H.; Werz, D. B. Automated synthesis of oligosaccharides as a basis for drug discovery. *Nature reviews. Drug discovery* **2005,** *4*, 751-763.
(170) Jones, G.; Willett, P.; Glen, R. C.; Leach, A. R.; Taylor, R. Development and validation of a genetic algorithm for flexible docking. *J. Mol. Biol.* **1997,** *267*, 727-748.
(171) Ferro, D. R.; Provasoli, A.; Ragazzi, M.; Casu, B.; Torri, G.; Bossennec, V.; Perly, B.; Sinay, P.; Petitou, M.; Choay, J. Conformer populations of L-iduronic acid residues in glycosaminoglycan sequences. *Carbohydr. Res.* **1990,** *195*, 157-167.
(172) Kirschner, K. N.; Yongye, A. B.; Tschampel, S. M.; Gonzalez-Outeirino, J.; Daniels, C. R.; Foley, B. L.; Woods, R. J. GLYCAM06: a generalizable biomolecular force field. Carbohydrates. *J. Comput. Chem.* **2008,** *29*, 622-655.
(173) McCoy, A. J.; Pei, X. Y.; Skinner, R.; Abrahams, J. P.; Carrell, R. W. Structure of beta-antithrombin and the effect of glycosylation on antithrombin's heparin affinity and activity. *J. Mol. Biol.* **2003,** *326*, 823-833.
(174) Pol-Fachin, L.; Verli, H. Depiction of the forces participating in the 2-O-sulfo-alpha-L-iduronic acid conformational preference in heparin sequences in aqueous solutions. *Carbohydr. Res.* **2008,** *343*, 1435-1445.

(175) Verdonk, M. L.; Cole, J. C.; Hartshorn, M. J.; Murray, C. W.; Taylor, R. D. Improved protein-ligand docking using GOLD. *Proteins* **2003,** *52*, 609-623.
(176) Gunnarsson, G. T.; Desai, U. R. Interaction of designed sulfated flavanoids with antithrombin: lessons on the design of organic activators. *J. Med. Chem.* **2002,** *45*, 4460-4470.
(177) Sidhu, P. S.; Liang, A.; Mehta, A. Y.; Abdel Aziz, M. H.; Zhou, Q.; Desai, U. R. Rational design of potent, small, synthetic allosteric inhibitors of thrombin. *J. Med. Chem.* **2011,** *54*, 5522-5531.
(178) Carlsson, P.; Kjellen, L. Heparin biosynthesis. *Handb. Exp. Pharmacol.* **2012**, 23-41.
(179) Esko, J. D.; Kimata, K.; Lindahl, U. Proteoglycans and Sulfated Glycosaminoglycans. In *Essentials of Glycobiology*, 2nd ed.; Varki, A.; Cummings, R. D.; Esko, J. D.; Freeze, H. H.; Stanley, P.; Bertozzi, C. R.; Hart, G. W.; Etzler, M. E., Eds. Cold Spring Harbor (NY), 2009.
(180) Esko, J. D.; Lindahl, U. Molecular diversity of heparan sulfate. *J. Clin. Invest.* **2001,** *108*, 169-173.
(181) Vives, R. R.; Seffouh, A.; Lortat-Jacob, H. Post-Synthetic Regulation of HS Structure: The Yin and Yang of the Sulfs in Cancer. *Front. Oncol.* **2014,** *3*, 331.
(182) Afratis, N.; Gialeli, C.; Nikitovic, D.; Tsegenidis, T.; Karousou, E.; Theocharis, A. D.; Pavao, M. S.; Tzanakakis, G. N.; Karamanos, N. K. Glycosaminoglycans: key players in cancer cell biology and treatment. *FEBS J.* **2012,** *279*, 1177-1197.
(183) Connell, B. J.; Lortat-Jacob, H. Human Immunodeficiency Virus and Heparan Sulfate: From Attachment to Entry Inhibition. *Front. Immunol.* **2013,** *4*, 385.
(184) Huntington, J. A. Mechanisms of glycosaminoglycan activation of the serpins in hemostasis. *J. Thromb. Haemost.* **2003,** *1*, 1535-1549.
(185) Shute, J. Glycosaminoglycan and chemokine/growth factor interactions. *Handb. Exp. Pharmacol.* **2012**, 307-324.
(186) Rein, C. M.; Desai, U. R.; Church, F. C. Serpin-glycosaminoglycan interactions. *Methods Enzymol.* **2011,** *501*, 105-137.
(187) Forster, M.; Mulloy, B. Computational approaches to the identification of heparin-binding sites on the surfaces of proteins. *Biochem. Soc. Trans.* **2006,** *34*, 431-434.
(188) Sage, J.; Mallevre, F.; Barbarin-Costes, F.; Samsonov, S. A.; Gehrcke, J. P.; Pisabarro, M. T.; Perrier, E.; Schnebert, S.; Roget, A.; Livache, T.; Nizard, C.; Lalmanach, G.; Lecaille, F. Binding of chondroitin 4-sulfate to cathepsin S regulates its enzymatic activity. *Biochemistry* **2013,** *52*, 6487-6498.
(189) Gandhi, N. S.; Freeman, C.; Parish, C. R.; Mancera, R. L. Computational analyses of the catalytic and heparin-binding sites and their interactions with glycosaminoglycans in glycoside hydrolase family 79 endo-beta-D-glucuronidase (heparanase). *Glycobiology* **2012,** *22*, 35-55.
(190) Gupta, V. K.; Gowda, L. R. Alpha-1-proteinase inhibitor is a heparin binding serpin: molecular interactions with the Lys rich cluster of helix-F domain. *Biochimie* **2008,** *90*, 749-761.

(191) Ballut, L.; Sapay, N.; Chautard, E.; Imberty, A.; Ricard-Blum, S. Mapping of heparin/heparan sulfate binding sites on alphavbeta3 integrin by molecular docking. *J. Mol. Recognit.* **2013,** *26*, 76-85.
(192) Nieto, L.; Canales, A.; Gimenez-Gallego, G.; Nieto, P. M.; Jimenez-Barbero, J. Conformational selection of the AGA*IA(M) heparin pentasaccharide when bound to the fibroblast growth factor receptor. *Chemistry* **2011,** *17*, 11204-11209.
(193) Knappe, M.; Bodevin, S.; Selinka, H. C.; Spillmann, D.; Streeck, R. E.; Chen, X. S.; Lindahl, U.; Sapp, M. Surface-exposed amino acid residues of HPV16 L1 protein mediating interaction with cell surface heparan sulfate. *J. Biol. Chem.* **2007,** *282*, 27913-27922.
(194) Gandhi, N. S.; Mancera, R. L. Prediction of heparin binding sites in bone morphogenetic proteins (BMPs). *Biochim. Biophys. Acta* **2012,** *1824*, 1374-1381.
(195) Fairweather, J. K.; Karoli, T.; Liu, L.; Bytheway, I.; Ferro, V. Synthesis of a heparan sulfate mimetic disaccharide with a conformationally locked residue from a common intermediate. *Carbohydr. Res.* **2009,** *344*, 2394-2398.
(196) Sapay, N.; Cabannes, E.; Petitou, M.; Imberty, A. Molecular modeling of the interaction between heparan sulfate and cellular growth factors: bringing pieces together. *Glycobiology* **2011,** *21*, 1181-1193.
(197) Tan, K.; Duquette, M.; Liu, J. H.; Shanmugasundaram, K.; Joachimiak, A.; Gallagher, J. T.; Rigby, A. C.; Wang, J. H.; Lawler, J. Heparin-induced cis- and trans-dimerization modes of the thrombospondin-1 N-terminal domain. *J. Biol. Chem.* **2008,** *283*, 3932-3941.
(198) Copeland, R.; Balasubramaniam, A.; Tiwari, V.; Zhang, F.; Bridges, A.; Linhardt, R. J.; Shukla, D.; Liu, J. Using a 3-O-sulfated heparin octasaccharide to inhibit the entry of herpes simplex virus type 1. *Biochemistry* **2008,** *47*, 5774-5783.
(199) Lindsay, G.; Scorer, H. J.; Carnegie, C. M. Safety and efficacy of temafloxacin versus ciprofloxacin in lower respiratory tract infections: a randomized, double-blind trial. *J. Antimicrob. Chemother.* **1992,** *30*, 89-100.
(200) van den Born, J.; Gunnarsson, K.; Bakker, M. A.; Kjellen, L.; Kusche-Gullberg, M.; Maccarana, M.; Berden, J. H.; Lindahl, U. Presence of N-unsubstituted glucosamine units in native heparan sulfate revealed by a monoclonal antibody. *J. Biol. Chem.* **1995,** *270*, 31303-31309.
(201) Bienkowski, M. J.; Conrad, H. E. Structural characterization of the oligosaccharides formed by depolymerization of heparin with nitrous acid. *J. Biol. Chem.* **1985,** *260*, 356-365.
(202) Rong, J.; Habuchi, H.; Kimata, K.; Lindahl, U.; Kusche-Gullberg, M. Expression of heparan sulphate L-iduronyl 2-O-sulphotransferase in human kidney 293 cells results in increased D-glucuronyl 2-O-sulphation. *Biochem. J.* **2000,** *346 Pt 2*, 463-468.
(203) Liu, J.; Shworak, N. W.; Sinay, P.; Schwartz, J. J.; Zhang, L.; Fritze, L. M.; Rosenberg, R. D. Expression of heparan sulfate D-glucosaminyl 3-O-sulfotransferase isoforms reveals novel substrate specificities. *J. Biol. Chem.* **1999,** *274*, 5185-5192.

(204) Shworak, N. W.; Liu, J.; Petros, L. M.; Zhang, L.; Kobayashi, M.; Copeland, N. G.; Jenkins, N. A.; Rosenberg, R. D. Multiple isoforms of heparan sulfate D-glucosaminyl 3-O-sulfotransferase. Isolation, characterization, and expression of human cdnas and identification of distinct genomic loci. *J. Biol. Chem.* **1999,** *274*, 5170-5184.
(205) Abdel Aziz, M. H.; Sidhu, P. S.; Liang, A.; Kim, J. Y.; Mosier, P. D.; Zhou, Q.; Farrell, D. H.; Desai, U. R. Designing allosteric regulators of thrombin. Monosulfated benzofuran dimers selectively interact with Arg173 of exosite 2 to induce inhibition. *J. Med. Chem.* **2012,** *55*, 6888-6897.
(206) Karuturi, R.; Al-Horani, R. A.; Mehta, S. C.; Gailani, D.; Desai, U. R. Discovery of allosteric modulators of factor XIa by targeting hydrophobic domains adjacent to its heparin-binding site. *J. Med. Chem.* **2013,** *56*, 2415-2428.
(207) Sidhu, P. S.; Abdel Aziz, M. H.; Sarkar, A.; Mehta, A. Y.; Zhou, Q.; Desai, U. R. Designing allosteric regulators of thrombin. Exosite 2 features multiple subsites that can be targeted by sulfated small molecules for inducing inhibition. *J. Med. Chem.* **2013,** *56*, 5059-5070.
(208) Jones, G.; Willett, P.; Glen, R. C. Molecular recognition of receptor sites using a genetic algorithm with a description of desolvation. *J. Mol. Biol.* **1995,** *245*, 43-53.
(209) Bottegoni, G.; Cavalli, A.; Recanatini, M. A comparative study on the application of hierarchical-agglomerative clustering approaches to organize outputs of reiterated docking runs. *J. Chem. Inf. Model* **2006,** *46*, 852-862.
(210) Bouvier, G.; Evrard-Todeschi, N.; Girault, J. P.; Bertho, G. Automatic clustering of docking poses in virtual screening process using self-organizing map. *Bioinformatics* **2010,** *26*, 53-60.
(211) Jones, C. J.; Membreno, N.; Larive, C. K. Insights into the mechanism of separation of heparin and heparan sulfate disaccharides by reverse-phase ion-pair chromatography. *J. Chromatogr. A* **2010,** *1217*, 479-488.
(212) Langeslay, D. J.; Urso, E.; Gardini, C.; Naggi, A.; Torri, G.; Larive, C. K. Reversed-phase ion-pair ultra-high-performance-liquid chromatography-mass spectrometry for fingerprinting low-molecular-weight heparins. *J. chromatogr. A* **2013,** *1292*, 201-210.
(213) Solakyildirim, K.; Zhang, Z.; Linhardt, R. J. Ultraperformance liquid chromatography with electrospray ionization ion trap mass spectrometry for chondroitin disaccharide analysis. *Anal. Biochem.* **2010,** *397*, 24-28.
(214) Abdel Aziz, M. H.; Mosier, P. D.; Desai, U. R. Identification of the site of binding of sulfated, low molecular weight lignins on thrombin. *Biochem. Biophys. Res. Commun.* **2011,** *413*, 348-352.
(215) Henry, B. L.; Abdel Aziz, M.; Zhou, Q.; Desai, U. R. Sulfated, low-molecular-weight lignins are potent inhibitorsof plasmin, in addition to thrombin and factor Xa: Novel opportunity for controlling complex pathologies. *Thromb. Haemost.* **2010,** *103*, 507-515.
(216) Olson, S. T.; Halvorson, H. R.; Bjork, I. Quantitative characterization of the thrombin-heparin interaction. Discrimination between specific and nonspecific binding models. *J. Biol. Chem.* **1991,** *266*, 6342-6352.

(217) Olson, S. T.; Bjork, I.; Sheffer, R.; Craig, P. A.; Shore, J. D.; Choay, J. Role of the antithrombin-binding pentasaccharide in heparin acceleration of antithrombin-proteinase reactions. Resolution of the antithrombin conformational change contribution to heparin rate enhancement. *J. Biol. Chem.* **1992,** *267*, 12528-12538.
(218) Ebalunode, J. O.; Ouyang, Z.; Liang, J.; Zheng, W. Novel approach to structure-based pharmacophore search using computational geometry and shape matching techniques. *J. Chem. Inf. Model* **2008,** *48*, 889-901.
(219) Bates, S. M.; Weitz, J. I. The status of new anticoagulants. *Br. J. Haematol.* **2006,** *134*, 3-19.
(220) Eikelboom, J. W.; Wallentin, L.; Connolly, S. J.; Ezekowitz, M.; Healey, J. S.; Oldgren, J.; Yang, S.; Alings, M.; Kaatz, S.; Hohnloser, S. H.; Diener, H. C.; Franzosi, M. G.; Huber, K.; Reilly, P.; Varrone, J.; Yusuf, S. Risk of bleeding with 2 doses of dabigatran compared with warfarin in older and younger patients with atrial fibrillation: an analysis of the randomized evaluation of long-term anticoagulant therapy (RE-LY) trial. *Circulation* **2011,** *123*, 2363-2372.
(221) Schumacher, W. A.; Luettgen, J. M.; Quan, M. L.; Seiffert, D. A. Inhibition of factor XIa as a new approach to anticoagulation. *Arterioscler. Thromb. Vasc. Biol.* **2010,** *30*, 388-392.
(222) Kreuger, J.; Spillmann, D.; Li, J. P.; Lindahl, U. Interactions between heparan sulfate and proteins: the concept of specificity. *J. Cell Biol.* **2006,** *174*, 323-327.
(223) Lindahl, U. Heparan sulfate-protein interactions--a concept for drug design? *Thromb. Haemost.* **2007,** *98*, 109-115.
(224) Sarrazin, S.; Bonnaffe, D.; Lubineau, A.; Lortat-Jacob, H. Heparan sulfate mimicry: a synthetic glycoconjugate that recognizes the heparin binding domain of interferon-gamma inhibits the cytokine activity. *J. Biol. Chem.* **2005,** *280*, 37558-37564.
(225) Saxena, K.; Schieborr, U.; Anderka, O.; Duchardt-Ferner, E.; Elshorst, B.; Gande, S. L.; Janzon, J.; Kudlinzki, D.; Sreeramulu, S.; Dreyer, M. K.; Wendt, K. U.; Herbert, C.; Duchaussoy, P.; Bianciotto, M.; Driguez, P. A.; Lassalle, G.; Savi, P.; Mohammadi, M.; Bono, F.; Schwalbe, H. Influence of heparin mimetics on assembly of the FGF.FGFR4 signaling complex. *J. Biol. Chem.* **2010,** *285*, 26628-26640.
(226) Turk, H.; Haag, R.; Alban, S. Dendritic polyglycerol sulfates as new heparin analogues and potent inhibitors of the complement system. *Bioconjug. Chem.* **2004,** *15*, 162-167.
(227) Correia-da-Silva, M.; Sousa, E.; Duarte, B.; Marques, F.; Carvalho, F.; Cunha-Ribeiro, L. M.; Pinto, M. M. Flavonoids with an oligopolysulfated moiety: a new class of anticoagulant agents. *J. Med. Chem.* **2011,** *54*, 95-106.
(228) Gunnarsson, G. T.; Riaz, M.; Adams, J.; Desai, U. R. Synthesis of per-sulfated flavonoids using 2,2,2-trichloro ethyl protecting group and their factor Xa inhibition potential. *Bioorg. Med. Chem.* **2005,** *13*, 1783-1789.
(229) Xia, Y.; Yang, Z. Y.; Hour, M. J.; Kuo, S. C.; Xia, P.; Bastow, K. F.; Nakanishi, Y.; Namrpoothiri, P.; Hackl, T.; Hamel, E.; Lee, H. K. Antitumor agents. Part 204:

synthesis and biological evaluation of substituted 2-aryl quinazolinones. *Bioorg. Med. Chem. Lett.* **2001,** *11*, 1193-1196.
(230) Henry, B. L.; Monien, B. H.; Bock, P. E.; Desai, U. R. A novel allosteric pathway of thrombin inhibition: Exosite II mediated potent inhibition of thrombin by chemo-enzymatic, sulfated dehydropolymers of 4-hydroxycinnamic acids. *J. Biol. Chem.* **2007,** *282*, 31891-31899.
(231) Al-Horani, R. A.; Desai, U. R. Chemical Sulfation of Small Molecules - Advances and Challenges. *Tetrahedron* **2010,** *66*, 2907-2918.
(232) Raghuraman, A.; Riaz, M.; Hindle, M.; Desai, U. R. Rapid and efficient microwave-assisted synthesis of highly sulfated organic scaffolds. *Tetrahedron Lett.* **2007,** *48*, 6754-6758.
(233) Henry, B. L.; Thakkar, J. N.; Liang, A.; Desai, U. R. Sulfated, low molecular weight lignins inhibit a select group of heparin-binding serine proteases. *Biochem. Biophys. Res. Commun.* **2012,** *417*, 382-386.

APPENDIX A

Naming convention for the H/HS monosaccharides and the 36 disaccharide building blocks derived from them.

Name[a]	Name	Conf.[b]	Anomer	Disaccharide Building Blocks		
uaA	IdoA*p*	$^1C_4$	α-	ZbB-YbCA	ua2A-	ua2A-
ua2A	IdoA*p*2S	$^1C_4$	α-	ZbB-	uc2A-	uc2A-
ucA	IdoA*p*	^2S_O	α-	ZbB-Yb2A	uaA-Yb2A	ucA-Yb2A
uc2A	IdoA*p*2S	^2S_O	α-	Zb2B-	ua2A-	uc2A-
Yb2A	GlcN*p*2S	$^4C_1$	α-	ZbB-	uc2A-	
Yb23A	GlcN*p*2S3S	$^4C_1$	α-	Zb2B-	uaA-	
Yb26A	GlcN*p*2S6S	$^4C_1$	α-	ZbB-	ucA-	
Yb236A	GlcN*p*2S3S6S	$^4C_1$	α-	Zb2B-	ua2A-	
Yb26A	GlcN*p*2S6S	$^4C_1$	α-	ZbB-	uc2A-	
YbCA	GlcN*p*2Ac	$^4C_1$	α-	ZbB-YbHA	uaA-	
YbC6A	GlcN*p*2Ac6S	$^4C_1$	α-	uaA-YbCA	ucA-	
YbHA	GlcN*p*	$^4C_1$	α-	ucA-YbCA	ua2A-	
YbH3A	GlcN*p*3S	$^4C_1$	α-	ua2A-	uaA-	
YbH36A	GlcN*p*3S6S	$^4C_1$	α-	uc2A-	ucA-	
ZbB	GlcA*p*	$^4C_1$	β-	uaA-	ua2A-	
Zb2B	GlcA*p*2S	$^4C_1$	β-	ucA-	uc2A-	

[a]Symbols: Z = *D*-GlcA*p*, u = *L*-IdoA*p*, Y = *D*-GlcN*p*. Ring conformations: a = $^1C_4$; b = $^4C_1$; c = ^2S_O. Substituents: H = No substitution at position 2; Ac = *N*-acetyl, S = sulfate; Anomer configuration: A = α, B = β. [b]Conformation.

APPENDIX B

Average torsion across the 1→4 inter-glycosidic bonds used in this CVLS study.

Disaccharide Building Block	**Φ** (O5-C1-O1-C4')	**Ψ** (C1-O1-C4'-C5')
GlcA*p*(1→4)GlcN*p*	-81.8	-114.0
IdoA*p*(1→4)GlcN*p*	-87.7	-128.3
GlcN*p*(1→4)GlcA*p*	91.1	-151.6
GlcN*p*(1→4)IdoA*p*	87.4	-132.3

VITA

Rio Boothello was born on the 3rd of June 1987 in Mumbai India. He is an Indian citizen and completed his Bachelors in Pharmaceutical Sciences at the Mumbai Educational Trust's institute of Pharmacy in 2005. He began his graduate studies at Virginia Commonwealth University in 2009.